EFFECTS OF OXIDATION STATES OF COPPER (Cu), NICKEL (Ni), PALLADIUM (Pd) AND SILVER (Ag) ON REJECTION BY NANOFILTRATION MEMBRANES

Thabo John Brooms

B. Tech. (Chemistry), Vaal University of Technology

This dissertation is presented in fulfilment of the requirements for the degree Magister Technologiae: Chemistry at Vaal University of Technology.

Supervisor: **Prof. S.J. Modise (BSc. Hons, M.Sc, Ph.D. (Chemistry)**

Co-supervisor: **Dr. S.M. Nelana (BSc. Hons, M.Sc, Ph.D. (Chemistry)**

DECLARATION BY CANDIDATE

I hereby declare that the dissertation/thesis submitted for M-Tech: Chemistry, at Vaal University of Technology has never been submitted to any other institution of higher learning. I further declare that all cited sources are acknowledged by list of referencing.

……

TJ Brooms June 2010

Vaal University of Technology 2010

ACKNOWLEDGEMENTS

Of all existing on this earth, I would like to thank **GOD the ALMIGHTY and ANGEL JOHN** for the grace when matters seemed impossible.

I will like to thank the following:

- My extremely patient and understanding supervisor, Prof. S. J. Modise for his love, support (academic and social), encouragement and his humbleness during the course of my confusions on the study. Without you, honestly I would not have made it.

- My sensitive co-supervisor, Dr. S. M. Nelana whom was a friend, brother and a colleague during the study. Thank you for the part of Inorganic chemistry. I will always cherish your contributions in my academic life.

- Research Department at VUT and NRF scholarship for funding the project from the onset till the end.

- The Chemistry Department for accessibility of AAS, FTIR and IC instrumentations.

- My partner and a friend during the study, Mr. B. M. Xaba, we made it through difficulties. I will always cherish you.

- My colleagues, M. Bucibo, T. Mashile, L. P. Motaung, G. Manzane and I. Ledwaba, thank you for believing in me.

- My family, Isaac, Esther, Xolani, Khanyisane, Khuzwayo, Mittah, Lindi, Dieketseng, Melita, Naledi and Lebohang. Thank you in advance for the support and the encouragement you have devoted to me.

- My social friends in and out of VUT, Mr. S. J. Phiri (spiritual partner), Mr. M. J. Mathejane (known as Tuks) and my soul-mate (Busisiwe D. Ngobeni), and the list is endless. Thank you in advanced for your contributions. I love u all.

DEDICATION

This study is dedicated to:

- My grandparents (deceased) Phillicks, Sannah and Mittah Brooms.
- My uncles (deceased) Joseph, Maletsatsi, Mbuti, Abel, Michael, Thandi and Nontozanele Toli. I know that you're behind me every time. Thank you.

ABSTRACT

Mining industry produces metals which are economical and serve as high valuable commodities in South Africa. This country is regarded as the world leading producer of precious metals such as platinum group metals (PGMs). Silver (Ag), which is also a precious metal, contribute to the country's economy wealth due to its significance during industrial applications. Base metals such as copper (Cu) and nickel (Ni), though they are low valued, play a significant role in the republics economic wealth. Mining wastewater contains some of these metals, which end up polluting the environment. A possibility to recover this was investigated using NF membranes. Mine effluent was simulated by using relevant reagents.

Characterization of NF90, NF- and NF270 membranes, was done by using scanning electron microscopy (SEM), clean water permeability, single charged salts of NaCl and $MgCl_2$ and binary mixture of NaCl/$MgCl_2$ studies. All the rejection experiments were conducted at pH 2.0 with varying pressure and concentrations. Flux measurements indicated that water permeability through the membranes trend, NF270 > NF90 > NF-. The experiments were performed at pressures of 5 bar, 10 bar, 15 bar and 20 bar.

For NF90 membrane, a rejection of Na^+ monovalent ion in 20 ppm solution was less than of Mg^{2+} (divalent) ion. Percentage rejections of 90% (Na^+) and 98% (Mg^{2+}) were achieved. NF- had rejection of 83% and 90% for Na^+ and Mg^{2+}, respectively. In the case of NF270, the membrane had rejection of 92% (Na^+) and 94% (Mg^{2+}), respectively.

At 100 ppm, all three membranes showed a decreasing trend in rejection while increasing pressure. For binary-solution mixture, Mg^{2+} ion still had the highest rejection compared to Na^+ ion with about 94% and 85% on NF90 than on NF270 and NF-. The high rejection of divalent ion as compared to monovalent ion for charged solutes was due to solute size and electrostatic interaction between the membrane surface layer and the solute.

In the case of transition metal rejection studies, Pd^{2+} ion had an average of 90%, with Ni^{2+} ion ≈ 95% and Cu^{2+} ion ≈ 98% as single salts on NF90 compared to NF270 and NF-. However, as for binary and trinary solution mixture, the competition amongst ions was high, where Pd^{2+} ion rejection was ≈ 99,0%, while Ni^{2+} and Cu^{2+} ions was > 90% on NF90 and NF-. Therefore it was excluded from the tests. For the monovalent metal ions (Ag^{+} and Cu^{+}), the rejection was > 90% in almost all concentrations mixtures. During membrane fouling evaluation, AgCl salt fouled the most, compared to other metal ions, forming a concentration polarization accumulation on the membrane surface for both 20 and 100 ppm solutions. This situation leads to cake layer formation which causes a flux decline, reduces membrane life time and lowers the rejection performance of NF membranes.

The aim of this study was to evaluate the performance of three commercial polymeric membranes (NF90, NF270 and NF-) during rejection of the metals.

List of Abbreviation and Symbols

Abbreviations

NF	Nanofiltration
UF	Ultrafiltration
SEM	Scanning Electron Microscopy
RO	Reverse Osmosis
TFC	Thin Film Composite
PGMs	Platinum Group Metals
FTIR	Fourier Transform Infrared
EDX	Energy Dispersive X-ray
IC	Ion Chromatography
AAS	Atomic Absorption Spectroscopy
IOP	Isoelectric Point
EMF	Electromotive Force

Symbols

MWCO	Molecular weight cut-off	(dalton)
MW	Molecular weight	($g.mol^{-1}$)
C_f	Feed concentration	(ppm)
C_r	Retentate concentration	(ppm)
C_p	Permeate concentration	(ppm)
J_w	Clean water flux	($\ell.m^{-2}.hr^{-1}$)
ΔP	Pressure difference	(bar)
η	Viscosity	(Pa.S)
t	Time	(hr)
ε	Porosity	(-)
ΔP	Pressure difference	(bar)

D_∞	Bulk diffusivity	($m^{-2}.s^{-1}$)
$\Delta\pi$	Osmotic pressure difference	(bar)
R	Retention coefficient	(-)
τ	Tortuosity	(-)
r_s	Stokes radius	(nm)
k_B	Boltman constant	($J.K^{-1}$)
T	Temperature	ºC or K

List of Figures

List of Tables

CHAPTER 1

INTRODUCTION

Table of Contents

1.1 Background of the study

The platinum group metals (PGMs), which comprise of platinum (Pt), palladium (Pd), rhodium (Rh), ruthenium (Ru), iridium (Ir) and osmium (Os), have some unique physical and chemical properties. They are industrially utilized as catalysts, electrical and corrosion-resistant materials, and therefore are contained in industrial wastes [1]. These PGMs possess also a wide range of both chemical and physical properties. In various environments they are increasingly finding vital uses. Amongst others, PGMs are used as hydrogen fuel cells and electronic computers [2].

South Africa (SA) is considered to be one of the leading producers of the precious metals such as PGMs [3, 4]. Silver (Ag), which is also a precious metal, is an important constituent of gold (Au) and platinum (Pt) ores in SA [5]. These precious metals, occur together with some of the world's largest reserve of chromium and vanadium ore in the Bushveld Igneous Complex, which is a geological formation that extends in an arc across three South African provinces (North-West, Limpopo and Mpumalanga) [6].

The PMGs and some of their alloys, serve a protective function due to their inert character and strength. The appearance and nobility of platinum metal further renders it as a useful material in the manufacturing of jewellery. For the catalytic and decorative purposes, these PGMs are often coated on to less expensive substrates. These PGMs are rare metals but they form part of South Africa's vast minerals resources [7]. They exist as sulphides from ore and are extracted by means of xanthate flotation. The resulting sulphide concentrate is roasted for the purpose of producing a so called converter matte, rich in copper (Cu), nickel (Ni) and PGMs [8].

The production process of the precious metals incorporates mining, concentrating, smelting and refining. The following seven commodities; manganese (Mn), chrome (Cr), vanadium (V), PGMs, gold (Au), vanadium (V) and vermiculite are classified as the

country's biggest minerals worldwide [9]. The mining expertise has made South Africa the world leader of minerals and metals producers over a period of a century, and confirmed that there is still more of other world class deposits to be discovered and yet to be explored [9, 10]. Table 1.1 represents the world reserves and production of commodities in South Africa. PGMs, gold (Au) and alumino-silicates are highly considered in terms of mineral ranges in the world. Highest ranking of PGMs productions of 57,8% indicates their vital uses and availability as minerals amongst other metals. Copper metal rank position 15 while nickel metal's ranking was not provided, but had 40% lower compare to copper with 102.6% of production during 2004. Silver had a good production of about 72% as a mineral. The availability of these minerals greatly boosts the economic moral as a whole.

Table 1.1 South Africa's mineral production, 2005 [9]

Commodity	Unit	Mass	%	World ranking
Aluminium	kt	866	2,9	10
Alumino-silicates	kt	235	38,0	1
Antimony	t	4967	3.2	3
Chrome ore	Kt	7645	44.5	
Coal	Mt	243	5,2	5
Copper	Kt	103	0.8	18
Fluorspar	Mt	365	-	5,0
Gold	t	341	13.8	1
Iron ore	Mt	39,2	3,3	
Lead	Mt	38	1.3	13
Manganese ore	Kt	4282	14,8	-
Nickel	Kt	40		
Phosphate rock	Kt	2735	1,9	-
PGMs	Kg	286 157	57,8	1
Silver	t	72	0,4	-
Titanium minerals	Kt	-	-	-
Uranium	t	887	2,1	4
Vanadium	Kt	23	48,0	1
Vermiculite	Kt	197	41,0	1
Zinc metal	Kt	32	0,4	22
Zirconium minerals	Kt	-	-	-
Mt = megaton, kt = kiloton, n/a = not available, t = ton, kg = kilogram, **Bold** = Metal to be considered on the project, Source: Mineral Bureau				

1.2 Statement of the problem

Mining and refinery industries generate waste, and have been connected with numerous environmental issues e.g. wastewater discharge from flotation process [11], and land pollution resulting from ore rocks. Wastewater produced in mining processing

contains lot of suspended solid particles, heavy metals ions, flotation reagents, organics and other pollutants resulting in environmental pollution. Therefore wastewater problem and reuse have much academic and practical significance [12].

According to Western Australia wastewater pollution control [13], coal and metal mining operations interfere with the natural circulation of water. The need to minimize pollution through wastewater has been recognized worldwide. Mostly, the majority of elements and compounds can be reused as valuable species through recycling process. But some of the metals discharged during mining refinery process, may need to be taken back to smelting plant and requires non-chemical additive during recycling processes [6].

The ongoing advances in membrane technology have rendered reverse osmosis (RO) as an increasingly cost-effective option to desalination, with the lower energy requirements than the alternative thermal processes [14]. The low pressure reverse osmosis (RO) and nanofiltration (NF) membranes can be used for secondary effluent wastewater treatment, since the total dissolved salts are not high (typically <1g/l). NF membranes have been successfully used in wastewater treatment [15].

These NF membranes have a charged surface material with small pores of about 1 nm, and their separation process is commonly based on electrical, dielectrical effects and size exclusion. Therefore, since the effective NF membrane pressure is relatively low in comparison to reverse osmosis, the application of NF membranes is extremely economically attractive. The economic rewards from increasing the degree of removal of precious metals provide huge environmental benefits [15]. Some of NF membrane researchers including Kaseoglu and Kitis [16], Bessbousse *et al.* [17] have applied the polymeric NF membrane for the recovery of metals from wastewater. Quite high percentage of metals was recovered between 96-99% for divalent metal ions and as lowest as 29-59% of monovalent ions were retained. This technique seems to favour divalent more than monovalent. This shows that NF membranes can be applied to recover metals in wastewater.

1.3 Aims and objectives

The aim of the study was to investigate the possibility of employing cost-effective and lesser energy consumption method (membrane technology) for the recovery of some of precious metals (palladium and silver) as well as base metals (copper and nickel) through their variations in oxidation states in mining wastewater. The objective of the work was to achieve the following:

- To characterize the polymeric flat sheet NF membranes used.
- To identify the NF membranes with maximum performance using NF membranes.
- To reject cations that are similar to those found in mining waste water.
- To introduce the process for membrane retentions that will be viable, rapid and controllable.

1.4 The hypothesis

It is stipulated that nanofiltration separation processes including recovery, has a potential for metal removal and is relevant to both mining and municipality industrial wastewater.

1.5 Scope of the study

This investigation is relevant to recovery of PGMs in mining and metal industries' effluents. The content of the work will be classified in the following approach:

Chapter 1 will state the problem, aims and objectives, scope of the study and the hypothesis will be described.

Introduction to metal industry, uses and physical properties of selected transition metals, metal oxidation states and membrane technology existence, will be discussed in Chapter 2.

Materials used and analytical instrumentations utilized, will be described in detail in Chapter 3.

In Chapter 4, the results of membrane characterization, salt (charged ion) retention capacity and transition metal rejection behaviour on different membranes, will be given and discussed.

For the last section (Chapter 5) of the study, conclusion of the result obtained and interpreted, will be given as well as evaluation and recommendation for future work.

References

1. T. Kakoi, N. Horinouchi, M. Goto, F. Nakashio. Selective recovery of palladium from water by liquid surfactants membranes process, *Journal of Membrane Science* **118** (1996) p63-71.

2. J. B. Glaister, G. M. Mudd. The environmental costs of platinum-PMG mining and sustainability: Is the glass half-full or half-empty? *Minerals Engineering* **23** (2010) p438-450.

3. P. Mwape, M. J. Roberts, E. Mokwena, L. Musi, T. Tjatjie, M. Phale, U. Pohlongo. South Africa's Mineral Industry General Review, Department of Minerals and Energy, 2004/2005.

4. S. Gwicana, N. Vorster, E. Jacobs. The use of a cationic surfactant for micellar-enhanced ultrafiltration of platinum group metal anions, *Desalination* **199** (2006) p504-506.

5. http://www.bullion.org.za/Education/Base.htm: date accessed: 01/03/2010.

6. M. Lydall. Backward linkage development in the South African PGM industry: A case study, *Resources Policy* **34** (2009) p112-120.

7. B. K. Ferreira. Electrochemical reactors for PGM recovery. M.Sc thesis, University of Witwatersrand, Johannesburg, South Africa (2004).

8. H. G. Julsing. The reclamation of the precious metals from acidic refinery effluent solutions using sodium formate, DTech thesis, Technikon Pretoria (2000).

9. http://www.gcis.gov.za/resource_centre/sa_info/pocketguide/2006/015_minerals.pdf. date accessed: 02/03/2010

10. www.southafrica.info/about/416221.htm: date accessed: 05/02/2010

11. R. S. Dobson, E. J. Burgess. Biological treatment of precious metal refinery wastewater, *Minerals Engineering* **20** (2007) p519-532.

12. C. Jian-Ming, L. Run-qing, S. Wei, Q. Guan-Zhou. Effects of mineral processing wastewater on flotation of sulfide minerals, *Transactions of Nonferrous Metals Society of China* **19** (2009) p454-457.

13. M. Nedved, J. Jansz. Waste Water pollution control in the Australian mining industry, *Journal of Cleaner Production* **14** (2008) p1118-1120.

14. A. Simon, L. D. Ngiehem, P. Le-Clech, S. J. Khan, J. E. and Drewes. Effects of membrane degradation on the removal of pharmaceutically active compounds (PhACs) by NF/RO filtration processes, *Journal of Membrane Science* **340** (2009) p16-25.

15. E. Chilyumova, J. Thöming. Nanofiltration of bivalent nickel cations-model parameter determination and process simulation, *Desalination* **224** (2008) p12-17.

16. H. Koseuglu, M. Kitis. The recovery of silver from mining wastewater using hybrid cyanidation and high-pressure membrane process, *Minerals Engineering* **22** (2009) p440-444.

17. H. Bessbousse, T. Rhalou, J. F. Verchère, L. Lebrun. Removal of heavy metals ions from aqueous solutions by filtration with a novel complexing membrane

containing poly (ethyleimine) in a poly (vivyl alcohol) matrix, *Journal of Membrane Science* **307** (2008) p249-259.

Table of Contents

CHAPTER 2

LITERATURE REVIEW

Introduction

World's mineral resources are critical to the well-being of modern civilization [1]. Most of the chemical elements which are crucially important as mineral resources are metals. Countries like South Africa, Russia, USA and Canada produces the most platinum group metals (PGMs) worldwide. According to the world mineral rankings (2007), South Africa is the highest in terms of mineral refinery worldwide with about 87.7% of PGMs. It is followed by Russia (8.3%), USA (2.5%) and Canada (0.5%) in fourth place [2]. These statistics indicate that South African mineral production mostly dominate the country's economic wealth.

Africa is richly endowed with abundant reserves of important minerals [3]. This continent holds about 30% of the world mineral reserves. Amongst them are gold (40%), cobalt (60%) and PGMs with 90%. Neighbouring countries including Zimbabwe, Tanzania, Ghana, Zambia and the Due Republic of Congo (DRC) dominate African PGM mining industry. They are also major producers of some minerals amongst 60 metals in Africa such as Diamonds, Uranium, Manganese, Chromium and Cobalt [3].

According to the report from Precious Metal Cluster (PMC) consultants [4], these neighbouring countries obtained 64% as an average global production of PGMs since 2005. Production of base metals such as copper, lead and zinc, is less than 7% when compared to PGMs in African mines. Therefore, the significance of PGMs against other minerals resources, mostly contribute economically as long term social benefit in an African continent [5]. Over the past century, South Africa has been and still is regarded as the world's leading producer of minerals (PGMs) [6]. PGMs in South Africa are mined as primary products while copper (Cu), nickel (Ni) and cobalt (Co) are treated as by-products. In Canada, PGMs are refined as by-products of Cu and Ni and this is due to their relatively small abundance [7, 8, 9].

In other countries including Russia and USA, Cu and Ni metals are refined as primary (major) products. PGMs are treated as by-products excluding platinum (Pt) which falls under platinum group metals, is regarded as a major product [10]. These major products are extremely scarce compared to precious metals (Pd and Ag). This is due to their low natural abundance and the complexity of the processes, which are required for their extraction and refining. Relative to other precious metals, the PGMs have high technological importance due to the number of properties they possess [7].

The demand for precious metals, especially silver and palladium has increasingly resulted in the scaling up of metal extraction and refinery operations globally [11]. The PGMs have wide range of applications as catalysts such as enabling petroleum and fuels. Platinum compounds, can also be used in cancer treatment drugs [12].

2.1 PGMs deposits and occurrences in South Africa

Bushveld Igneous Complex is an area in South Africa where some of the main PGM ore are located. The deposits containing Ni, Cu and PGMs sulphides are usually associated with mafic and ultramafic rocks. They can also be obtained on other mines like Noril'sk (Ural Mountains in Russia), Sudbury (at Ontarion in Canada), Hartley mine (Zimbabwe) and in the USA (Still-water Complex in Montana) [12, 13]. The mineral ore deposits in South Africa are subdivided into two groups, and can be distinguished as follows;

i) Ores with Ni and Cu

Ores with Ni and Cu are considered as the principal products, whereas PGMs and Au are treated as by-products. These ores contain more than 10% of sulphide minerals e.g. Sudbury, Noril'sk and others [14]. The ores rarely occurs as orebodies at the base of komatiite channel, except in an impact that is related to Sudbury meltsheet.

ii) Ores with PGMs

Ores where PGMs are main products with Ni and Cu deposited as by products, occur in two types of reefs e.g. the Merensky reef and the UG-2 reef of the Bushveld Igneous Complex [12, 15]. The Merensky reef contains much more sulphide, and the minerals are found in a silica substrate. The UG-2 reef contains a chromite matrix.

PGMs' association with other base metal sulphides occurs as Sperrylite and Braggite and are classified as platinoid minerals. While in copper, nickel, cobalt and iron-bearing sulphide minerals, they occur as Pentlandite, Pyrrhotite and Chalcopyrite. On nickel mining, PGMs are produced as by products in Mpumalanga Province on the Uitkomst Complex area [2, 14]. Metals such as nickel, copper, titanium, manganese etc, are found at usable levels as the base metals, this is because of their wide industrial applications [12]. With the demand from both industrial and automobile manufacturing sectors, PGMs will continue to be most useful and vital to the mineral users globally.

2.2 PGM Separation Process

South Africa has the highest concentration of primary PGMs' producing companies. Each of these has their own approach to smelting and are governed to a large extend by the type of ore they process. Some of PGMs are concentrated in the Merensky reef, the Plaatreef (ore similar to Merensky but higher in copper and nickel content), and the UG-2 chromite reef ores [16, 17]. Bernardis *et al.* [8] outlined a typical separation process of PGMs in South Africa from the sulphide ore concentrate as presented in Figure 2.1. The deposits of the concentration are less than 10 grams per tonne (g/t) of an ore. Therefore processes such as physicalmetallurgy and pyrometallurgy, which are applied as metals separation processes, can be employed for concentrating the PGMs.

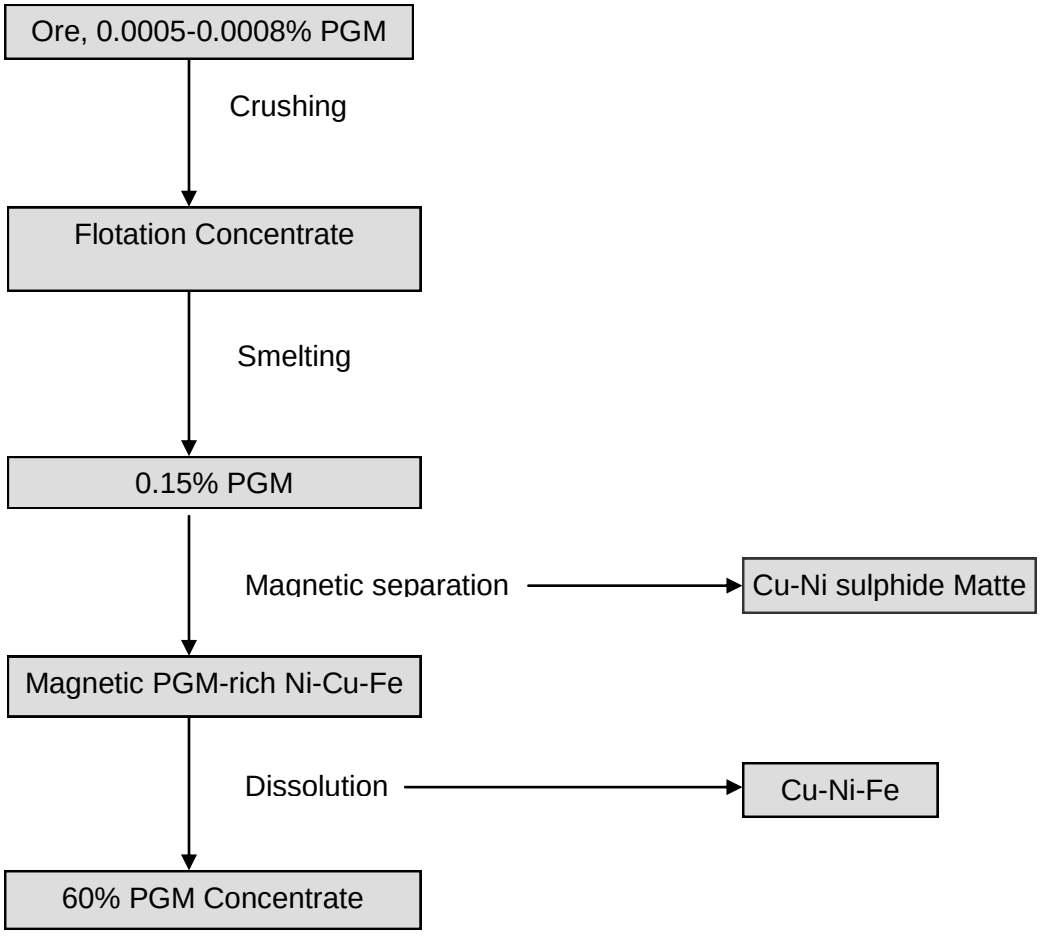

Figure 2.1 A schematic diagram of concentration process for PGMs from sulphide ore [6].

Each process is designed to increase the concentration of the valuable components of the original ore, which is done by reducing the bulk of the ore. The mined ore undergoes communition (conversion of larger particle into smaller particles) and the gravity concentrate is extracted.

The flotation concentrates undergoes smelting and are converted to produce a PGM-containing nickel-copper matte. This is done after flotation is concentrated by the sulphides. Before reaching the final PGM concentrate, the matte is treated using

hydrometallurgical process for separation of the base metals from precious metals. Lastly, the PGM concentrates are refined to separate precious metals in their pure forms [7].

2.3 Occurrence, uses and health hazard of copper (Cu) metal

Copper is the 25th most abundant element in the earth's crust [18]. It occurs naturally throughout the environment, in rocks, soil, water and air. It is found in native and in variety with other minerals in plants and animals. This element can be found as a metal in sulphides, carbonates, chloride, nitrates and so on. Leaching with dilute sulphuric acid or by solvent extraction are usually wet processes used for extraction of copper from ores. The metal can be refined by electrolysis process [19].

Although humans need copper for industrial purposes, it can still pose some danger into our lives. At high (10 ppm) or low (0.01 ppm) level of exposure, the metal can cause an illness called Wilson's disease if it is ingested. This disease can lead to severe liver damage, brain damage, nausea, vomiting, diarrhoea, dizziness, stomach cramps and it could even lead to death [20]. Therefore, standard levels of copper are essential for human good health maintenance.

There are countless applications of copper industrially, some include production of wire brass, boiler pipe, cooking utensils [21] and sheet metals [20]. Other applications of copper include uses for roofing, building construction, chemicals and so forth.

2.4 Occurrence, uses and health hazard of nickel (Ni) metal

Nickel is a universal trace metal and it can occur in soil, water, air and in the biosphere [22]. As a base metal, nickel occurs within both laterite and sulphide ores and it can also be associated with deep-sea nodules. This metal ranks below copper metal

as 24th element in abundance [23]. Nickel is also essential in maintaining good health in animals. A small amount of nickel is needed by humans, though at low level, the metal possesses no danger or some sort of health effects.

Statement issued by State of Ohio Environmental Protection Agency (EPA) [24] indicates that, the most common adverse effect of nickel is an allergic reaction in humans. During skin contact with the metal, one might suffer from skin irritation. Excessive exposure to the metal, humans might suffer from kidney failure. Research conducted by Demir's [22] revealed that exposure to nickel, pose an acute toxicity in humans, which leads to air-way irritation, allergic eczema and respiratory cancers. Purely refined nickel is marketed in variety of forms suited for the requirements of different users, ranging from metallic products of iron (Fe) and steel makers. Nickel is also a special alloy to form chemical compounds for catalyst manufacturing and electroplaters [25].

2.5 Occurrence, uses and health hazard of silver (Ag) metal

The first metals to be discovered and used by ancient man were gold, copper and silver [26]. Silver metal is rear but naturally occurring, and it can be deposited as the mineral ore in association with other elements. The metal is comparatively rare in the earth and is the 67th natural abundant in order of elements [27]. Discharge of silver at its high toxicity level in wastewater without treatment, becomes harmful to human life. Environmental protection agency [27] reported that even at low level, silver ions in solution are also considered to be harmful.

In 1990, about 50% of the refined silver consumed in the United State of America (USA), was used to manufacture photographic and X-ray products. Regarding the metal industrial production; 25% of electronic and electrical equipments were produced. The 10% were of jewellery and electroplate wares, and only 5% in brazing alloys was also produced. [28]. One on the common uses of silver metals is in silverware production, and it can also be applied in food processing and beverages.

2.6 Occurrence, uses and health hazard of palladium (Pd) metal

The precious metal (Pd) has vital significance in human life. This metal occurs in nature in base metal ores. During mining operational processes such as smelting, refining or recycling industries, Pd metal exposure leads to health effect on the immune systems especially to workers. Some of the symptoms include swelling of lips and cheeks, dizziness and asthma [29].

The demand for palladium as metal has increased in both ordinary and advanced fields of industry e.g. electronics, heat and corrosion resistance apparatus and catalysis [30, 31]. Based on the production distribution of this metal worldwide, Carrington *et al.* [32] reported that 10% of palladium is used for catalytic reactions in chemical and petrochemical industries. About 46% is used for electronic components manufacturing and about 25% is used in dentistry.

Some of Pd catalysts are employed during hydrogenation, hydrochlorination, hydrogenolysis and oxidation processes [33, 34, 35].

2.7 Physical/Chemical properties of selected metals

2.7.4 Copper (Cu)

The metal (copper) has been utilised by man for continuous period of nearly 6000 years. Its applications fluctuate with time as more knowledge about its properties becomes available [36]. According to Cotton and Wilkinson [19] copper is a tough, soft, ductile and reddish metal. The metal is also very malleable with a wide range of strength values.

Copper is in sub group 1B in the Periodic Table with an atomic number 29. It has properties that resemble those of gold (Au) and silver (Ag). The metal occurs as two isotopes namely; Cu^{63} and Cu^{65}. Cu^{63} has 69.09% in abundance while Cu^{65} has 30.91%

and it has no allotropic modification [36]. Copper falls in the first long period followed by iron (Fe), cobalt (Co) and nickel (Ni) while zinc (Zn) falls on the last. Table 2.2 outlines chemical properties of pure copper metal at 20 °C.

Table 2.2 Physical properties of Copper metal [36]

Properties	Values
Atomic radius	1.275 Å
Atomic number	29
Atomic weight (mass)	63.54 $g.mol^{-1}$
Valence	1 and 2
Density at 20 °C	8.96 $g.cm^{-3}$
Density of liquid just above melting point	8.53 $g.km^{-3}$
Specific heat capacity at 25°C	385 $J.kg^{-1}.K^{-1}$
Boiling point	2590 °C
Melting point	1083 °C

2.7.5 Nickel (Ni)

Nickel occurs in the first long period together with cobalt (Co) and iron (Fe) as ferromagnetic metals [25]. It has a high resistance to atmospheric tarnishing and can be used with other metals as an electrodeposited coating material. When nickel comes into contact with water (distilled or natural), it exhibits and extra extremely high resistant property. With regard to its physical property and wide range of applications, the metal can be rolled, forged, drawn and polished depending on the purpose of its employment.

The density of liquid nickel at the melting and boiling point is reported to be 7900 kg/m^3. When temperature increases linearly up to 2500°C during nickel production, the density of the metal falls approximately to 7000 kg/m^3. The density of nickel when operated at 20°C is 8.908 g/cm^3, which is about the same as copper metal [37]. Table 2.3 list the physical properties of nickel as representative of the highest-purity material.

Table 2.3 Physical properties of nickel metal [25]

Properties	Values
Atomic radius	1.24 Å
Atomic number	28
Atomic weight	58.71 $g.mol^{-1}$
Valence	2 [38]
Density at 20°C	8.908 $g.cm^{-3}$
Density of liquid nickel at melting point	7900 $kg.m^{-3}$
Specific heat capacity	425 $J.kg^{-1}.K^{-1}$
Boiling point	2910°C
Melting point	1453 °C

The average value of specific heat capacity over the temperature ranges from 0-100 °C was found at 425 J/kg.K, and within that temperature range, nickel tend to loose its ferromagnetism. The naturally occurring element of nickel composes of five different stable isotopes. The isotopes of the metal isotopes are estimated in the following order of their natural abundances; Ni^{58} (67.7%), Ni^{60} (26.2%), Ni^{61} (1.25%), Ni^{62} (3.66%) and Ni^{64} (1.16%) [25].

2.7.6 Silver (Ag)

The metal (Ag) has the highest electrical and thermal conductivity amongst all transition metals [26]. Silver has two stable isotopes Ag^{107} and Ag^{109}, which are found in Group 1 on Subgroup IB of the Periodic Table. The percentage distribution of silver atoms with an atomic number of 47 appeared to be about 51.84 (Ag^{107}) and 48.18 (Ag^{109}). The melting and boiling points of Cu and Ag, are very closely grouped at much higher temperature, but considerably lower than on Ni and Pd metals. Table 2.4 list the physical properties of silver during chemical processing and even in nature form.

Table 2.4 Physical properties of silver metal [26]

Properties	Values
Atomic radius	1.44 Å
Atomic number	47
Atomic weight	107.88 $g.mol^{-1}$
Valence	1
Density at 20°C	10.49 $g.cm^{-3}$
Density of liquid at melting point	961 °C
Specific heat capacity at 25°C	0.23 $J.Kg^{-1}.K^{-1}$
Boiling point	2180 °C
Melting point	960.5 °C

The metal has the highest electrical and thermal conductivity; it is followed by Cu. But the silver has the lowest electrical contact resistance compared to other metals [39]. Electrical conductivity of silver in usual volumetric basis is about 8% above that of copper, while thermal conductivity of silver metal is about one-third greater than that of copper. Therefore this indicates that silver dominates all other substances in conductivity with regard to both heat and electricity.

2.7.7 Palladium (Pd)

Palladium is a scarce and costly metal, and it has unusual properties. It is the least dense metal amongst other PGM members and it does not tarnish in air. When annealed, the metal becomes soft and ductile. The metal resembles its PGM member (Pt) very closely by having same diamagnetic characteristic in its compounds. These two metals (Pd and Pt) are sometimes called noble metals as result of their superior ability to withstand oxidation and corrosion [40]. In general, these two metals share almost the same physical and chemical properties.

Palladium is attacked mostly by various reagents than any of its PGM member. Most of all, it has the ability to absorb hydrogen up to 900 times of volumes extremely far than any other metals [38, 39]. As the temperature rises from zero to red heat (>950°C), the amount absorbed falls up to 600°C and tends to lower slightly above the mentioned temperature. This situation occurs when the metal is in the colloidal, powdered or even in a compact form. The hardness and other mechanical properties as with other metals, depends on the amount of cold working or annealing to which species of the metal are subjected. Table 2.5 list some of the metal physical properties as it is found in nature and during chemical processes.

Table 2.5 Physical properties of palladium metal [39]

Properties	Values
Atomic radius	1.79 Å
Atomic number	46
Atomic weight	106.4 g/mol
Valence	2, 3 or 4 [38]
Density at 20°C	12.02 g/cm^3
Density of liquid at melting point	10.38 g/cm^3
Specific heat capacity	0.058 J(Kg/K)
Boiling point	3167 °C
Melting point	1555 °C

2.8 Transition metals and their oxidation states

2.8.1 Transition metals

Transition metals are defined as metals or elements that have partially filled *d* orbital shell either in the neutral atom or in a common oxidation state e.g. Cu, Ag and Pd and others [41]. These types of metals are the most important mainly due to the presence of

strong inter-atomic bonding. The presence of the inter-atomic bond on the metals, results in excellent mechanical properties and thus high melting points. Atoms of the elements (Ag and Cu) have one *s* electron in their outer orbital, but tend to differ from Group 1 elements in second last shell with ten *d* electron. Therefore, the transition metal definition expand to include oxidation states of the metals like nickel (Ni) which has incomplete filled *d* orbital as seen on Table 2.6 and the table list the outer electronic configurations of the atoms. Group 1 metals are situated or found at the top of the electrochemical series. These metals are regarded as the most reactive elements in the Periodic Table [37].

Table 2.6 Electronic configurations and oxidation states of selected metals

Elements	**Electronic structure**	**Oxidation states**
Cu	[Ar] $3d^{10}4s^{1}$	1, ***2***, 3 [37, 42]
Ni	[Ar] $3d^{8}4s^{2}$	0, 1, ***2***, 3, 4 [37, 19]
Ag	[Ar] $4d^{10}5s^{1}$	***1***, 2, 3 [19, 42]
Pd	[Kr] $4d^{10}$	0, ***2***, 3, 4 [37, 38]

Bolded: Most common and stable oxidation states of the element.

2.8.2 What is an oxidation state?

Oxidation state can defined as addition of oxygen, loss of hydrogen or one or more electrons [41, 43]. An understanding of an oxidation reaction involves the reduction step to complete it. The transfer of electrons is basically accompanied by transfer of atoms. Details about the selected transition metal oxidation states are discussed below in the following section.

2.8.2.1 Copper oxidation states

The common oxidation states of copper metal are +1 and +2 as indicated in Table 2.6. Even though +3 state of the metal exist, it is very scarce. The +1 state is fairly stable and is produced by the decomposition of Cu^{2+} compounds [42]. Cu^{+} compounds are water insoluble and display diamagnetic properties, except from where they results from anion or charge-transfer bands. During the charge transfer of the ion, the colour in solution becomes colourless. Cu^{2+} compounds are most stable and water soluble compared to Cu^{+} compounds [19]. The potential values given in (Equation 2.1 and 2.2), are the relative stability of Cu^{+} and Cu^{2+} electromotive force (e.m.f) values. The standard redox potential values are given in the following:

$$Cu^{+}_{(aq)} + e^{-} \rightarrow Cu_{(s)} \qquad E^{\circ} = 0.52V \qquad \text{(Equation 2.1)}$$

$$Cu^{2+}_{(aq)} + e^{-} \rightarrow Cu^{+}_{(aq)} \qquad E^{\circ} = 0.153V \qquad \text{(Equation 2.2)}$$

Liptrot [41], Cotton and Wilkinson [19] confirm that, the positive e.m.f for Cu^{+} in an aqueous solution is thermodynamically unstable with respect to Cu^{2+} in solution. Therefore Cu^{+} undergoes self oxidation-reduction reaction. Cu^{+} and Cu^{2+} relative stability depends very strongly on the nature of ions and other ligands present. These cations considerably vary with solvent or the nature of neighbouring atoms in a crystal in an aqueous solution. Only low equilibrium concentration of Cu^{+} ($<10^{-2}$ M) can exist and the only simple compound that are stable to water are highly insoluble compounds such as CuCl or CuCN.

2.8.2.2 Nickel oxidation states

Nickel as Ni^{2+} ion, is more reactive compared to other metals ions e.g. Cu^{+} and Cu^{2+}, but less reactive compared to iron (Fe) and cobalt (Co) ions under acidic conditions [37].

The main oxidation state of nickel as a metal is 2+ and it is ionic. Ni^{2+} state is considered as the most important ion and stable in all five nickel elemental oxidation states and it can form many complexes, and be reduced to Ni^{+} complexes. In Ni^{3+} complexes, oxidation process becomes a bit difficult or impossible.

The Ni^{2+} complexes have an octahedral, tetrahedral or square planar shape, these conditions are determined by number of orbital used [41]. The metal standard redox potential value is given for the reaction in (Equation 2.3).

$$Ni^{2+}_{(aq)} + 2e \rightarrow Ni_{(s)} \qquad E^{\circ} = -0.24V \qquad \textbf{(}\text{Equation 2.3)}$$

The negative e.m.f value indicates that nickel in 2+ states, is thermodynamically stable in an aqueous solution. This ion (Ni^{2+}) is resistant to attack by air or water at ordinary temperature. The metal halides are usually known in the anhydrous state, and all are water soluble, except for the fluoride which is moderately soluble [19].

2.8.2.3 Silver (Ag) oxidation states

Silver in the +1 state forms many simple compounds which are ionic and stable in water as indicated in Table 2.6. But the most stable and important oxidation state is 1+ [19, 41, 42]. $AgNO_3$ is one of the silver 1+ compounds and the most important silver salt, this is due to its wide range of applications. One of its common uses in the chemical laboratory is gravimetric analysis for halides. Another Ag^{+} compound (AgCl), is insoluble in water but soluble in dilute ammonia, sodium thiosulphate aqueous solutions. AgBr can is also be dissolved in ammonia solution, both AgCl and AgBr form ammine complex $[NH_3 \rightarrow Ag \rightarrow NH_3]^{+}$, which are linear in shape. Although Ag^{2+} compounds are known and present in the oxide (AgO) and fluoride (AgF_2), they are unstable but powerful oxidizing agent [41, 43]. Another oxidation state of silver include Ag^{3+} ion, is unstable to water and exist only as insoluble compound or even one of the complexed

species. Equation 2.4 is the intercomparisons of silver ions according to the standard potential [41]. Silver metal ion strongly depends on nature of the anion. Therefore, the standard redox potential reaction given below, indicate the instability of Ag^{2+} against Ag^{+} in an aqueous solutions:

$$Ag^{2+} \xrightarrow{1.98} Ag^{+} \xrightarrow{0.799} Ag \qquad \text{(Equation 2.4)}$$

The positive electromotive force (e.m.f) values for silver ions imply that, Ag^{2+} can be oxidized to Ag^{+} under thermodynamic conditions. But Ag^{+} conversion to Ag^{2+} and Ag, become impossible since that potential value is recorded to be negative and thus leading to disproportionally of the silver ion.

2.8.2.4 Palladium (Pd) oxidation states

Palladium principal oxidation states are 2+ and 4+. But the 2+ state is the most stable compared to 4+ states. Pd and Pt metal compounds resemble each other very closely than any other pair of PGMs [41]. Compounds of the Pd^{2+} and Pt^{2+} usually exist as halides, sulphates, nitrates and oxides compounds [19].

The metal in an anhydrous solid form is generally ionic. PdF_2 is apparently ionic whereas $PdCl_2$ forms linear polymer in the solid state. The stability of the 2+ state increases from $Ni^{2+} \rightarrow Pd^{2+} \rightarrow Pt^{2+}$, and the complexes of Pd^{2+} and is square planar. Cotton and Wilkinson [19] mentioned that Pd^{2+} prefers co-ordination number of 4 while Pd^{4+} prefers an octahedral type of structure and has co-ordination number 6. Some of ion salts that are formed by 2+ states include $PdCl_2$ and PdO, while for 4+ state is $[PdCl_6]^{2-}$. The Pd^{4+} salts can quickly get hydrolysed by water.

Generally, palladium resembles platinum very closely with some of its physical or chemical properties [38]. The tetravalent state of Pd metal is much less stable than the

divalent, but for Pt metal both are equally stable. The reaction on Equation 2.5 [44] indicate the standard electromotive force potential value, and is also given as follows:

$$Pd^{2+}_{(aq)} + 2e^{-} \rightarrow Pd_{(s)} \qquad E^{\circ} = +0.987V \qquad \text{(Equation 2.5)}$$

The positive e.m.f value indicates the stability of Pd^{2+} during reduction to Pd^{0}. Therefore, the Pd^{2+} is certainly more stable ion compare to Pd^{4+}. Only Pt^{4+} is stable especially as complex compound [45].

2.9 Mining wastewater treatment

2.9.1 What is wastewater?

Wastewater is a combination of liquids or waste carried in water from various sources, this include industries such as mining, residential areas and commercial centres [46]. This wastewater that is produced in the mineral processing contains lot of suspended solid particles, heavy metal ions, flotation reagents, organic and other pollutants resulting in environmental pollution. A report from Caribbean Alliances for Sustainable Tourism (CAST) [47] stated that, wastewater can be classified into four categories:

- Domestic-wastewater discharge from residence and commercial, institution.
- Infiltration or inflow of extraneous water that enters the sewer through indirect and direct means, this includes cracks, leaking joint and porous walls.
- Wastewater accumulation from production companies.
- Storm water-runoff resulting from flooding due to rainfall.

Schutte and Pretorius [48] mentioned that some of the activities in petrochemical industry, mining and power generation plants consume about 12.5% of the total amount of water available in South Africa. This high consumption makes water to be the most

widely used commodity during industrial processes, and concurrently creating a huge amount of wastewater.

A report by Mack *et al*. [11] states that wastewater in mining industry, contain high concentration of chlorides of platinum group metals (PGMs) at low pH conditions, which are basically in the form of anionic chloro-complexes. The high demand of precious metals (PGMs) especially palladium and platinum, has resulted in the scale-up of metal extraction and refinery processes worldwide. Although minerals from mining industries contribute economically, metal discharge results in wastewater. Penalties of the untreated wastewater discharge, pose a large financial pressures on industries.

Research in operational cost reduction primarily focuses on the recovery of metals and by-products from the wastewater streams. Treatment of wastewater streams to meet environmental or process standard, is fast becoming another focused area to reduce operational costs [46]. In some instances recovery might be very important since wastewater contains appreciable amounts of valuable metals.

Due to environmental wastewater pollution, treatment of wastewater has become a major priority in the world for the mere fact that it is vital to human life and environment. Various wastewater treatment processes are being employed and they include chemical precipitation, coagulation-flocculation and flotation [49].
A research study [46] reports the use of solar evaporation in holding ponds for the treatment of wastewater from PGMs extraction refinery. This technique is used to reduce the amount of wastewater and to concentrate trace of metals still remaining in the holding ponds. The solar process allows wastewater to rise outside the ponds, and that results in surface evaporation occurring. Therefore, solar energy results in desired reduction of volume and increased metals recovery through concentration of the wastewater.

2.10 Mining wastewater metal recovery

Wastewater is vastly considered to be a severe worldwide pollution crisis. Countries like Australia and China are mostly affected by wastewater originating from mining industry. Wastewater from Australian mine ore processing plants are contaminated with waste sludge, insoluble (finely ground rocks) and soluble (heavy metals, sulphates) substances [50]. In China, mining industries discharge wastewater containing heavy metals, suspended solid particles and other pollutants. Therefore, this wastewater results in environmental pollution [49]. The need for the treatment and recovery of the valuable substances is fast becoming a priority to many countries.

In South Africa, Mine Health and Safety Inspectorate (MHSI) [51] is responsible for the health and safety of persons employed in the mining industry. This Department is identifying the strategies and programmes that could be efficient to minimize wastewater pollution, maximize and broaden the economy linkages regarding metals as minerals. These can naturally arise from the need to extract process and refine the country's mineral resources [6].

The demand and supply symmetry of the precious metals is changing because of the present economical need. Several different methods e.g. Convection methods such as chemical precipitation and cementations, have been put into practice for recovery of heavy metals from wastewater in general. Each method conducted had its individual advantages and disadvantages.

Convection methods are limited on processes such as chemical precipitations and cementations [52]. Chemical precipitation has been proven to be an efficient technology for metals removal and other inorganic substance that can be found in wastewater. According to Amine *et al.* [53] cementation or metal displacement is the most effective technique for the removal of valuable metals and toxic substances that can also be found in industrial waste solutions. Majority of metal removal techniques such

complexation are still employed in wastewater treatment processes. When PGMs are strongly complexed in solution, although high percentage recovery of precious metals are obtained, they result in further chemical contamination on the waste steams which might need a further treatment before any disposal.

Another technique for metal removal in wastewater is called biosorption. This technique has emerged as a low-cost and often low technology option for removal and recovery of base and precious metals from aqueous industrial wastewater [6]. The process uses mechanisms such as electrostatic interaction, ion exchange and metal ion chelation or complexation that are based on physico-chemical interaction between metal ions and the functional groups present in the cell surface.

Göksungur *et al.* [54] reports that the disadvantages of using convectional methods such as ion exchange and chemical precipitation for the recovery of metals in wastewater, leads to an incomplete metals removal and provide high capital costs, high reagent utilization, high energy consumption and concurrently generate a toxic sludge or other waste products that will require disposal.

Ferreira [52] used electrochemical process by employing electrochemical reactor for treatment and recovery of PGMs in an effluent streams. Separation of metals occurred during electrodeposition and further combustion of graphite particles can also be employed for recovery of the metals. Although different methods have been employed for the treatment of wastewater, is still an internationally existing crisis. Research continues globally to find cost effective and highly efficient metal removal methods, which can concurrently reduce toxicity levels in the environment.

2.11 Membrane Technology Existence

2.11.1 History of membrane technology

Membrane technology phenomena can be traced to the philosopher scientists of the early eighteenth century. In the year 1748 Abbé Notel coined the word ‘osmosis’ which described permeation of water through a diaphragm [55]. During the nineteenth century’s, membranes had no industrial or even commercial uses, but were used as laboratory tools for development of physical or chemical theories. In the year 1907, Benchhold devised a technique to prepare nitrocellulose membranes of grade pore sizes, which can be determined using a bubble test [56]. But 20 years later, microfiltration membranes technique were found and expanded to polymer materials notably cellulose acetate (CA). And the first historic membranes application was in testing of drinking water towards end of World War II.

The elements of modern membrane science had been developed but were specifically used only in few laboratories, and small specialised industrial applications. From 1960 until 1980, a significant change in status of the membrane was implemented. The interfacial polymerization, multilayer composite casting and coating, were developed for making high performance types of membranes [55, 56].

Li *et al*. [57] mentioned that around the 1970’s, nanofiltration membranes were developed from reverse osmosis (RO) membranes with the intentions of providing reasonable water flux at relatively low pressures. The high pressure RO membranes resulted in a considerable energy cost. On the other hand these RO membranes provided a very good quality permeate. During 1980s, this low pressure RO membranes became known as nanofiltration (NF) membrane and their first application were reported [55, 56]. By the year 1980, microfiltration, ultrafiltration, reverse osmosis and electrodialysis were all established processes with large plants installed worldwide [55].

2.11.2 Introduction to membrane technology

Membrane technology is a promising and emerging technology that can be used in a wide range of separation processes, this is due to its multidisciplinary character [58]. Today membrane processes are used in wide range of applications and the number of such applications is still growing. Membrane can defined as a selective barrier between two phases, and this means that its performance is determined by two parameters; selectivity and flow through the membrane. Membranes can be thick or thin, homogeneous or heterogeneous and their transport mechanism can be active or passive. The driving force can be gradients in pressure, concentration and temperature differences. In addition to NF membranes, it can either be neutral, synthetic or charged.

Synthetic membrane are usually subdivided into organic (polymeric or liquid), and inorganic (ceramic, metal) membranes. Verissimo *et al.* and Yang *et al.* [59, 60] emphasised that, nowadays applications of membrane technology can be found in various industries such as water and wastewater treatment, pharmaceutical, biochemical, metallurgical, textile, pulp and paper, beverage and foods and so on. The first generation processes from economical point of view are microfiltration (MF), ultrafiltration (UF), nanofiltration (NF), reverse osmosis (RO), electrodialysis (ED), membrane electrolysis (ME), diffusion dialysis (DD) and dialysis. The second generation membrane processes include gas separation (GS), vapour permeation (VP), perforation (PV) and membrane contactors [58, 61].

As every process has its own advantage and disadvantages, membrane advantages are summarised as follows [61]:

- Separation process can be carried out continuously
- Energy consumption can be operated out at low levels
- Separation can be carried out under mild conditions
- Additives are not required

- Up-scaling is easy

Membrane disadvantages are summarized as follows:

- Concentration polarisation or membrane fouling accumulation
- Short lifetimes
- Low selectivity or flux

2.11.3 Nanofiltration (NF) membrane

Nanotechnology is described as the study of matter, typically measuring less than 100 nanometres (nm) on the atomic and molecular scale [62]. Due to numerous and far-reaching nanotechnology applications, they range from electrical engineering and biology to environment engineering. Léandre [62] also reported that nanotechnology is vital for water or wastewater treatment. The thin composite polymer can be formulated into modified membranes that give the remarkable separation qualities or characteristics.

Nanofiltration (NF) membrane shares the properties of RO and UF membranes [57]. It is regarded as loose reverse osmosis. NF membranes are organic polymers. Typically NF polymers membranes are aromatic, polyamides, polysulfone or poly (ethersulfone) or sulfonated polysulfone, polyimide and poly (piperazine amide). They consist of thin film composite (TFC) layer on top of the substrate UF layer.

Tang *et al.* [63] emphasized that, TFC membranes are characterised by an ultra-thin separating selective layer supported on a porous substrate. Figure 2.2 shows the spiral wound NF membrane sketch. The schematic diagram shows the path of the feed (solution to undergo separation) to permeate (solution penetrated through membrane) flow channel, through impermeable flat sheet membrane (FSM). The separation process of NF membrane is based on electrical and dielectrical effects. The NF membrane contains smallest void size (pore size) of about 1 nm [64, 65].

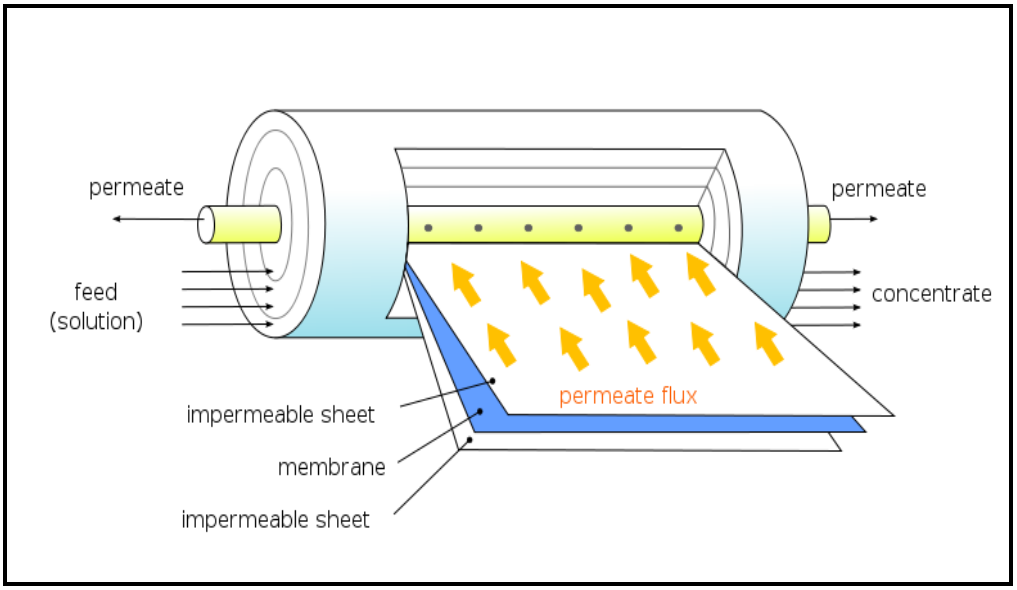

Figure 2.2 Schematic representation of spiral wound NF membrane module

Mulder *et al.* [61] defines the spiral wound membrane element as the plate and frame system, which is centrally wrapped around a central collection pipe. The element is rolled in a sandwich fashion. Membrane layers and permeate–side spacer material are glued along three edges to build a membrane. The movement of the feed flows axially through a cylindrical module, and it is situated parallel along the central pipe. The permeate flows radically towards the central pipe. According to the diagram in Figure 2.2, the membrane is centrally placed between two impermeable membranes. The unwrapped membrane layer is unfolded from the module and is used as flat sheet (FS) membrane.

2.11.4 Applications of NF membranes

The processes for NF membranes have been emerging recently. It has shown very promising properties for water purification of brackish water and surface water. It has

also been used in many aspects as one of the water treatment techniques including drinking water treatment and wastewater effluent reclamations [66]. Table 2.7 Illustrate the properties of NF membranes as adopted from Mulder [58]. NF molecular weight cut off (MWCO) for solutes range of 150 to 1000 Dalton (Da) [57]. Some of the NF membranes applications include wastewater treatment [67], removal of micropollutants (herbicides, pesticides, insecticides) [68], retention of dyes (textile industry) [69] and also in metal industry [70].

Table 2.7 Properties of Nanofiltration (NF) membrane [58]

Nanofiltration compared to other pressure membrane processes				
	Applied Pressure	***Flux range ($\ell.m^{-2}.hr^{-1}.bar^{-1}$)***	***Transport mechanism***	***Application ranges***

Microfiltration	0.1-2 bar	> 50	Sieving	Removal of particles
Ultrafiltration	1-5 bar	10-50	Sieving	Removal of Macromolecules
Nanofiltration	**5-15 bar**	**1.4-12**	**Sieving diffusion charge effects**	**Removal of multivalent ions and relatively (small) organic molecules**
Reverse Osmosis	10-100 bar	0.05-1.4	Diffusion	Removal of ions and (small) organic molecules

2.11.5 NF membrane surface charge

Polymeric NF membranes consist of surface active layers that are charged either negative, neutral or positive [61] and they also contain different functional groups, charge on the membrane surface is dependent on the pH of the solution.

Studies on the rejection of organic substances by NF and ultra-low pressure (RO) membranes have proven that, the retention of solutes depends on solute properties such as size, polarity and charge. On the other hand the retention on the membranes depends on the pore size, charge and hydrophobicity [71, 72]. Therefore, high rejection has been reported on the organic solutes having the same sign (negative charge) as that of membrane surface. This observation was due to the electrostatic interaction between membrane surface and solutes.

Other studies have reported the rejection of inorganic ions such as sodium (Na), magnesium (Mg), and heavy metals [73, 74]. They found an increase in rejection of ions during conditions favouring membrane surface, which was caused by an electrostatic repulsion between the membrane surface charge and the inorganic ions.

Generally, NF membranes are negatively charged at neutral pH and above pH 7.0, and they become positively charged at pH below 7.0 (amphoteric behaviour) [75, 76]. The isoelectric points (*point where membrane encounters a zero or neutral charge*) of some membranes are found at pH between 3.0 and 4.0 [61], while IOP of other NF membranes are found at pH 4.0 and 5.0 respectively [63]. These isoelectric points on the NF membranes depend on the functional groups of the polymer.

The thin film composite (TFC) nanofiltration membranes have charge characteristics that influence the separation capabilities, and these characteristics can be altered by the pH of the solution [77]. Tang *et al.* [63] used charged TFC membranes containing amino functional group on the membrane surface, and mentioned that this amino group can be adjusted relative to ions being investigated. The following reaction in (Equation 2.6) [58], illustrate an amphoteric behaviour of the amino acid, which contain contains both acidic and basic group, depending on the pH of the solution.

$$H_2NCHRCOO^- \leftrightarrow^+ HNCHROO^- \leftrightarrow^+ HNCROOH \qquad \text{(Equation 2.6)}$$

At high pH, the amino acid is negatively charged (*structure a*) and this charge migrates towards the anode when an electric field is applied. But at low pH the amino acids becomes positively charged (*structure c*) and this charge migrates towards the cathode. If the structure (*a)* and (*c)* are found to be exactly in balance, this equation implies that there is no net charge (*structure b*), this is called an isoelectric point (IOP). This implies that the amino acid will definitely not migrate in an electric field. TFC membranes (NF90 and NF200), were employed for the evaluation of NF membrane charge [76]. Zeta potential was utilized to measure electrophoteric mobility (EM) on NaCl solute and streaming potential (SP) on KCl in an aqueous solution as shown in Figure 2.3. Streaming potential measurements on NF200 indicate that an effective surface charge was less negative than during electrophoretic mobility measurements. NF200 isoelectric

point was observed at pH 4.0. It is reported that at pH 4.00, both NF membranes have a zero charge.

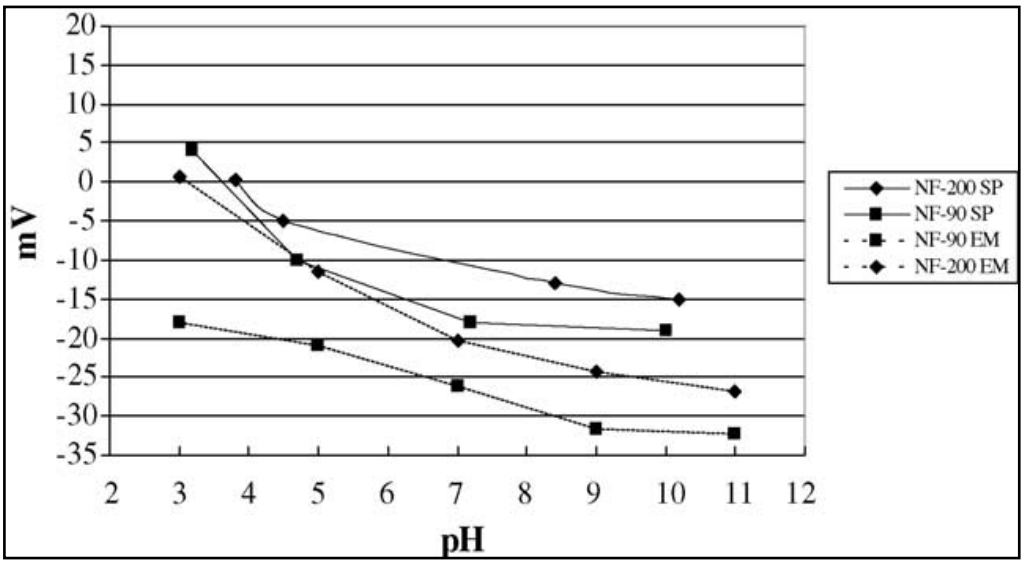

Figure 2.3 Zeta potential measurements for NF90 and NF200 membranes (Adapted from Bellona and Drewes) [76]

2.11.6 Effect of pH on polymeric (NF) membrane surface

The role of pH is significant in determining the charge stability on the membrane surface. Since NF polymeric membranes have a negative, neutral or positive charge surface, an electrostatic repulsion between the charge on the membrane surface and solute significantly influence the separation of ions as mentioned above [77, 78].

During the research study by Ahmad *et al.* [68] pesticides (Antrazine and dimethoate) were exposed to the following TFC membranes namely; NF90, NF270, NF200 and DK. These experiments were performed at pH 4.0 and pH 9.0. NF90 gave high rejection

regardless of solution's pH changes. The trend of pesticides rejections obtained for NF200, NF270 and DK increased with an increase in pH from 4.0 to 9.0, but decrease during permeate flux performances.

Desal-5 NF membrane was employed for the recovery of Na ions in $NaNO_3$ and NaCl which can be found in town water [77]. The water had pH values of 4.25, 4.50 and 4.55 respectively. The pH value above isoelectric point for Desal-5 membrane is 4.0, which was very close pH value found in town water. They observed that Na^+ ion rejection decreased, due to the reduction of the electrostatic repulsion. While its anion (NO_3^-), increased by shielding most of positively charged groups on the membrane at high salt concentration. The reason behind an increase and decrease in rejection of these ions was an electrostatic repulsion, which occurred between the proton and positively charged membrane at pH < 1.6. On the hand the anion (Cl^-) encountered a decrease in retention with regards to opposite of the charge with the membrane surface (counter ion). This proved that the charge of NF polyamide membranes, does influences the separation capabilities by altering the pH of the solution.

2.11.7 Metals recovery studies on NF membranes

Metal recovery process such as solvent extraction, is a well known hydrometallurgical process. This process can achieve a highly selective separation and concentration of metals from dilute aqueous solutions. Solvent extraction can achieve an effective enrichment of metals, therefore large amounts of extractants and solvents are needed to complete the separation process [79]. Although the technique is effective, the following disadvantages are encountered during the process of PGMs recovery;

- extraction rates of the metals are generally lower
- large amounts of extractant and solvent are needed to make up separation process.

Therefore, metal recovery still requires a method that could minimize the operational cost.

A lot of work has been done in the application of membrane technology as an alternative technique for metal recovery. Nanofiltration membranes, having the ability to recover metals such as PGMs, heavy metals and charged solutes were tested and applied by several researchers.

Feini *at al.* [80] used self prepared cellulose acetate (CA) membranes for the recovery of Na^{+}, Mg^{2+} and Ca^{2+} cations. Na^{+} was recovered fairly with almost 80% as compared to Ca^{2+} and Mg^{2+} which gave >80% of recovery. The poor recovery of Na^{+} resulted from low molecular weight cut-off (MWCO) and the charge of the cation. This recovery behaviour of the CA membranes was influenced by high pressure operation.

Ahmad and Ooi [21] also used CA membranes for the recovery of Cu^{2+} in $CuSO_4$ compound. Highest recovery of 92% of the metal was achieved. The MWCO and charge of $CuSO_4$ had a huge influence on the recovery by the membranes. They conclude that, although pH has a less influence on Cu^{2+} recovery, the CA membranes can be operated at acidic conditions.

In another study [64] commercial polyamide NF membranes (NF90 and NF-), were employed for the recovery for Ni^{2+}. The entire membrane processes were operated at constant pressure of 5 bar. The retention of Ni^{2+} as $NiNO_3$ salts was found to be 95.3% and 99.82% at pH 2.4, and as for pH 3.2 it was found to be 94% and 99.85% for NF90 and NF- membranes respectively. The highest retention favoured NF90 membrane is due to its small pore size as compared to NF-. The above statement clearly shows that, NF membranes are not only pH or concentration depended but also pressure dependent.

2.12 NF membranes fouling

Charge characteristics and fouling tendency, play a vital role in the membrane performance [81]. Fouling is described as the reduction in permeate flux that is irretrievable. This irretrievable process reduces the efficiency of the membrane processes by decreasing the flux and hence influencing the desired retention values [82]. The fouling concept on the membranes is regarded as a major constraint in the areas of membrane applications such industrial wastewater treatment [83], groundwater and river treatment [84] and water purification institutions.

Fouling results from an increase of solute concentration at the membrane surface. Such concentration build up generates a diffusive flow back to the bulk of the feed, only for a given duration of time when steady state condition is achieved. This phenomenon is called concentration polarization. It is a regular occurrence during dead-end operation of the membranes [32, 82].

During membrane operation, suspended solid tends to settle inside pores or on membrane surface causing a decrease in flux. This decrease in flux results when foulants (particulates or material that block the membrane pores for permeation) increases on the surface layer. Figure 2.4, is the graphical illustration of membrane fouling caused by high concentrations of foulants. Membrane pore fouling on (A) is caused by adsorption of particles, while on (B) fouling occurs on the surface of the membrane.

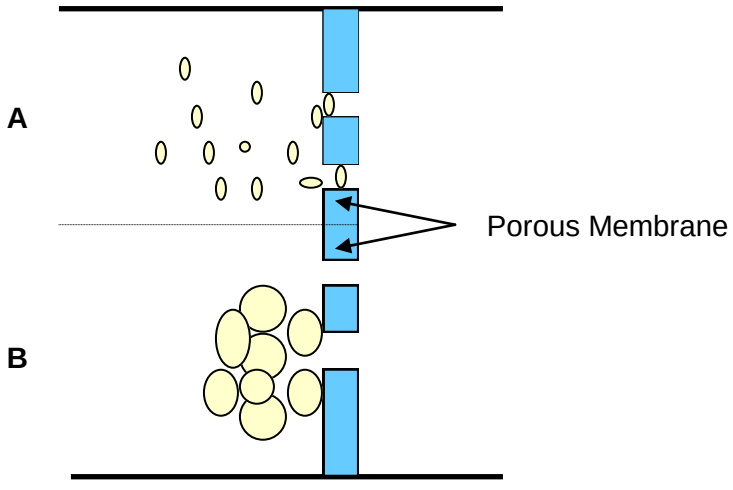

Figure 2.4 Fouling mechanism: (A) Membrane pore fouling; (B) Membrane surface fouling (adapted from Stolp) [82]

Membrane fouling is also referred to as reversible and irreversible decrease in permeate fluxubility. The deterioration in flux performance is due to concentration polarization or fouling phenomena. Schäfer *et al*. [85] clarify that foulants (organics, solutes etc.) at surface of the membrane exert an influence on passage of solutes through the membrane.

The major cause will be cake porosity and blocked membranes. One of the critical effects of fouling has to do with pore size. Foulants which are larger than the membrane pore size will cause surface fouling due to reduction of pore sizes. Therefore, fouling influence membrane rejection behaviour [85]. Fouling does not only reduces the permeate flux intensity, it also causes an increase in capital cost and reduction in applicability of membrane processes.

2.13 History of South African membrane technology application

The earliest membrane research in South Africa started in the early 1953's on electrodialysis systems (ED). This operation was conducted at Council of Scientific and Industrial Research (CSIR). The development of polymeric membranes started in 1973 at the Institute for Polymeric Studies (IPS) at Stellenbosch University (currently known as Institute for Polymer Science) [86]. Some of the membrane developments at Potchefstroom University include: alumina or chitosan composite membranes. These membranes were employed for the removal of metals such as Cu^{2+}, Pb^{2+} and Zn^{2+} ions from polluted water [87].

2.14 Membrane Technology viability in South Africa

The Department of Water Affairs and Forestry (DWAF) [88] is fuelling the demand for the technology solution, that can resolve a huge challenge faced by water users in South Africa. A report from this department (DWAF) further stated that, the demand of water and wastewater treatment has been considered and given attention. The advances in separation technology especially membrane applications, have a huge significance in wastewater treatment technology worldwide. Water Research Commission [89] reported that, apart from fouling which serve as a disadvantage during membrane operations, membranes are now being acknowledged as the viable option in the treatment of water and wastewater effluents in South Africa.

According to membrane designers (Weir-Envig Membrane Company) based in South Africa [90], clients such as Eskom, Impala Platinum and Clover use the membrane units in the desalination plants. Other clients such as Sasol technology (Sastech), African Products and Saldahna Steel employ membrane elements for industrial effluent treatment. Therefore, the above mentioned statements show that membrane application is growing in SA.

Literature on nanofiltration membranes discussed in Chapter 2, indicates that NF membranes can be used for the recovery of metals from wastewater at an acidic medium. The next Chapter 3 will describe the experimental methods applied to accomplish the rejections of metal as synthetic mining wastewater.

References

1. E. S. Manchan. Environmental Chemistry, 8th Edition, CRC Press, London (2005).

2. www.dme.gov.za/pdfs/**mine**rals/D6%20**2007**.pdf: date accessed: 02/03/2010.

3. www.mbendi.com/indy/ming/mingaf.htm: date accessed: 01/04/2010.

4. www.bmconsultancy.net/preciousmetals.html: date accessed: 05/04/2010.

5. S. Ndlovu. Biohydrometallurgy for sustainable development in the African minerals industry, *Hydrometallurgy* **91** (2008) p20-27.

6. M. Lydall. Backward linkage development in the South African PGM industry: A case study, *Resources Policy* **34** (2009) p112-120

7. Z. Xiao, A. R. Laplante. Characterizing and recovering the platinum group minerals-a review, *Minerals Engineering* **17** (2004) p961-979.

8. F. L. Bernadis, R.A. Grant, D. C. Sherrington. A review of methods for separation of the platinum group metals through their chloro-complexes, *Reactive and Functional Polymer* **65** (2005) p205-217.

9. P. M. Cole, K. C. Sole, A. M. Feather. Solvent extraction development in southern Africa, *Tsinghua Science and Technology* **11** (2006) p153-159.

10. www.atlapedia.com/online/countries/**russia**.htm: date accessed: 03/04/2010.

11. C. Mack, B. Welhelmi, J. R. Duncan, J. E. Burges. Biosorption of precious metals, *Biotechnology Advances* **25** (2007) p264-271.

12. C. R. M. Rao, G. S. Reddi. Platinum group metals (PGM): Occurrence, use and recent trends in their determination, *Trends In Analytical Chemistry* **19** (2000) 565-586.

13. W. D. Maier. Platinum-group elements (PGE) deposits and occurrences: Mineralization styles, genetic concepts, and exploration criteria, *Journal of African Earth Sciences* **41** (2005) p165-191.

14. R. T. Jones. An overview of Southern African PGM smelting, Mintek, South Africa. Retrieved from website: www.pyro.co.za/Mintek/Files/2005Jones**PGMsmelting**.pdf: date accessed: 03/02/2010

15. J. Nell. Melting of platinum group metal concentrates in South Africa, *The Journal of South African Institute of Mining and Metallurgy* (2004) p423-428. Retrieved from website: http://www.saimm.co.za/Journal/v104n07p423.pdf: 05/03/2010

16. S-R. Barnes, W. D. Maier, L. D. Ashwal. Platinum-group element distribution in the Main Zone and Upper Zone of the Bushveld Complex, South Africa, *Chemical Geology* **208** (2004) p293-317.

17. J. J. Bezuidenhout. Computational Fluid Dynamic Modelling of an Electric Smelting Furnace in the Platinum Recovery Process, M.Sc thesis, Stellenbosch University, Cape Town (2008).

18. I. Giannopoulou, D. Panias. Copper recovery and nickel from acidic polymetallic aqueous solutions, *Minerals Engineering* **20** (2007) p753-760.

19. F. A. Cotton, G. Wilkinson. Advanced Inorganic Chemistry, 5th Edition, John Wiley and Sons, USA (1988).

20. www.helium.com/items/920502-symptoms-of-copper-allergies: date accessed: 05/03/2010.

21. A. L. Ahmad, B. S. Ooi. A study on acid reclamation and copper recovery using low pressure nanofiltration membrane, *Chemical Engineering Journal* **156** (2010) p257-263.

22. T. A. Demir, B. Isikli, S. M. Urer, A. Berber, T. Akar, M. Canbek, C. Kalyoncu. Nickel exposure and its effects, *Biometals* **18** (2005) p7-13.

23. R. R. Moskalyk, A. M. Alfantazi. Nickel laterite processing and electrowinning practice*, Mineral Engineering* **15** (2002) p593-605.

24 Nickel and nickel compounds: This site can be retrieved from the website http*:* www.epa.ohio.gov/portals/41/p2/mercury_pbt/fact96.pdf: date accessed: 03/03/2010.

25. W. Betteridge. Nickel and its alloy, Ellishorwood limited, England (1984).

26. A. Butts, C. D. Coxe. Silver: Economics, Metallurgy and Use, Robert E, Krieger Publishing Company, New York (1967).

27. P. D. Howe, S. Dobson. Silver and Silver Compounds: Environmental Aspects, World Health Organisation, Geneva (2002).

28. K. L. Gering, J.F. Scamehorn. Use of electrodialysis to remove heavy metals from water, *Separation Science and Technology* **23** (1988) p2231-2267.

29 World Health Organization (WHO), International Programme on Chemical Safety (IPCS) Environmental Health Criteria. Palladium, Geneva (2002).

30 J. Kielhorn, C. Melber, D. Keller, I. Mangelsdorf. Palladium–a review of exposure and effects of to human health, *Introduction to Journal of Hygiene Environmental Health* **205** (2002) p417-462.

31. E. Birinci, M. Gülfen, A. O. Aydin. Separation and recovery of palladium (II) from base metal ions by melamine-formaldehyde-thiourea (MFT) chelating resin, *Hydrometallurgy* **95** (2009) p15-21.

32. N. A. Carrington, D. L. Rodman, Z. L. Xue. Palladium and the electrochemical quartz crystal microbalance: A new method for the in situ analysis of the precious metal in aqueous solutions, *Analytica Chimica Acta* **572** (2006) p303-308.

33. T. A. Nijhuis, G. Van Koten, J. A. Moulijn. Optimized palladium catalyst systems for selective liquid-phase hydrogenation of functionalised alkynes, *Application of Catalyst* **238** (2003) p259-271.

34. Q. Chen. Towards cleaner production of hydrogen peroxide in China, *Journal of Cleaner Production* **14** (2006) p708–712.

35. T. G. Kang, J. H. Kim, S. G. Kang, G. Seo. Promotion of methane combustion activity of Pd catalyst by titania loading, *Catalyst Today* **59** (2000) p87–93.

36. E. G. West. Copper and its alloy, Ellis Horwood Limited, Chichester (1982).

37. J. D. Lee. Concise Inorganic Chemistry, 2nd Edition, D. Van Nostrand Company Ltd, London (1965).

38. N. V. Sidgwick. The Chemical Elements and their Compounds, Clarendon Press, Oxford (1950).

39. J. C. Bailar, H. J. Emeléus, R. Nyholm, A. F. Trotman-Dickenson. Comprehensive Inorganic Chemistry, P. Van Nostrand Ltd Company, London (1973).

40. www.unctad.org/infocomm/anglais/**palladium/characteristics**.htm: date accessed: 05/03/2010.

41. G. F. Liptrot. Modern Inorganic Chemistry, 4th Edition, Collins Educational, Eton College, London (1983).

42. M. C. Sneed, J. L. Maynard, R. C. Brasted. Comprehensive Inorganic Chemistry, B. Van Nostrand Ltd Company, Princeton (1954).

43. D. F. Shriver, P. W. Atkins. Inorganic Chemistry, 3rd Edition, Oxford University Press, New York (1999).

44. J. R. Davis. Handbook of materials for medical devices-Google Books Result: date accessed: 12/04/2010.

45. S. A. Cotton, F. A. Hart. The heavy transition elements, John Wiley and Sons Publishers, New York (1975).

46. R. S. Dobson, J. E. Burgers. Biological treatment of precious metal refinery wastewater: A review, *Mineral Engineering* **20** (2007) p519-532.

47. Caribbean Alliance for Sustainable Tourism (CAST): Can be retrieved on the website http: www.caribbean-innkeeper.com (under wastewater conservation toolkit): date accessed: 01/02/2010.

48. C. F. Schutte, W. A. Pretorius, Water Demand and population growth. *Water SA* **23**(2), (1997) 127-133. Cited in: B. Thompson, comment on "Water demand and population growth", *Water SA* **24** (2), (1998) p265-268.

49. C. Jian-ming, L. Ruin-qing, S. Wei, Q. Zhou. Effects of mineral processing wastewater on flotation of sulphide minerals, *Transactions of Non-ferrous Metals Society of China* **19** (2009) p454-457.

50. Editorial. Waste water pollution control in the Australian mining industry, *Journal of Cleaner Production* **14** (2006) p1118-1120.

51. Z-X. Li, J-J. Li, C-P, Li, S-Y. Liu. Overview of the South African mine health and safety standardization and regulation systems, *Journal of Coal Science and Engineering* 14 (2008) p329-333.

52. B. K. Ferreira. Electrochemical Reactors for PGM Recovery, M.Sc thesis, University of Witwatersrand, South Africa (2004).

53. N. K. Amin, E-S. Z. El-Ashtoukhy, O. Abdelwahab. Rate of cadmium ion removal from dilute solutions by cementation on zinc using fixed bed reactor, *Hydrometallurgy* **89** (2007) p224-232.

54. Y. Gösungur Y, Güvens U. Biosorption of cadmium and lead by ethanol treated waste baker's yeast biomass, *Bioresouces Technology* **96** (2005) p103-109.

55. R. W. Baker. Membrane Technology and applications, 2nd Edition, John Wiley and Sons Ltd, Chichester, London (2004).

56. J. Glater, The early history of reverse osmosis membrane development, *Desalination* **117** (1998) p279-309.

57. N. N. Li, A. G. Fane, W. S. Winston Ho, T. Matsura. Advanced Membrane Technology and its Applications, John Wiley and Sons Incorporation, New Jersey (2008).

58. M. Mulder. Basic Principle of Membrane Technology, 2nd Edition, Kluwer Academic Publishers, The Netherlands (1996).

59. S. Verissimo, K. V. Peinemann, J. Bordado. New composite hollow fiber membrane for nanofiltration, *Desalination* **184** (1-3) (2005).

60. F. J. Yang, S. H. Zhang, D. L. Yang, X. G. Jian. Preparation and characterisation of polypiperazine amide/PPRSK hollow fiber composite nanofiltration membrane, *Journal of Membrane Science* **301** (2007) p85-92.

61. M. Mulder, J. Thelon, W. Maaskant. European Membrane Guide, Alinea Publisher, Netherlands (1997).

62. V. Léandre. Characterisation of thin film polyamide nanofiltration membranes, Visit site, http://www.nnin.org/doc/2008NNINreuLeandre.pdf: date accessed: 03/03/2010.

63. B. Tang, Z. Huo, P. Wu. Study on novel polyester composite nanofiltration membrane by interfacial polymerisation of triehanolamine (TEOA) and trimesoyl chloride (TMC). I. Preparation, characterisation and nanofiltration properties test of membrane, *Journal of Membrane Science* **320** (2008) p198-205.

64. E. Chilyumova, J. Thoming. Nanofiltration of bivalent cations-model parameter determination and process simulation, *Desalination* **224** (2008) p12-17.

65. K. Boussu, Y. Zhang, J. Cocquyt, P. Van der Meeren, A. Volodin, C. Van Haesendonck, J. A. Martens, B. Van der Bruggen. Characterization of polymeric nanofiltration membranes for systematic analysis of membrane performance, *Journal of Membrane Science* **278** (2006) p418-427.

66. K. Listiarini, W. Chu, D. D. Sun, J. O, Leckie. Fouling mechanism and resistance of systems containing sodium alginate, calcium, alum and their combination in dead–end fouling of nanofiltration membranes, *Journal of Membrane Science* **344** (2009) p244-251.

67. J. M. Gozálvez-Zafrilla, D. Sanz-Escribano, J. Lora-García, M. C. León Hidalgo. Nanofiltration of secondary effluent for wastewater reuse in the textile industry, *Desalination* **222** (2008) p272-279.

68. A. L. Ahmad, L. S. Tan, A. Shulor. The role of pH in nanofiltration of antrazine and dimethoate from aqueous solution, *Journal of Hazardous Material* **154** (2008) p633-638.

69. Z. Ji, Y. He, G. Zhang. Treatment of wastewater during the production of reactive dyestuff using a spiral nanofiltration membrane system, *Desalination* **201** (2006) p255-266.

70. N. Hilal, G. Busca, N. Hankins, A. Wahab Mohammad, The use of nanofiltration membranes in the treatment of metal-working fluids, *Desalination* **167** (2004) p227-238.

71. B. Van der Bruggen, J. Schaep, D. Wilms, C. Vandercasteele. Influence of molecular size, polarity and charge on the retention of organic molecules by nanofiltration, *Journal of Membrane Science* **156** (2001) p29-41.

72. Y. Kiso, Y. Sigiura, T. Kitao, K. Nitsimura. Effects of hydrophobicity and molecular size on the rejection of aromatic pesticides with nanofiltration membrane, *Journal of Membrane Science* **192** (2001) p1-10.

73. J. Tanninen, M. Nystrom. Separation of ions in an acidic conditions using NF, *Desalination* **147** (2002) p295-299.

74. J. Yoon, G. Amy, Y. Yoon, P. Brandhuber, J. Pellegrino. Rejection of target ion anions, hexavalent chromium (CrO_4^{2-}) perchlorate (ClO_4^-) and arsenate ($H_2AsO_4^-$ /$HAsO_4^{2-}$), by negatively charged membranes, in: Proceedings of the American Water Works, Association Membrane Technology Conference, Atlanta, GA (2003).

75. S. Bandini, J. Drei, D. Vezzani. The role of pH and concentration on the ion rejection in polyamide nanofiltration membranes, *Journal of Membrane Science* **264** (2005) p65-74.

76. C. Bellona, J. E. Drewes. The role of membrane surface charge and solute physico-chemical properties in the rejection of organic acids by NF membranes, *Journal of Membrane Science* **249** (2005) p227-234.

77. A. L. Ahmad, S. W. Puasa, M. M. D. Zulkali. Micellar-enhanced ultrafiltration for removal of reactive dyes from an aqueous solutions, *Desalination* **191** (2006) p153-161.

78. J-J. Qin, M-H. Ooi, H. Lee. B. Coniglio. Effects of feed pH on permeate pH and ion rejection under acidic conditions in NF process, *Journal of Membrane Science* **232** (2004) p153-159.

79. T. Kakoi, N. Horinouchi, M. Goto, F. Nakashio. Selective recovery of palladium from a simulated industrial wastewater by liquid surfactants membrane process, *Journal of Membrane Science* **118** (1996) p63-71.

80. L. Feini, Z. Guoliang, M. Qin, Z. Hongzi. Performance of nanofiltration and reverse osmosis membrane in metal effluent treatment, *Journal of Chemical Engineering* **16** (2008) p441-445.

81. H. Matsumoto, Y-C. Chen, R. Yamamoto, Y. Konosu, M. Minagawa, A. Tanioka. Membrane potentials across nanofiltration membranes: effect of nanoscaled cavity structure, *Journal of Molecular Structure* **739** (2005) p99-104.

82. W. Stolp. Nickel recovery from spent electrolyte by nanofiltration, M.Sc thesis, North West University, Potchefstroom (2007).

83. N. Her, G. Amy, A. Plutto-Pecheux, Y. Yoon. Identification of membrane foulants, *Water Research Organization*, France (2003).

84. L. J. Moitsheki, Nanofiltration: Fouling and chemical cleaning. M.Sc thesis, Potchefstroom University, South Africa (2003).

85. A. I. Schäfer, A. G. Fane, T. D. Waite. Fouling effects on rejection in the membrane filtration of natural waters, *Desalination* **131** (2000) p215-224.

86. http://www.scienceinafrica.co.za/2002/february/membrane.htm: date accessed: 03/03/2010.

87. J. J. Smit, L. R. Koekemoer. The extraction of nickel with the use of supported liquid membrane capsules, *Water SA* **22** (1996) p249-259.

88. South African Water and Wastewater Treatment Equipment Markets, Can be viewed on http://www.researchandmarkets.com/reports/362402/. Date accessed: 05/04/2010.

89. G. Offringa, Membrane Development in South Africa, Water Research Commission, South Africa (2002).

90. http://www.weirenvig.co.za/projects.htm: date accessed: 05/08/2009.

CHAPTER 3

EXPERIMENTAL METHODS

Table of Contents

Introduction

In this Chapter, experimental methods are described to investigate NF membranes. Different materials and chemicals used including the suppliers will be listed. Dead-end unit (bench scale) set up employed for membranes characterization and rejection of salts, will be discussed. Experimental procedures conducted during membranes testing will be described. Instrumentation used to quantify ions (cations and anions) including scanning electron microscopy (SEM) for membranes surface morphologies, will also be discussed.

3.1 Materials and methods

3.1.1 NF Membranes

Three flat sheets membranes (NF90, NF270, and NF-) used in the study were obtained from Dow/Filmtec (South Africa). They were all stored wet at room temperature before being used. Details and operational conditions of the NF membranes used from the supplier's datasheet are listed in Table 3.1.

Table 3.1 Properties of different (NF) membranes and their suppliers

Membrane	***NF90***	***NF270***	***NF-***
Manufactures	Dow/Filmtec	Dow/Filmtec	Dow/Filmtec
Material	Polyamide	Polyamide	Polypiperazine amide
Membrane type	FS	FS	FS
Max. Operating temp. (°C)	45	45	45
Surface charge @ pH 7	Negative [1, 2]	Negative [1, 2]	Negative [1, 3]
pH range	2-11	2-11	3-10
MWCO (Da)	90	150	150

MWCO = Molecular Weight Cut-Off, **FS** = Flat Sheet, Da = Dalton

3.1.2 Chemicals

Various commercial chemical salts were used in the study. All chemicals employed are an AR grade and were directly used without undergoing any purification. Chemicals used and their suppliers are listed in Table 3.2.

Table 3.2 Specifications of commercial chemicals used.

Inorganic	***Supplier***	***Purity (%)***	***MW (g.mol^{-1})***
$PdCl_2$	Sigma Aldrich	99.99	177.32
$(NH_4)_2PdCl_6$	Sigma Aldrich	99.99	355.20
$NiCl_2{\cdot}6H_2O$	LabChem	99.99	237.65
CuCl	LabChem	99.99	99.00
$CuCl_2{\cdot}\,2H_2O$	SMM Instrument	99.98	170.47
AgCl	Merck	99.90	143.32
NaCl	SaarChem	99.50	58.40
$MgCl_2$	Merck	99.50	95.21
HCl	Merck	37	36.46

$AgCl_{(s)}$ was stored in a dark black container before and after use. This was to avoid decomposition of silver Ag^+ into Ag^0 during contact with UV-visible light. Deionised water with a conductivity of < 2µS.cm^{-1}, was used for the experiments.

3.2 Experimental set up

3.2.1 Dead end unit

Dead end (bench scale) unit with loading capacity of ~ 1,2 ℓ was used. The unit has a top opening to allow solution (feed inlet) through as illustrated on Scheme 3.1. It could be operated at maximum pressure of up to 20 bar. A magnetic stirrer fitted inside the module is used to homogenize the samples. The stainless steel unit has a circular flat sheet cell with two halves fastened together to tighten the bolts, and a porous support to

allow permeation. Nitrogen gas (N_2) was preferably used as the driving force throughout the whole experiment. All the experiments were operated at room temperature.

A scissor/blade was used to cut the membranes into required size area. The FS membranes have an active area of 0.00636 m^2. The FS membranes were kept wet after being immersed in deionised water for 24 hrs before use (for wetting the membrane pores), and were introduced into the unit.

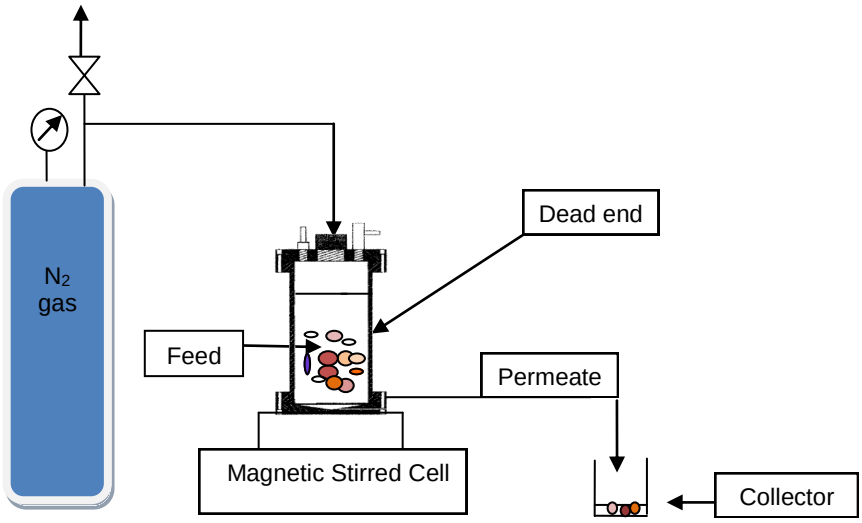

Legend:

: Pressure regulator : Valve

Scheme 3.1 Schematic diagram of high pressure set up.

3.3 Instrumentation

3.3.1 Scanning Electron Microscopy *(SEM)*

A Zeiss ULTRA 55 FEGSEM was used to characterise the properties of NF membranes layers. A clear image of an overall membranes structure as a top surface, cross-section and bottom surface was viewed. The instrument uses a field emission tungsten hairpin filament with a ZrO reserve as an electron source. Elemental analyses for SEM were also performed. This was done by using a Bruker XFlash SDD detector that is controlled by Bruker ESPIRIT software. Micrographs for the pore sizes, the pore size distribution and surface porosity can also be observed. SEM instrument's analyses were outsourced from Sasol Technology (Sastech) division based in Sasolburg.

3.3.2 Ion Chromatography (*IC*)

Dionex ICS 1000 ion chromatographic instrument was used to quantify synthetic charged ions (Na^{+}, Mg^{2+} and Cl^{-}) in samples solutions. The instrument is coupled with an automated-sampler (AS40) which can accommodate volume of 10 ml per sample vials, conductivity detector (ED142 Conductivity Cell), column for anion (AS 22) and for cations (CS 12A), both Ionpack type), suppressor type (*CAES*) for cations and (*ASRS-4mm*) for anion.

The eluents used were 0.4 M methanesulfonic acid/ultrapure water mixture for cations, and 4.5 mM sodium carbonate/ultrapure water mixture for anion. Operating pressure for cations and anion was ≈ 1300psi and ≈ 1100psi respectively. Pump flow rate was kept constant at (1.20 and 1.00 $ml \cdot min^{-1}$) for anions and cations during the course of instrumental analyses. The parameters were controlled using Chromeleon 6.80 software.

3.3.3 Atomic Absorption Spectroscopy (*AAS)*

Shimadzu AA 7000 instrumentation coupled with auto-sampler (ASC-7000) was employed for quantifying inorganic metals (Pd, Ni, Cu and Ag). The instrument was operated using WizAArd 5.0 software. The instrument was calibrated using a

commercial standard solution with a concentration of 1000 ppm (99.99% purity). The operating conditions for the unit in analysing metals are shown in Table 3.3.

Table 3.3 Transition element's analytical conditions for analysis on AAS.

Element	***Pd***	***Ni***	***Cu***	***Ag***
Wavelength (nm)	247.6	232.0	324.8	328.1
Lamp current (mA)	10	12	8	10
Support	Air	Air	Air	Air
Slit width	0.7	0.2	0.7	0.7
Fuel	Acetylene	Acetylene	Acetylene	Acetylene

3.3.4 Fourier Transform Infrared (*FT-IR/FT*) Spectrophotometer

Perkin-Elmer Spectrum 400 Model FT-IR/FT Spectrophotometer was used to identify the functional groups present per membrane as part of membrane characterization. Dry specimen of the membrane samples were placed on crystal size and mounted in a near infrared (NIR) cell. The spectra were collected at spectral resolution of 4.0 cm^{-1} and 148 scans were accumulated. The measurement ranges for wavenumber was (4000-650 cm^{-1}). The spectra were baseline corrected with the use of Spectrum software.

3.3.5 pH meter

Crimson 31+ pH meter was used to monitor pH values of sample solutions. Three pH buffer solutions (*4.00, 7.00* and *10.00*) were employed to calibrate the instrument for the intended purposes. This apparatus uses platinum electrode probe ion sensor.

3.4 SECTION A: Membrane Characterization

3.4.1 Surface morphology

In a typical analysis, a piece of virgin or used dry flat sheet NF membrane of about 2 cm length, was cut and placed on an aluminium stub (sample holder). This stub was covered with a double-sided carbon tape. A conducting layer (gold-palladium) is applied as coating material to the NF flat sheet membrane samples. This was done to avoid membrane surface layer being burned or damaged due to high voltage applied. The top surface cross-section and bottom surface of the membranes were analysed to achieve surface micrographs or images including elemental composition of the membranes using SEM/EDAX. The membranes images magnifications during SEM analysis are listed in Table 3.4.

Table 3.4 Magnifications of three distinct NF membranes during SEM analysis

Membranes	***Magnification***
NF90	X200
NF270	X1000
NF-	X300

3.4.2 Clean water flux

The membranes were characterised in terms of pure water permeability and rejection of solutes. The law describe by Darcy [4] for water flux through a membrane is shown on (Equation 3.1):

$$J_W = A_W \cdot (\Delta P - \sigma \Delta \pi) \qquad \text{(Equation 3.1)}$$

where A_W is the water permeability ($\ell.m^{-2}.h^{-1}.bar^{-1}$), which can be determined experimentally from the plot of J_W versus ΔP (shown in (Equation 3.2), ΔP is the trans-membrane pressure (bar) and $\Delta \pi$ is the osmotic pressure difference. This implies that if

the feed and the retentate contain pure water, i.e. the osmotic pressure difference across the membrane become zero, therefore the (Equation 3.1), will be reduced to:

$$J_W = A_W \cdot \Delta P \qquad \text{(Equation 3.2)}$$

An alternative approach for expressing water flux through membrane is by using Hagen-Pouseuille [5] (Equation 3.3):

$$J_W = \frac{\varepsilon \cdot r^2}{8 \cdot \eta \cdot \tau} \cdot \frac{\Delta P}{\Delta x} \qquad \text{(Equation 3.3)}$$

where Δx, is the thickness of the membrane (m) and η is the viscosity of water (Pa.S). If both Darcy and Hagen–Poisseuille (Equation 3.2 and 3.3) are combined, quantification of water permeability becomes (Equation 3.4):

$$A_w = \frac{\varepsilon}{\tau} \cdot \frac{r^2}{8 \cdot \eta \cdot \Delta x} \qquad \text{(Equation 3.4)}$$

where ε indicate the porosity, which can approximately reveal how many pores can be found in a medium, and τ is the membrane tortuosity. In (Equation 3.5), for the cylindrical pores perpendicular to the membrane surface, τ = 1[5]. Therefore, when it is approximated that:

$$\varepsilon \approx \frac{1}{\tau} \qquad \text{(Equation 3.5)}$$

When combining (Equation 3.4 and 3.5) the following (Equation 3.6) is obtained:

$$\varepsilon \cdot r^2 = 8 \cdot \eta \cdot \Delta x \cdot A_W \qquad \text{(Equation 3.6)}$$

These experiments were performed at trans-pressure of 5, 10, 15 and 20 bar. But, before measuring permeate, the first 10 ml of permeate was discarded to remove any preservatives in the membrane. The flow as volume flux was measured using a

measuring cylinder. Performances of the membranes were evaluated using dead end module.

3.4.3 Fluxes of charged solutes

Synthetic sample solutions of charged solutes (NaCl and $MgCl_2$) were prepared according to the following concentration ranges; 20, 50 and 100 ppm. The solution mixtures were prepared from 100 ppm stock solution. The pH of the solutions was adjusted to pH values of 2.0, 3.0, 5.0 and 7.0. Flux measurements using single-salt experiments of NaCl, were performed at pressure of 5, 10, 15 and 20 bar at pH value of 2.0. The solution mixtures with varying concentrations were exposed to all membrane tested. This was to evaluate ion movement and charge on NF membranes. NF90 was used to monitor the effects of pH for NaCl and $MgCl_2$ during flux measurements.

3.4.4 Charged solute rejection

Charged solute rejection experiments on the single-salts (NaCl and $MgCl_2$) and binary-salts (NaCl/$MgCl_2$) mixture were performed at 5, 10, 15 and 20 bar. Ratio of the ions was kept 1:1 in all the experiments. Permeate of the solutions was collected through varying 10 min intervals. Retention of cations was calculated in order to evaluate the retention capacities of the membranes used with the use of (Equation 3.7):

The procedure used to quantify cations (Na^+ and Mg^{2+}) was adopted from the instrument manual. The retention coefficient (R) was obtained using (Equation 3.7):

$$R = 1 - \frac{C_p}{C_f} \qquad \text{(Equation 3.7)}$$

Where C_p (permeate concentration, ppm) which was obtained after solution permeated through the membrane, and C_f (feed concentration, ppm) was obtained from the

average initial concentration and retentate (feed solution remaining in the unit at the end of the experiment) is the feed concentration (ppm).

3.5 SECTION B: Rejection of metals

3.5.1 Synthetic feed solutions

Inorganic mining wastewater sample solutions were prepared in the similar approach as charged salts. Solution with the concentration ranges of 20, 50 and 100 ppm were also prepared. $PdCl_{2(s)}$ (Pd^{2+}) and $CuCl_{(s)}$ (Cu^{+}) salts were dissolved with concentrated HCl aqueous solution. While $CuCl_2{\cdot}2H_2O_{(s)}$ (Cu^{2+}), $(NH_4)_2PdCl_{6(s)}$ (Pd^{4+}) and $NiCl_2{\cdot}6H_2O_{(s)}$ (Ni^{2+}) salts were dissolved using deionised water. In the case of $AgCl_{(s)}$, 1 M $Na_2S_2O_{3(aq)}$ solution was used to dissolve the salt.

3.5.2 Rejection of metals

Single-salt metal ion experiments (Pd^{2+}, Pd^{4+}, Ni^{2+}, Cu^{2+}, Cu^{+} and Ag^{+}) and binary salts metal ions experiments (Pd^{2+}/Cu^{2+}, Ni^{2+}/Cu^{2+}, Pd^{2+}/Ni^{2+}) mixtures, were also performed at varying pressure of 5, 10, 15 and 20 bar. The pH of the solutions was kept at pH 2.0 and 3.0. Time (min) intervals were also varied. As for trinary-salt mixtures (Pd^{2+}/ Ni^{2+}/Cu^{2+}) experiments were also performed at pressure of 5 bar and 20 bar at pH 2.0. Retentate, feed and permeate solutions, were collected and quantified while the metal retention was also calculated in the manner as with charged solutes.

References

1. A. N. Zhu, F. Long, X. L. Wang, W. P. Zhu, J. D. Ma. The negative rejection of H^+ in NF of carbonate solutions and its influences on membrane performance, *Chemosphere* **67** (2007) p1558-1565.

2. L. D. Nghiem, P. J. Coleman. NF/RO filtration of the hydrophobic ionogenic compound triclosan: Transport mechanisms and their influence of membrane fouling, *Separation and Purification Technology* **62** (2008) p709-716.

3. M. Mänttäri, T. Pekuri, M. Nyström, NF270, a new membrane having promising characteristics and being suitable for treatment of dilute effluents from the paper industry, *Journal of Membrane Science* **242** (2004) p107-116.

4. T. J. Visser, Performance of nanofiltration membranes for the removal of sulphates from acids solutions, M.Sc thesis, Potchefstroom University, Potchefstroom. South Africa (2000).

5. M. Mulder. Basic Principles of Membrane Technology, 2nd Edition, Kluwer Academic publishers, The Netherlands (1997).

CHAPTER 4

RESULTS AND DISCUSSION: SECTION A

Table of Contents

Introduction

This Chapter is divided into two sections (A and B). In section (A), data collected in this study will be interpreted and discussed. Firstly, NF membranes were characterised using SEM. The clean water permeability experiments were also performed to evaluate membrane porosity. Flux measurements and rejection of charged solutes will be discussed. Lastly, the functional groups of NF membranes tested will be identified and interpreted using FTIR instrumentation.

4.1 Characterization by Scanning Electron Microscopy (SEM)

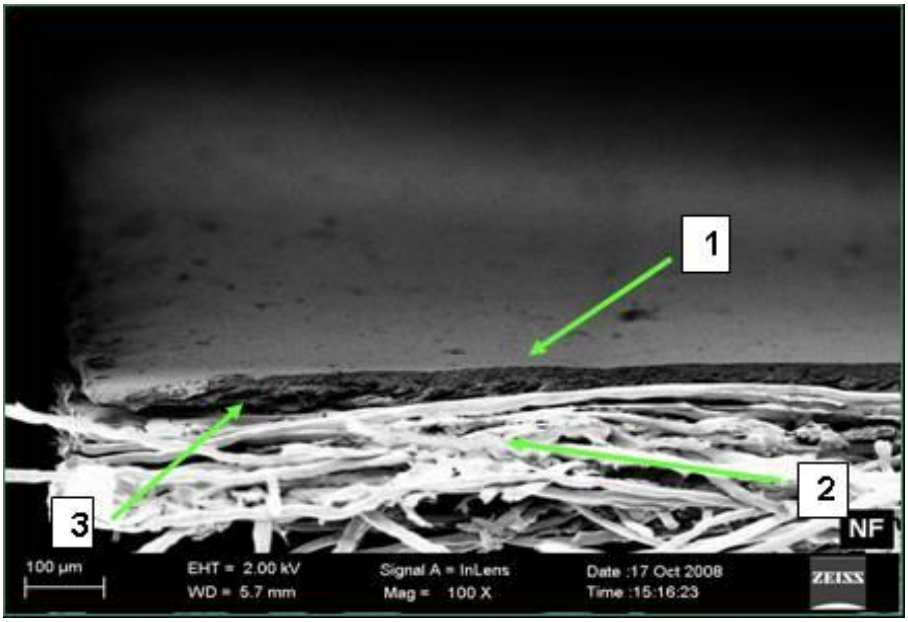

Figure 4.1 Cross sectional view of NF- Membrane

Thin film composite (TFC) membranes images of NF90, NF270 and NF-, were captured by SEM to provide membrane's morphology. Figure 4.1 shows the cross-section of NF- indicating three distinct layers namely top polymer (1), porous support (2) and non-woven layer (3). Top layer is the most important layer during membrane separation

processes [1]. Due to the fact that, it is where charge density is found and rejections are taking place. Porous support and non-woven layer allow permeation during membrane processes. These layers are observed in all the NF membranes investigated in this study. Figure 4.2 shows the top view of NF90.

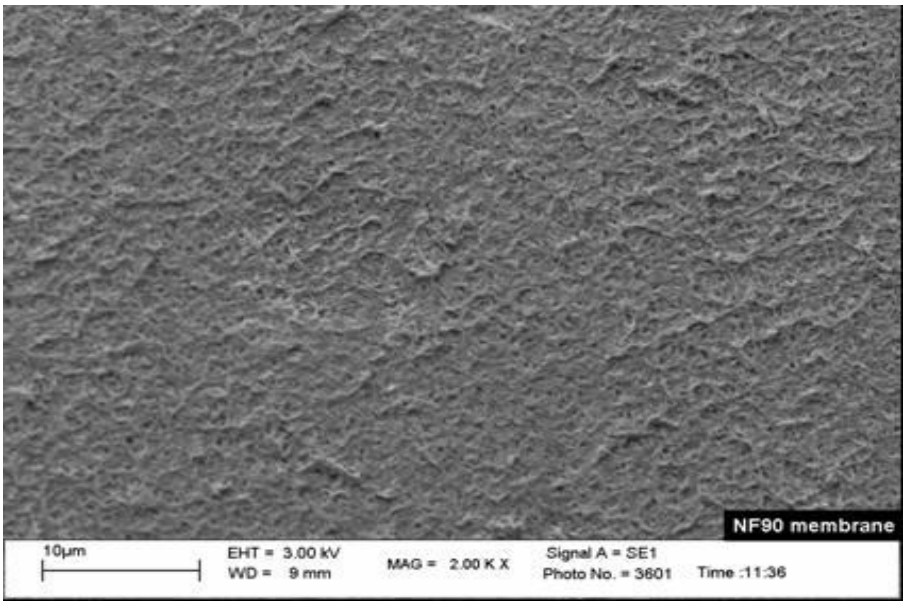

Figure 4.2 Top view of NF90

The top layer of the membrane (NF90), is a microporous polysulphone supporting layer [2]. It has a rough surface layer as shown in Figure 4.2.

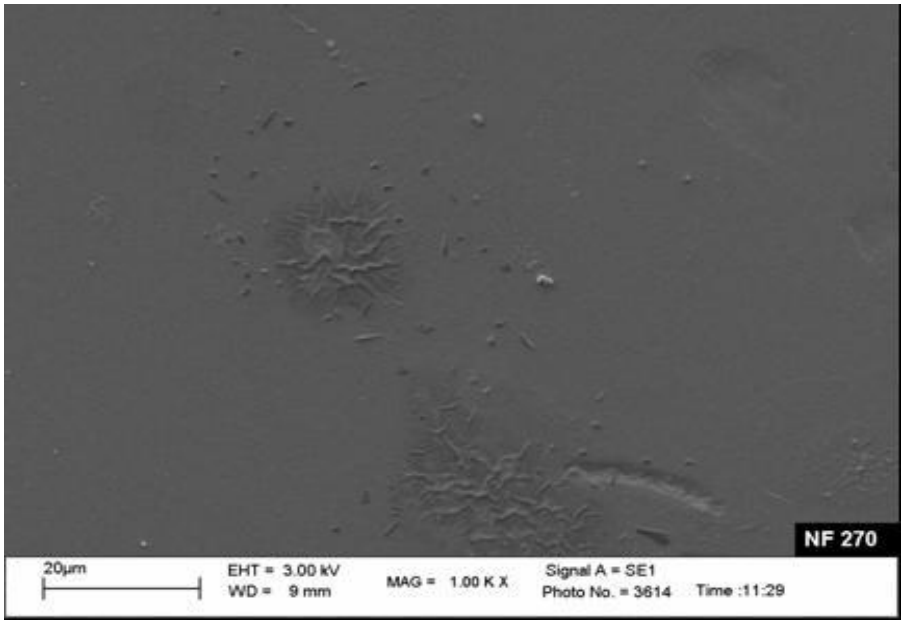

Figure 4.3. Top view of NF270

In Figure 4.3, NF270 reflects the smooth surface top-layer with no indication of pores.

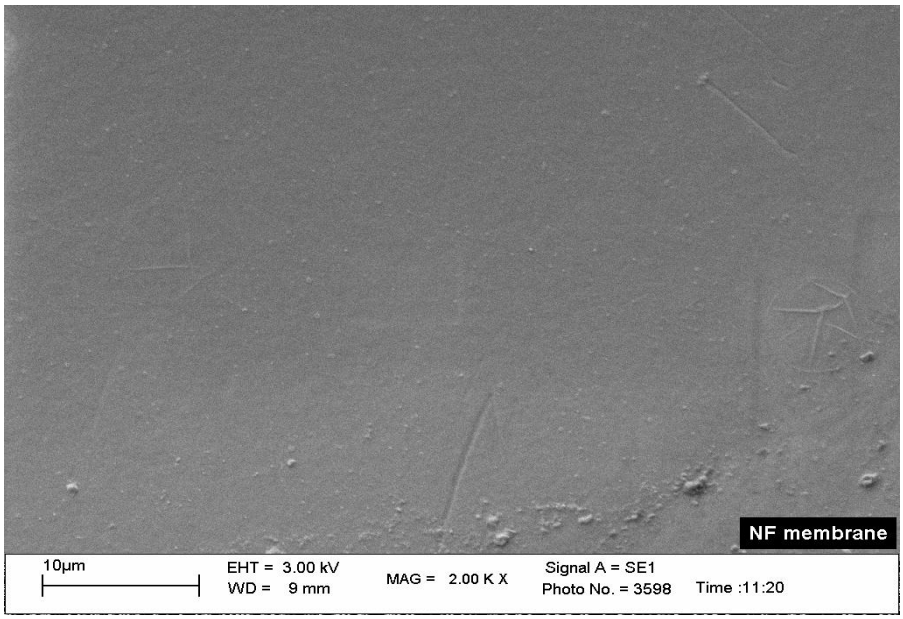

Figure 4.4 Top view of NF-

In the case of NF-, the membrane has the smoothest surface top layer resembling NF270 as seen in Figure 4.4. It can be assumed that both membranes (NF270 and NF-) will have similar performances (permeability, rejection) based on their smooth surface layer. However, these two membranes differ in their performance due to the membrane surface layer functional group.

4.2 Clean water flux

Clean water permeability (A_w, $\ell.m^{-2}.h^{-1}.bar^{-1}$) experiments, were performed on all three NF membranes. The permeate flow shows a linear trend as shown in Figure 4.5. An increase in applied pressure yields a linear increase in flow rate in all membranes.

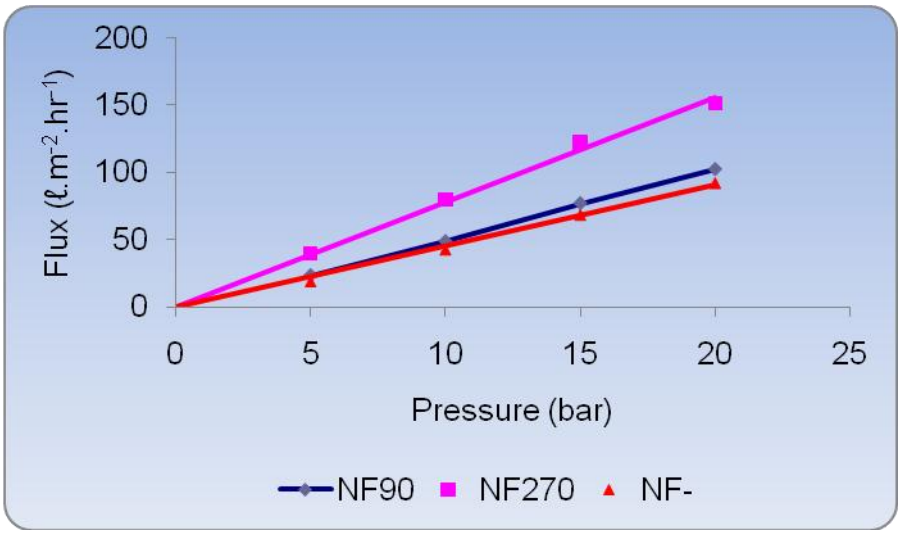

Figure 4.5 Plot of pressure vs. flux on various membranes at room temperature.

NF270 was found to have the highest flux (160 $\ell.m^{-2}.h^{-1}$ at 20 bar). This could be due to the large pore size distribution of this membrane, compared to the other two membranes (NF90 and NF-). Their permeability values are listed in Table 4.1. NF90

and NF- showed lower fluxes of 109 ℓ.m^{-2}.h^{-1} and 98 ℓ.m^{-2}.h^{-1} at 20 bar, and have the lowest permeability values compared to NF270. This observation could be due to unequal void sizes amongst NF membranes tested. All the membranes exhibit a linear increasing trend in flux as pressure increases.

Table 4.1 Clean water permeability value for NF membranes (dead end module)

Membrane	*A_w (ℓ.m^{-2}.hr^{-1}.bar^{-1})*
NF90	5.10
NF-	4.54
NF270	7.50

Specifications of NF membrane's permeability values range between 1.4 ℓ.m^{-2}.hr^{-1}.bar^{-1} and 12 ℓ.m^{-2}.hr^{-1}.bar^{-1} with applied pressure between 5 bar and 20 bar [3]. These results were in accord with the ones found by Lou *et al.* [4]. All the membranes tested, adhered to the specification ranges stated and are an indication that they are indeed NF membranes. Therefore, the behaviour of these membranes can be related to their pore sizes and polymer charge density.

4.3 Single salt flux

4.3.1 NaCl salt

Flux measurements for single salt (NaCl) solution, were performed to investigate the permeability of ions (Na^+ and Cl^-) on NF membranes. Figure 4.6, 4.7 and 4.8, illustrate various NF membranes tested for different salt concentrations during flux measurements. As can be seen in Figure 4.6 at pH 2 and concentration of 20 ppm, NF270 shows an increasing NaCl flux with increasing pressure (from 5 bar to 20 bar).

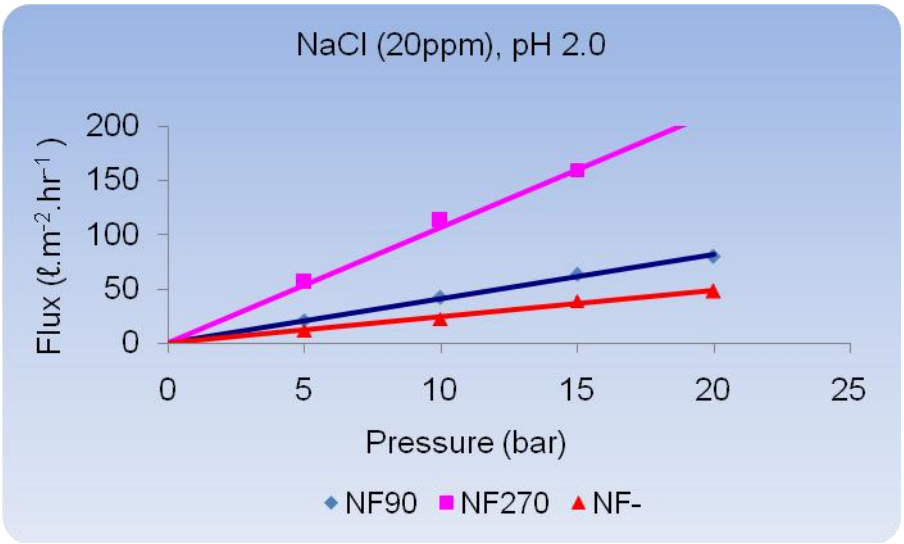

Figure 4.6 Plot of flux vs pressure of NaCl on three NF membranes at 20 ppm.

Values of flux increase from 50 $\ell.m^{-2}.h^{-1}$ at 5 bar to 200 $\ell.m^{-2}.h^{-1}$ at 20 bar. However, NaCl flux on NF90 and NF- also increases but at lower flux rate compared to that of NF270. At 50 ppm (Figure 4.7), the trend in flux is similar to that at 20 ppm. However, unlike at 20 ppm, the flux values on NF90 were higher compared to NF-.

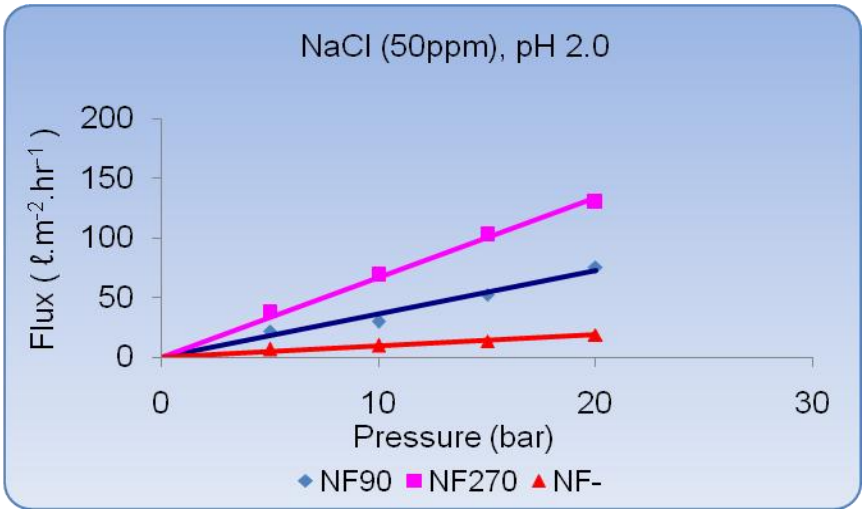

Figure 4.7 Plot of flux vs pressure of NaCl on three NF membranes at 50 ppm.

An increasing trend in NaCl flux on these membranes resembles the clean water flux measurement shown in Figure 4.5 above. This indicates that, NF- has the smallest pore sizes amongst the two membranes. In order to further investigate the influence of concentration, experiments were conducted at 100 ppm (Figure 4.8). The flux for NaCl solution had the same increasing trend as that at 20 ppm and 50 ppm on all membranes as shown in Figure 4.8.

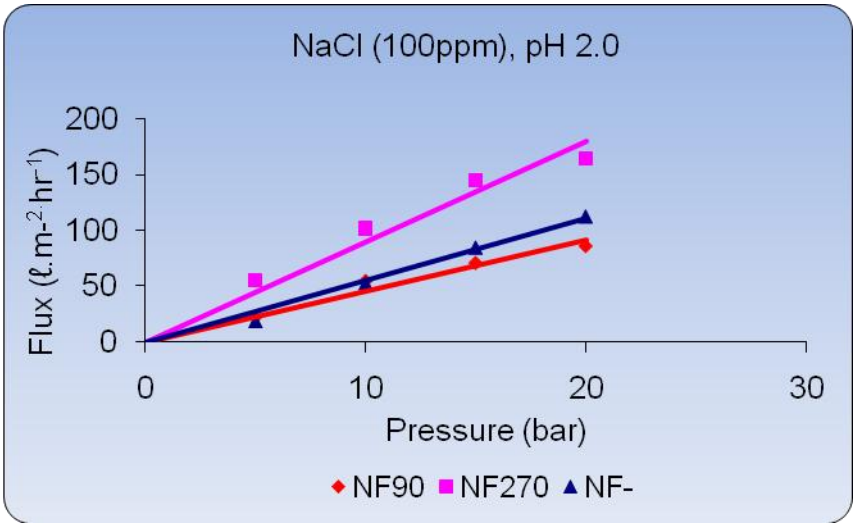

Figure 4.8 Plot of flux vs pressure of NaCl on three NF membranes at 100 ppm.

The increasing trend at 50 ppm and 100 ppm was lower compared to the one at 20 ppm. This observation at 50 ppm and 100 ppm, was due to adsorption of Na^+ and Cl^- ions on NF membranes leading to possibility of concentration polarization accumulation. Therefore, adsorption of these ions excludes them from being transported through the permeable FS membranes. Modise [5] reported the same result for NF90 membrane at concentrations of 20 ppm, 50 ppm and 100 ppm (NaCl) solutions at neutral pH. Table 4.2 list the fluxibility measurement values of NaCl on various concentrations and membranes at pH 2.0.

Table 4.2 Fluxibilty measurements of NaCl on three NF membranes

	Concentrations (ppm)		
Membranes	20	50	100
NF90	10.18	6.14	7.34
NF-	3.96	3.7	6.28
NF270	2.57	0.8	4.10

In Table 4.2, fluxibility of NaCl on NF90 is higher at 20 ppm than at 50 ppm and 100 ppm. In the case of NF-, fluxibility of NaCl observed was higher than that of NF270 on all concentrations varied. This shows that, movement of ions (Na^+ and Cl^-) was higher than on NF- and N270.

4.3.2 Effects of pH on NF membranes flux for charged solutes

Figure 4.9 shows the effect of pH on NF90 membrane using NaCl and $MgCl_2$ solutions during flux measurements. Solution mixtures were adjusted to pH 2.0, 3.0, 5.0 and 6.95 (to monitor flux during movement of Na^+ and Mg^{2+} ions at varying pH conditions). The concentration used in this case was 100 ppm, and the pressure applied was kept constant at 20 bar.

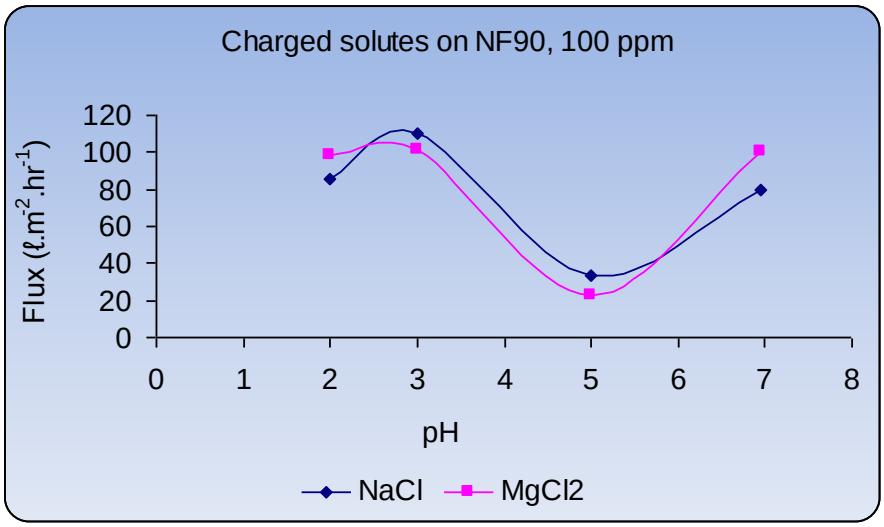

Figure 4.9 Plot of flux vs pH of NaCl and $MgCl_2$ at 20 bar.

Flux measurement of NaCl increases from 100 $\ell.m^{-2}.h^{-1}$ at pH 2.0 to 150 $\ell.m^{-2}.h^{-1}$ at pH 3.0. However at pH values between 3.0 and 5.0, the values decrease but increase again between pH 5.0 and 7.0. The maximum flux was observed at 112 $\ell.m^{-2}.h^{-1}$ (NaCl) between pH 2.0 and 3.0, while for $MgCl_2$ it was observed at 102 $\ell.m^{-2}.h^{-1}$ between 2.0 and 3.0. At pH above 3.0, the decrease in flux measurement on NF90, is due to the isoelectric point (IOP), indicating that the membrane encounters a zero or negative charge. Minimum flux was observed at 36 $\ell.m^{-2}.h^{-1}$ (NaCl) between pH 5.0 and 6.0, while for $MgCl_2$ it was observed at 28 $\ell.m^{-2}.h^{-1}$ between pH 5.0 and 6.0. At pH 7.0, the membrane charge density seems to be more of H^+ which lead to R_3HN^+, showing an increase in flux from pH 5.0 to 7.0. The similar results obtained during flux measurements on NF membranes, were reported in another study [7] with varying pH levels using NaCl solution.

The signoidal-shaped trend in flux measurements for $MgCl_2$ on NF90 was obtained as shown in Figure 4.9. A decrease in flux at pH 3.0 for $MgCl_2$ was similar to a decrease obtained for NaCl flux measurement. This behaviour can also be interpreted as reaching an IOP of the membrane. The values for Mg^{2+} ion seem to be lower compared to those of Na^+ since Mg^{2+} has larger ion size compared to Na^+ ion. Hilal *et al.* [6]

reported also that Mg^{2+} ion has large ion size compared to Na^{+} ion. This could have an effect during ion flux measurements The same IOP flux results were obtained on TFC membrane and were reported by Tang *et al.* [7], while Ooi *et al.* [8] found that, the IOP of the laboratory prepared NF membrane is found between pH 3.5 and pH 4.5. Therefore, pH conditions have an effect on flux measurement of charged solutes.

4.4 Effects of charged solute concentrations on rejection

4.4.1 Charged ion properties

According to charged solutes properties of monovalent (Na^{+}) and divalent (Mg^{2+}) cations and anion (Cl^{-}) given in Table 4.3, the salt bulk diffusivity (D_∞) of Na^{+} ion is less than that of Mg^{2+} ion. While in the case of Stokes radius (r_s) or solute size, Mg^{2+} ion is larger than that of Na^{+} ion. The Stokes radius (r_s) can be calculated using the following equation by Stokes-Einstein relationship (Equation 3.8):

$$r_s = \frac{k_B T}{6\pi\eta_0 D_\infty} \qquad \text{(Equation 3.8)}$$

where r_s is Stokes radius (nm), k_B the Boltman constant ($J.K^{-1}$), η_0 as the solvent viscosity ($Pa.s^{-1}$), T is the temperature (K) and D_∞ is bulk diffusivities ($m^{-2}.s^{-1}$) at infinite dilution. The values are an indication of molecular diameter of a solute and the Stokes radius (solute size).

Table 4.3 Ion characteristics of charged solutes (physical properties of the species) [9, 10]

Ions	D_∞ *× 10^{-9} (m^2. s^{-1})*	r_s *(nm)*
Na^+	1.33	0.18
Mg^{2+}	0.71	0.35
Cl^-	2.03	0.12

4.5 Rejections of charged solute

4.5.1 Single salt: *NaCl*

The rejection behaviour of charged solute (NaCl) as single-salt on NF90 membrane was evaluated at pH 2.0. It is experimentally proven that at low pH, the membrane surface charge density becomes positive [1, 11, 12]. Separation of ions which occurs at membrane solution interface, is established by Donnan equilibrium, which brings about equity between the total charge of species in the membrane and those in the solution [3, 13]. Donnan principle indicates that, the ion (cation or anion) having the same charge as that of the membrane surface (co-ion) will be repelled, and ions with opposite charge (counter-ion) will be attracted to the membrane surface as reported by Mulder [3].

Figure 4.10 shows NaCl rejection data on NF90 at pH 2.0 with varying concentration (20, 50 and 100 ppm) and varying pressure (5 to 20 bar). Rejection of Na^+ ion on NF90 of 90% at 5 bar and 96% at 20 bar, were achieved at 20 ppm. While at 10 and 15 bar, the rejection was almost constant achieving between 90% and 94% with a linear increasing trend.

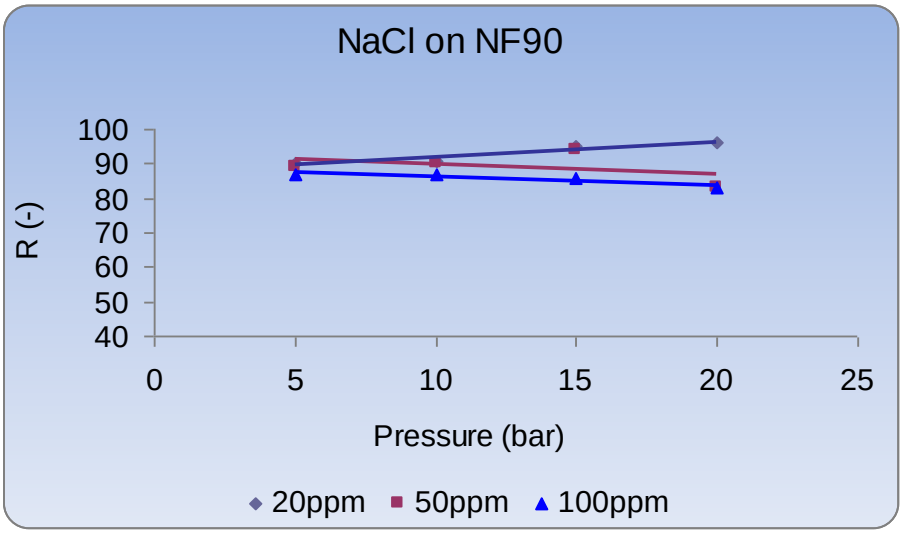

Figure 4.10 Plot of rejection vs pressure of NaCl solute on NF90 at pH 2.0.

While at 50 ppm, rejection of 90% at 5 bar and 85% at 20 bar, was achieved. This indicates that the membrane (NF90) is not influenced by concentration during separation process. Therefore, an electrostatic interaction between the membrane and the solute had an influence causing an increase in rejection. Also a typical reason leading to an increase in rejection is membranes void (pores) size. However, at 100 ppm the rejection was between 80% and 87%, showing a decreasing linear trend as compared to 20 and 50 ppm as the applied pressure was increased.

For NF- (Figure 4.11), highest NaCl as Na^+ ion rejection observed was between 83% and 75% also 20ppm at 5 bar and 20 bar. While for 50 ppm, similar rejection trend was observed as 20 ppm at 5 and 20 bar respectively. A linear trend was observed showing an increase when pressure was increased.

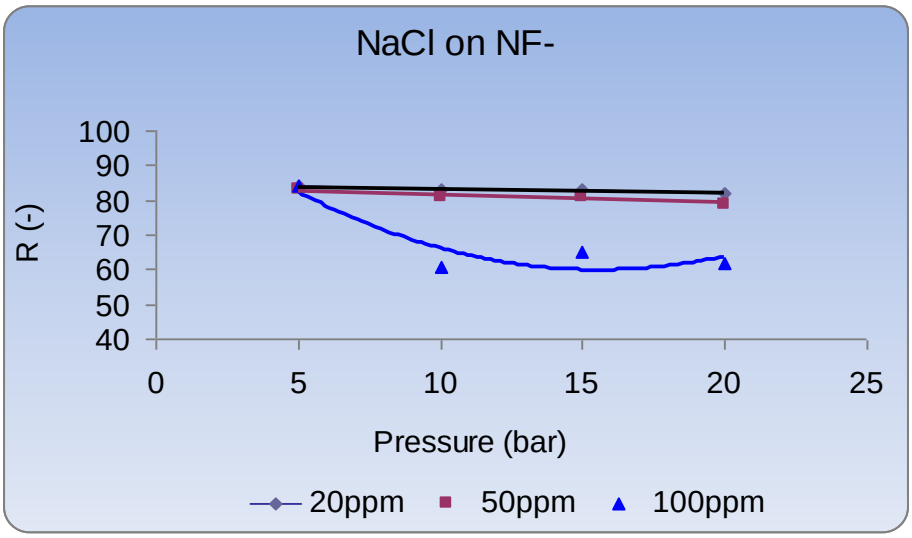

Figure 4.11 Plot of rejection vs pressure of NaCl on NF- at pH 2.0.

For the highest concentration (100 ppm) solution, a decrease in rejection from 83% to 60% at 5 bar and 10 bar was achieved. While from 10 bar to 20 bar, rejection was almost constant at ≈60%. This indicates that, the higher the NaCl concentration solution exposed on NF-, as with NF90, the lower the rejection capacity on the membrane. The lower rejection of NaCl on the membrane indicates the possibility of concentration polarization accumulation on the top surface membrane layer. Chilyumova and Thöming [14] reported almost the same results using lower concentration of NaCl solution.

NF270 (highest permeate flux) had the highest NaCl rejection of 92% at 20 ppm and 71% at 50 ppm, were observed at 20 bar as seen in Figure 4.12. At 50 ppm, the rejection trend was linear whether pressure was continuously applied from 5 bar to 20 bar. This implied that the pressure had no influence on the rejection values. For 100 ppm, the linear rejection trend was observed from 5 bar to 20 bar. An interpretation in this case indicates that, although this membrane has high permeate flux amongst other two membranes, a high rejection obtained was due to high membrane surface charge [15], and electrostatic interaction between the surface layer and the solute.

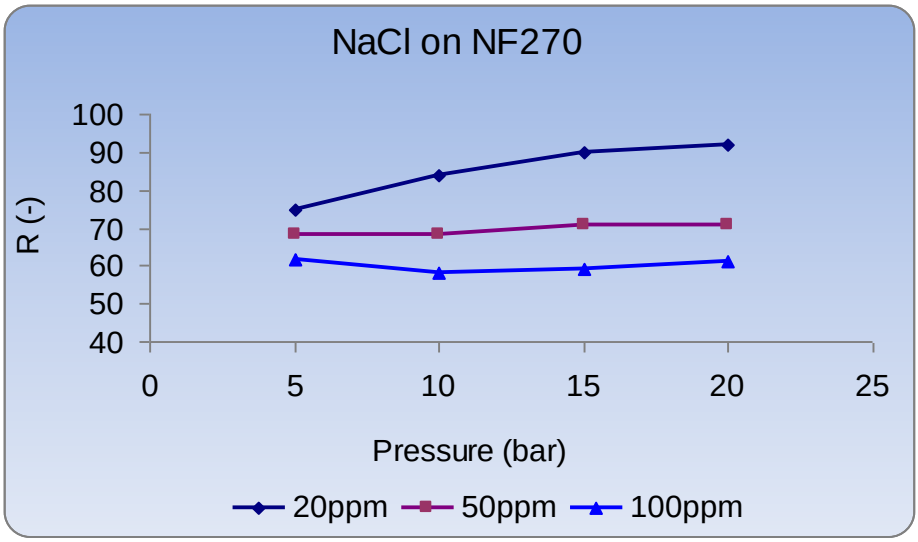

Figure 4.12 Plot of rejection vs pressure of NaCl on NF270 at pH 2.0.

Rejection of anion (Cl^-) presented in Figure 4.13, shows a decrease in rejection trend as applied pressure increases almost in all membranes employed for the study. According to ion characteristics of charged solutes listed in Table 4.3, the 0.12 nm Stokes radius (solute size) for Cl^- ion, suggests an easy transportation of the ion through the membrane than Na^+ ion with 0.18 nm.

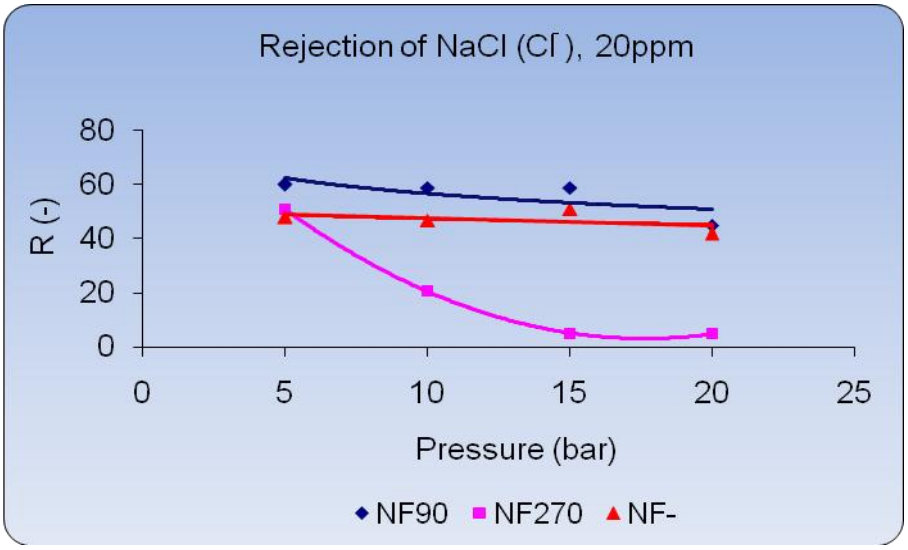

Figure 4.13 Plot of rejection vs pressure of NaCl (Cl^-) on NF membranes at 20 ppm.

Rejection of 60% was the highest on NF90 as compared to 51% and 48% through a positively charged density membrane surface on NF270 and NF- respectively at 5 bar. The rejection sequence of Cl^- ion for all membrane tested was that NF90 > NF- > NF270 as observed. High rejection observed on NF90 was due to small pore size, while the lowest rejection on NF270 was due to membrane large pore sizes [16]. The monovalent diffusion through the membrane decreased when the membrane pressure was increased. Due to opposite charge of the surface and the ion (counter-ion), Cl^- species will be attracted to the surface material thus leading to low rejection performance on the membranes. Therefore, Donnan equilibrium was compensated since the ion (Cl^-) had an opposite charge as the membrane's positive surface charge density, thus leading to low rejection of the anion.

4.5.2 Single salt: *$MgCl_2$*

A divalent (Mg^{2+}) ion has a larger solute size (0.35 nm) as compared to monovalent (Na^+) ion with (0.18 nm) according to the charge ion properties listed in Table 4.3. The large solute size of this divalent ion can influence membrane rejection behaviour, which

can result in high rejection on the membranes. High rejections of up to 98%, was achieved at 20 ppm for Mg^{2+} ion on NF90 irrespective of pressure (Figure 4.14). The high rejection achieved was due to high molecular weight and larger solute size [9, 10] of Mg^{2+} ion as compared to Na^{+} ion.

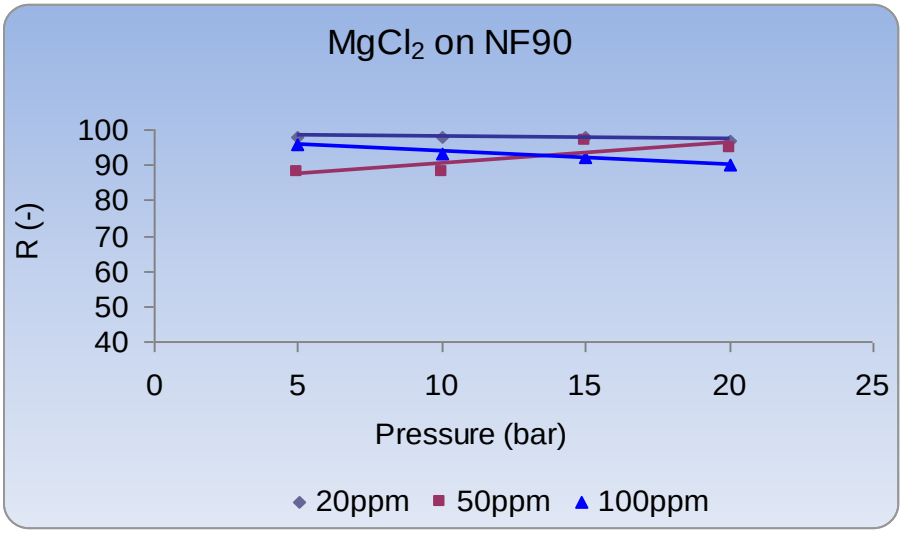

Figure 4.14 Plot of rejection vs pressure of $MgCl_2$ on NF90 at pH 2.0.

At 50 ppm, $MgCl_2$ rejection slightly increased from 88% to 97% at 10 bar and 15 bar, respectively. An increase in applied pressure operation results in an increase in rejection capacity (indicating that the more pressure applied on the membrane, the more Mg^{2+} ion strongly interacts with the surface layer). While at 100 ppm, a linear decrease in rejection on NF90 from 96% to 92% was obtained from 5 bar to 20 bar, respectively. Again, this decrease in rejection trend leads to possibility of membrane fouling (concentration polarization) to occur during membrane processes. It is clear that an increase in rejection has partly to do with molecular weight of the ion (Mg^{2+}). This also includes an electrostatic interaction between positively charged membrane surface and the solute, when compared to Na^{+} ion.

In Figure 4.15, NF- rejection was almost constant with ≈ 90% at 20 ppm irrespective of the applied pressure. At 50 ppm, the rejection behaviour of NF- was almost the same as

at 20 ppm. In this case the membrane was not influenced by concentration variation. At 100 ppm, a decrease in rejection of Mg^{2+} was from 80% to 60% at 5-20 bar. Therefore, the concentration of Mg^{2+} ion had an influence on membrane surface layer which indicated that the larger the solute size, the higher the rejection by NF-membrane.

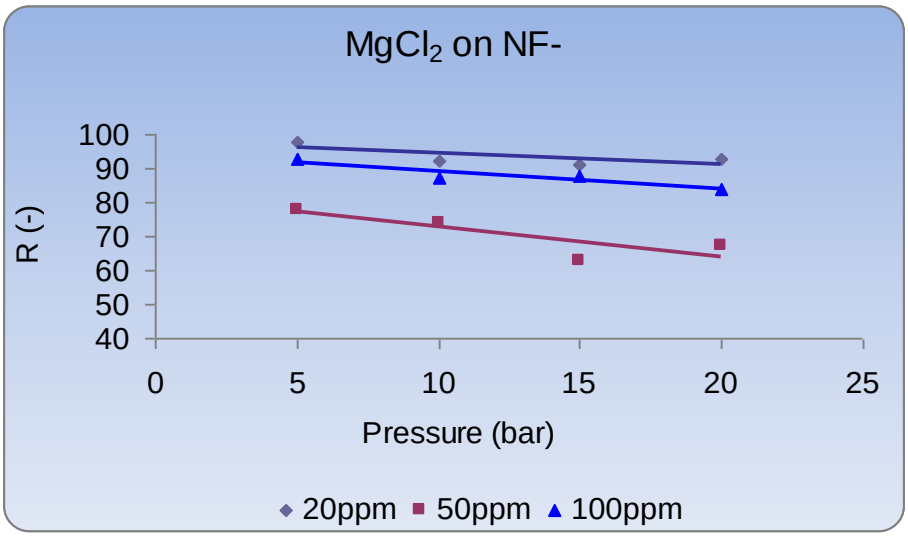

Figure 4.15 Plot of rejection vs pressure of $MgCl_2$ on NF- at pH 2.0.

Figure 4.16 shows a linear rejection trend of 95% and 90% from 5 bar to 20 bar at 20 ppm on NF270. At 50 ppm, the membrane has the rejection of between 50% and 60% from 5 bar to 20 bar, of which it was lower compared to 20 ppm. But at 100 ppm, a constant rejection trend of ≈ 98% was observed from 5 bar to 20 bar, which was the highest rejection compare to 20 ppm and 50 ppm. This indicates that at 100 ppm, the membrane was independent of pressure. This can further be explained that, since NF270 has the highest permeability compared to the other two membranes, this could be due to the predicted large pore sizes of the membrane. However, the high rejection of Mg^{2+} ion at high concentration level was due to high positive charge membranes surface layer on NF270 [15].

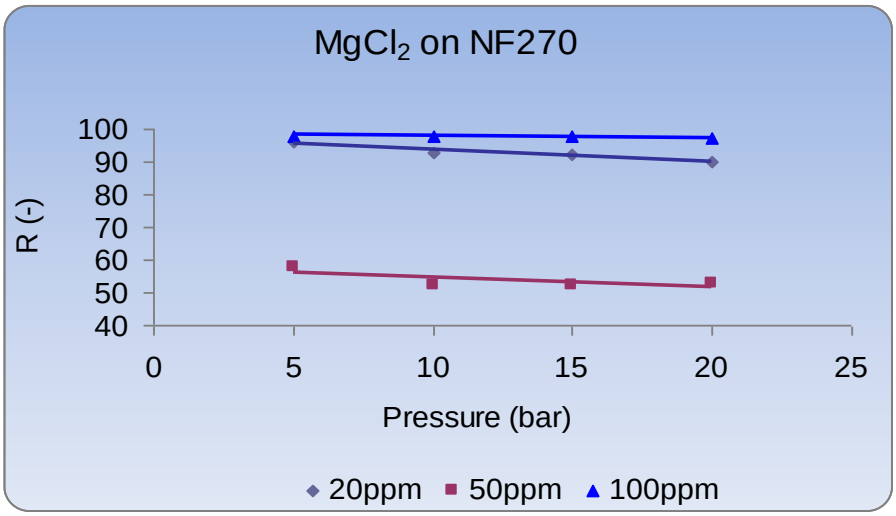

Figure 4.16 Plot of rejection vs pressure of $MgCl_2$ on NF270 at pH 2.0.

4.6 Effect of pH on NF membranes rejection

The pH (either acidic or basic medium) influences the separation capability of the charged NF membranes [8]. Figure 4.17, illustrates the rejection of (Mg^{2+}) ion as $MgCl_2$ and (Na^{+}) ion as NaCl on NF90 in all pH medium (2.0, 3.0, 5.0 and 7.0) at pressure of 5 bar and concentration of 20 ppm.

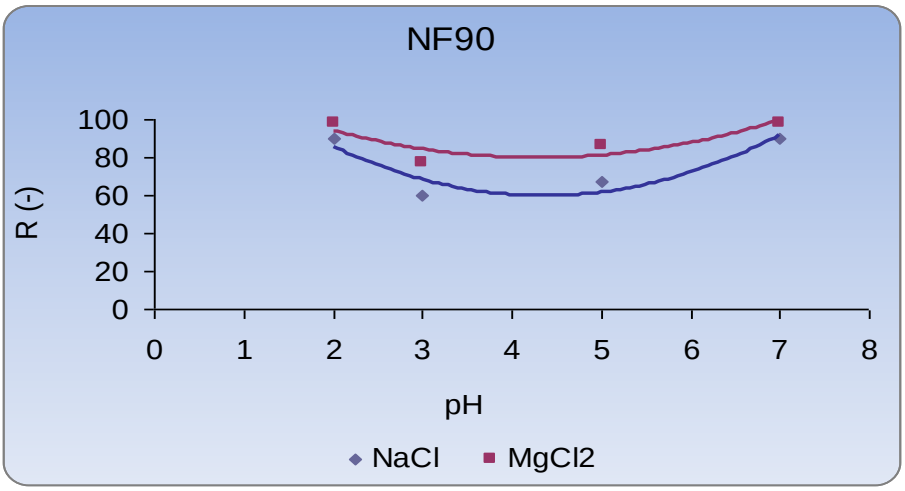

Figure 4.17 Plot of rejection vs pH of $MgCl_2$ and NaCl on NF90, 20 ppm.

In Figure 4.17, rejection of 98% was achieved for Mg^{2+} ion on NF90 at pH 2.0 and 7.0, while 77% was rejected at pH 3.0. At pH 5.0, 85% was rejected on the membrane. The U-shaped like rejection trend was observed indicating that pH medium influenced the rejection of Mg^{2+} ion on the membrane as mentioned. In the case of the monovalent ion (Na^{+}), rejection of 90% and 60% were observed at pH 2.0 and 7.0 respectively. However, the lower rejection performance of the membrane at pH 3.0 was due to the same IOP observed during flux measurements in Figure 4.9.

4.7 pH effect on rejection of $MgCl_2$

Polymeric membrane are charged (positive or negative) due to their functional group depending on the monomers during polymerisation process [16]. Figure 4.18 illustrates the influence of charged solute ($MgCl_2$) on all membranes at pH 2.0, 3.0, 5.0 and 7.0 performed at 5 bar.

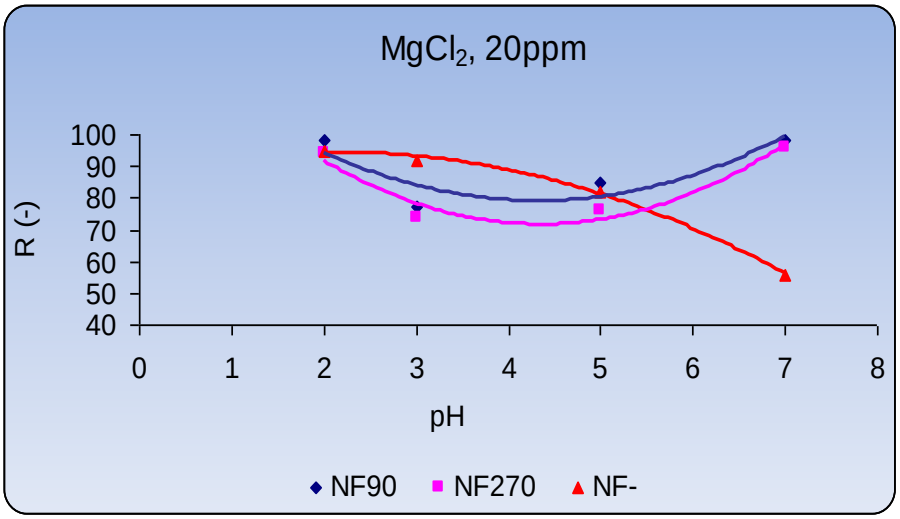

Figure 4.18 Plot of rejection vs pH of $MgCl_2$ on NF membranes at 5 bar, 20 ppm.

In Figure 4.18, $MgCl_2$ was used to evaluate pH variation with respect to the performance of NF membranes. Rejection trend on NF90 and NF270 membranes was almost similar from pH 2.0 to pH 7.0. A U-shaped like trend was observed on NF90

rejecting 98% and 77% at pH 2.0 and pH 3.0 respectively while pressure was kept constant at 5 bar. For pH 5.0 and 7.0, the rejection behaviour of the membrane increased from 88% to 97%. In essence, an increase from pH 5.0 to 7.0 indicates that the membranes are pH dependent.

In the case of NF270, rejection of 94% and 74% at pH 2.0 and 3.0 were achieved. At pH 3.0, a decrease in rejection was observed for both membranes (NF90 and NF270), was due to deprotonation of H^+ in the solution when pH was increased. However, at pH 5.0 and 7.0, the same rejection behaviour trend was observed as with NF90, 96% and 76% were observed indicating dependency of the membranes on pH medium. NF-, showed a decrease in rejection with an increase pH variation from pH 2.0, 3.0, 5.0 and 6.95. A decrease in rejection varied from 95% at pH 2.0 to 56% at pH 7.0. The trend implies that, these NF membranes are pH dependent. In general, NF membranes can be conducted under acidic pH medium.

4.8 Salt mixture: $NaCl/MgCl_2$ (Na^+/Mg^{2+})

The binary salt ($NaCl/MgCl_2$) mixtures were carried out at 20 ppm on pH 2.0 medium in all three NF membranes at ratio 1:1. This was to evaluate ion distribution on membranes as binary mixture during permeation measurements. The difference between single salt (NaCl and $MgCl_2$) mixture and rejection performance of NF membranes is shown in Figure 4.19, Figure 4.20 and Figure 4.21.

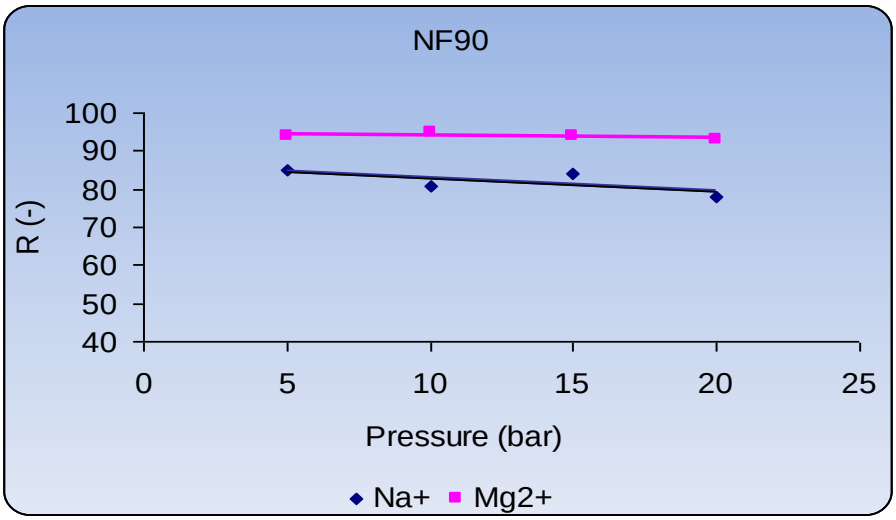

Figure 4.19 Plot of rejection vs pressure for NaCl/$MgCl_2$ at 20 ppm.

Figure 4.19 shows that Mg^{2+} ion was rejected higher than Na^{+} ion at 5-20 bar. A constant rejection of ≈ 94% was achieved at (5-20 bar) on NF90. On the other hand, Na^{+} ion had 85% and 82% at 5 and 10 bar respectively, with 84% and 79% at (15-20 bar) on NF- membrane respectively. Therefore, movement of Na^{+} ion seems to be faster as compared to Mg^{2+} ion, which leads to lower rejection due to its small solute size [9, 10].

In the case of NF- (Figure 4.20), Mg^{2+} ion rejections of 85% and 89% at (5-10 bar) were observed. While at (15-20 bar), 70% and 86% were achieved, respectively. However, according to ion characteristics of charge solute, ion with larger solute size lead to low rejection on polymeric NF membrane [9].

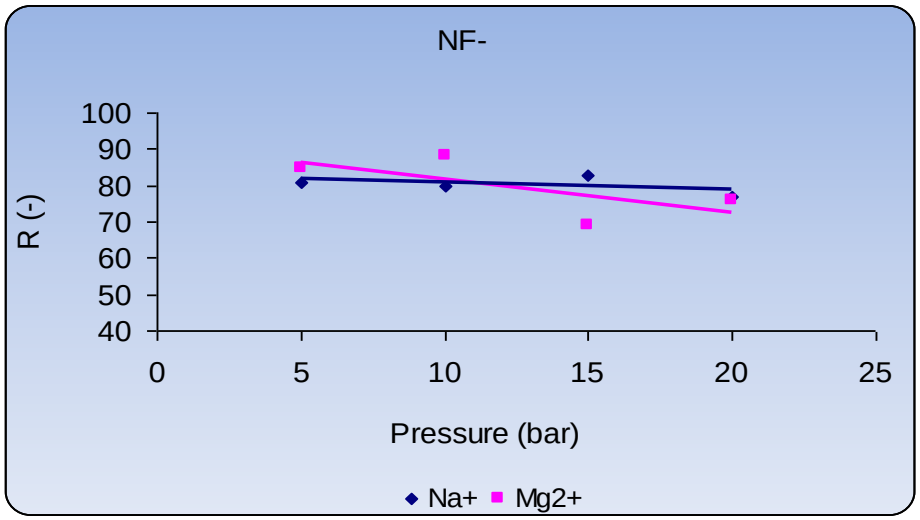

Figure 4.20 Plot of rejection vs pressure of NaCl/$MgCl_2$ at 20 ppm.

In Figure 4.21 (NF270), the performance of the membrane was interesting since lower retention of cation was expected due to the largest pore size. However, a linear rejection trend of ≈ 94% and 90% for Mg^{2+} ion at (5-20 bar). On the other hand, 90% and 76% for Na^{+} ion at (5-20 bar) were achieved. It could be explained that, the lower the membrane pressure operation, the higher the rejection of solute, depending on the ionic size and charge of the solute.

The question could be raised with regard to largest pore sized membrane (NF270), on the rejection performance of heavy metals e.g. PGMs. One of the reasons that make NF270 performance high during rejection for charged solute, had to do with the electrostatic charge since it has a high negative charge density compare to NF90 and NF-.

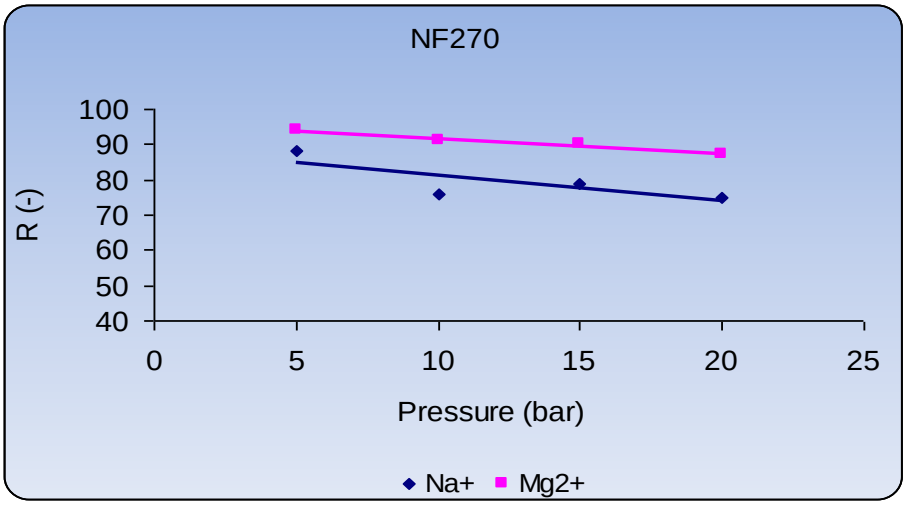

Figure 4.21 Plot of rejection vs pressure for NaCl/ $MgCl_2$ at 20 ppm.

4.9 Surface layer characterization

Scheme 4.1 and Scheme 4.2, are adopted structures of typical NF polymeric membranes functional groups during interfacial polymerization from Chuyang *et al.* [17]. NF90 is a fully aromatic polyamide material, which is made from 1, 3 phenylene diamine and benzenetricarbonyl trichloride as starting materials during interfacial polymerisation process [16]. NF270 is a polyamide TFC membrane which is made from piperazine and benzenetricarbonyl trichloride as starting materials [17]. As for NF-, the membrane is a polypiperazine amide contains carboxylic ($COOH^-$) and amide (NH^-) functional groups [18].

The purpose of employing FTIR is to identify relative amount of polymeric species (functional group) present in NF membranes used. The spectra of 3 overlapping membranes, analysed using FTIR over wavenumbers ranging from 4000-650 cm^{-1}, are presented in Figure 4.22.

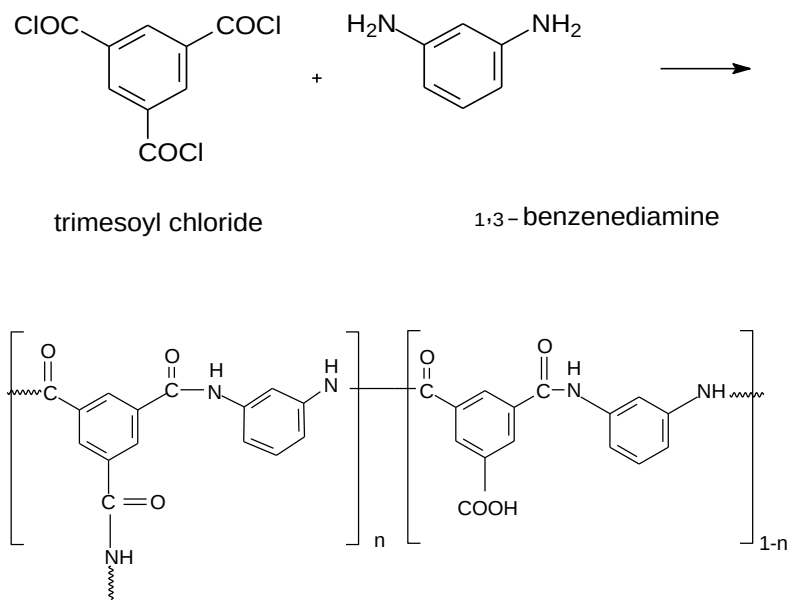

Scheme 4.1. Interfacially formed polyamide.

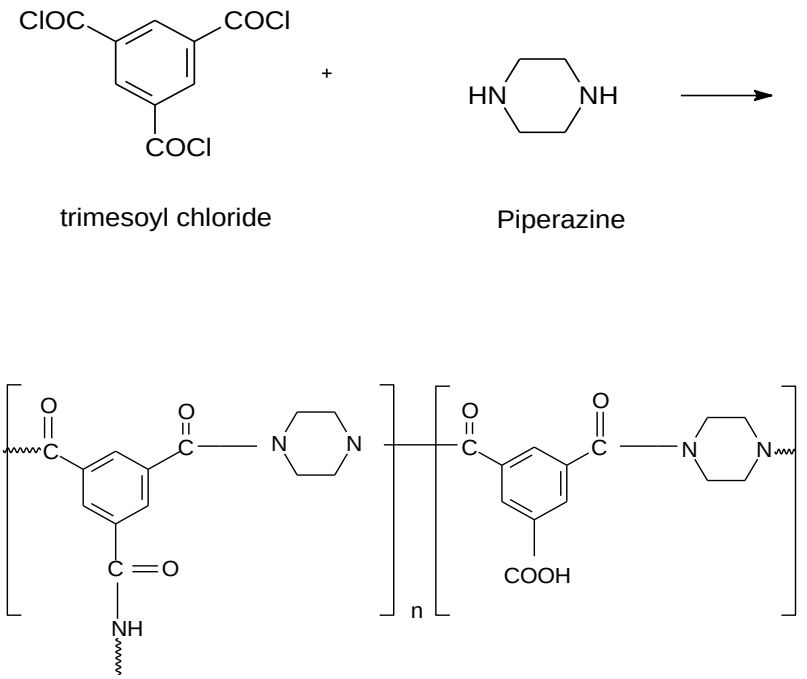

Scheme 4.2. Interfacially formed poly (piperazineamide).

In Figure 4.22, NF90 membrane's top layer (polysulfone) was associated with the strongest peak at 1240 cm^{-1} [17, 19], while the carbonyl (C=O) gave the strong band in the region 1700-1720 cm^{-1}, but was picked at 1713 cm^{-1}. An aromatic stretching band in the region 3100-3000 cm^{-1}, was absorbed as a weak peak at 3053,3 cm^{-1} for this membrane, and are in accord with the previous study [20]. The halide (Cl^-) which had a strong stretching vibration, was associated in the region 785-540 cm^{-1}, which was peaked at 691,8 cm^{-1} as primary chloride [19].

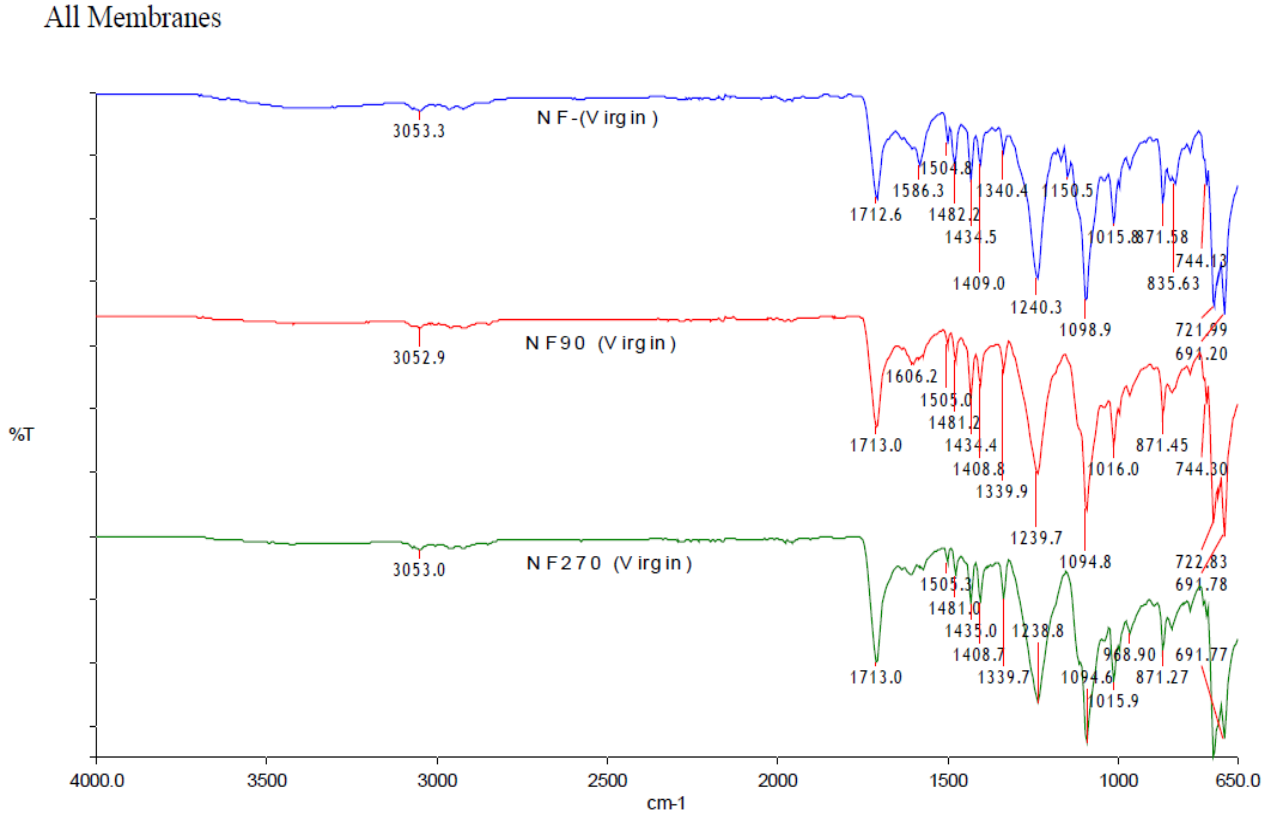

Figure 4.22 NF membranes analysis for functional group determination by FTIR.

The diamine group which was used to prepare NF270 was associated as a small band in the range at 1640-1550 cm^{-1}, but absorbed nearly at ≈1505 cm^{-1} (Figure 4.22). This also includes chloride, which was picked in the same region as NF90. Therefore, polyamide membranes (NF90 and NF270) exhibited the almost same

functional groups with regards to their spectra. In the case of NF-, almost the same region of polysulfone, chloride and carbonyl group, were associated.

References

1. S. Bandini, J. Drei, D. Vezzani. The role of pH and concentration on the ion rejection in polyamide nanofiltration membranes, *Journal of Membrane Science* **264** (2005) p65-74.

2. L. D, Nghiem, S. Hawkes, Effects of membrane fouling on the nanofiltration of pharmaceutically active compound (PhACs): Mechanisms and role of membrane pore size, *Separation and Purification Technology* **57** (2007) p176-184.

3. M. Mulder, Basic Principle of Membrane Technology, 2nd Edition, Kluwer Academic Publishers, The Netherlands (1996).

4. J. Lou, L. Ding, X. Chen, Y. Wan, Desalination of soy sauce by nanofiltration, *Separation and Purification Technology* **66** (2009) p429-437

5. S. J. Modise, South African rural water. Analysis and treatment of inorganics with nanofiltration and adsorption, PhD thesis, Potchestroom University, Potchefstroom, South Africa.

6. N. Hilal, H. Al-Zoubi, N. A. Darwish, A. W. Mohammad, Nanofiltration of magnesium chloride, sodium chloride, sodium carbonate, and calcium sulphate in salt solutions, *Separation Science and Technology* **40** (2005) p3299-3321.

7. B. Tang, Z. Huo, P. Wu. Study on a novel composite nanofiltration membrane by interfacial polymerization of triethanolamine (TEOA) and trimesoyl chloride (TMC) I. Preparation, Characterization and nanofiltration properties test of membrane, *Journal of Membrane Science* **320** (2008) p198-205.

8. J-J. Qin, M-H. Ooi, H. Lee. B. Coniglio, Effects of feed pH on permeate pH and ion rejection under acidic conditions in NF process, *Journal of Membrane Science* **232** (2004) p153-159.

9. A. L. Ahmad, B. S. Ooi, A. W. Mohammad, J. P. Choudhury, Composite Nanofiltration Polyamide Membrane: A study on the diamine ratio and its performance evaluation, *Industrial Engineering Chemicals* **43** (2004) p8074-8082.

10. L. Ouyang, R. Malaisamy, M. L. Bruening, Multilayer polyelectrolyte films as nanofiltration membranes for separating monovalent and divalent cations, *Journal of Membrane Science* **310** (2008) 76-84.

11. M. R. Teixeira, M. J. Rosa, M. Nyström, The role of membrane charge on nanofiltration performance, *Journal of Membrane Science* **265** (2005) p160-166

12. A. L. Ahmad, B. S. Ooi, A study on an acid reclamation and copper recovery using low pressure nanofiltration membrane, *Chemical Engineering Journal* **156** (2010) p257-263

13. W. R, Bowen, J. S. Welfoot, Modelling of the performance of membrane nanofiltration-critical assessment and model development, *Chemical Engineering Science* **57** (2002) p1121-1137

14. E. Chilyumova, J. Thöming. Nanofiltration of bivalent nickel cations-model parameter determination and process simulation, *Desalination* **224** (2008) p12-17

15. G. Artuğ, J. Hapke. Characterization of nanofiltration membranes by their morphology, charge and filtration performance parameters, *Desalination* **200** (2006) p178-180

16. K. Boussu, Y. Zhang, J. Cocquyt, P. Van der Meeren, A. Volodin, C. Van Haesendonck, J. A. Martens, B. Van der Bruggen. Characterization of polymeric nanofiltration membranes for systematic analysis of membrane performance, *Journal of Membrane Science* **278** (2006) p418-427

17. T. Y. Chayang, Y-N. Kwon, O. J. Leckie. Effects of membrane chemistry and coating layer on physiochemical properties on thin film composite polyamide RO and NF membranes. I. FTIR and XPS characterization of polyamide and coating layer chemistry, *Desalination* **242** (2009) p149-167.

18. C. Schaep, C. Vandecasteele, Evaluating the charge of nanofiltration membranes, *Journal of Membrane Science* **188** (2001) p129-136.

19. D. L. Pavia, G. M. Lampman, G. S. Kriz. Introduction to spectroscopy, 2nd edition, Saunders College Publishers, USA (1996).

20. C. Y. Tang, Y-N, Kwon, J. O. Leckie. Probing the nano-and micro-scales of reverse osmosis membranes-A comprehensive characterization of physicochemical properties of uncoated and coated membranes by XPS, TEM, ATR-FTIR, and streaming potential measurements, *Journal of Membrane Science* **287** (2007) p146-156.

CHAPTER 4

RESULTS AND DISCUSSIONS: SECTION B

Table of Contents

Introduction

This section (B), illustrates the effects of varying oxidation states metal rejections to different pH medium, concentration levels and applied pressure on all three tested membranes, are given and discussed. Rejection of single, binary and trinary solution mixtures of metals on NF membranes is discussed. Fouled membrane images captured on SEM/EDX, are also given and discussed.

4.10 Rejection of metal ions

Synthetic metal salt solutions of $PdCl_2$, $(NH_4)_2PdCl_6$, CuCl, $CuCl_2{\cdot}2H_2O$, $NiCl_2{\cdot}6H_2O$ and AgCl, were filtered in a similar manner as charged solutes (NaCl and $MgCl_2$) on three NF membranes (NF90, NF270 and NF-). These NF membranes have a negative surface charge density at ≥ pH 7.0 [1, 2]. The surface layer of these NF membranes become positive charge at low pH medium due to the protonation of the amide functional group [3, 4]. In this study, all the experiments were performed at pH 2.0. The influence of concentration (20, 50 and 100 ppm) on the rejection behaviour of the NF membranes was investigated at varying pressures of 5, 10, 15 and 20 bar. As for the halide (Cl^-) ion, its close proximity to the NF membranes results in an increase in membrane surface charge [5]. However, in this study, its influence in rejection measurement is not considered. Only metal ions (Pd^{2+}, Pd^{4+}, Cu^{2+}, Cu^{+}, Ni^{2+} and Ag^{+}) in their oxidation states were considered for the rejection on different membranes.

4.10.1 Single salt rejection: *Pd^{2+}as ($PdCl_2$)*

Solution of $PdCl_2$ was exposed on three NF membranes. Figure 4.23 illustrates the rejection of Pd^{2+} ion on NF membranes conducted at 20 ppm and at varying pressure (5, 10, 15 and 20 bar).

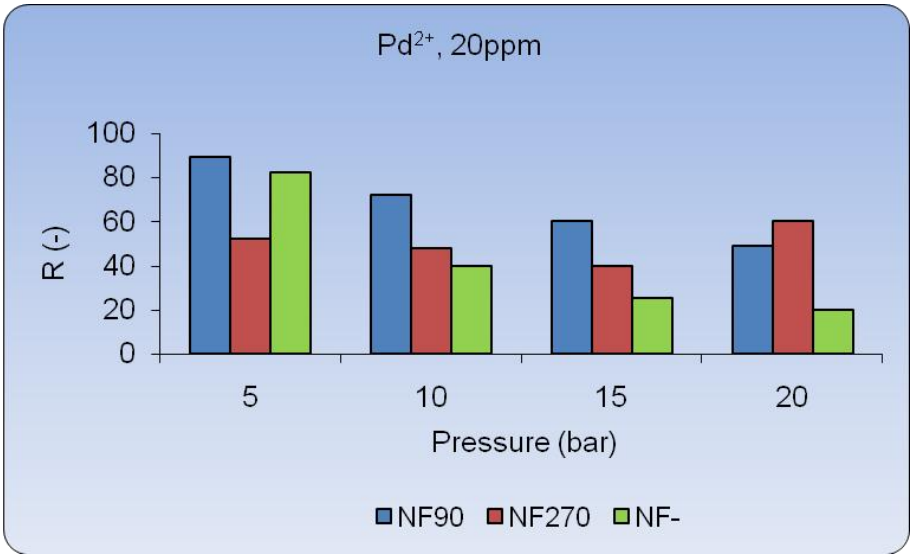

Figure 4.23 Plot of rejection vs pressure of $PdCl_2$ on NF membranes at 20 ppm.

Figure 4.23 shows that Pd^{2+} ion had a rejection of 89% and 74% at 5 bar and 10 bar respectively. 60% and 49% was rejected at 15 and 20 bar respectively on NF90. In the case of NF-, 81% and 40% rejections were achieved at 5 and 10 bar, while at 15 and 20 bar rejections decreased to 20% and 17%, respectively. It appears that rejection on the NF90 and NF- decreases as pressure increases. In the case of NF270, rejection of about 50% was achieved at 5, 10 and 15 bar respectively. At 20 bar, the rejection further decreased to 20%. At 20 ppm the performance amongst these three NF membranes indicates that, higher rejections were achieved on NF90 followed by NF- and NF270. The high rejection observed on NF90 with rough surface layer, was due to its small pore size [6]. The intermolecular repulsion between the solute and membrane surface layer, lead to high rejection behaviour of the membrane, since the membrane become positively charged at low pH causing repulsion of cations [4]. While for NF- with smooth surface layer, the rejection was influenced by its small pore size. In the case of NF270 with smooth surface layer, low rejections observed were due to its larger pore size. Similar results on NF90 and NF270 were also reported by Chuyang *et al*. [7]

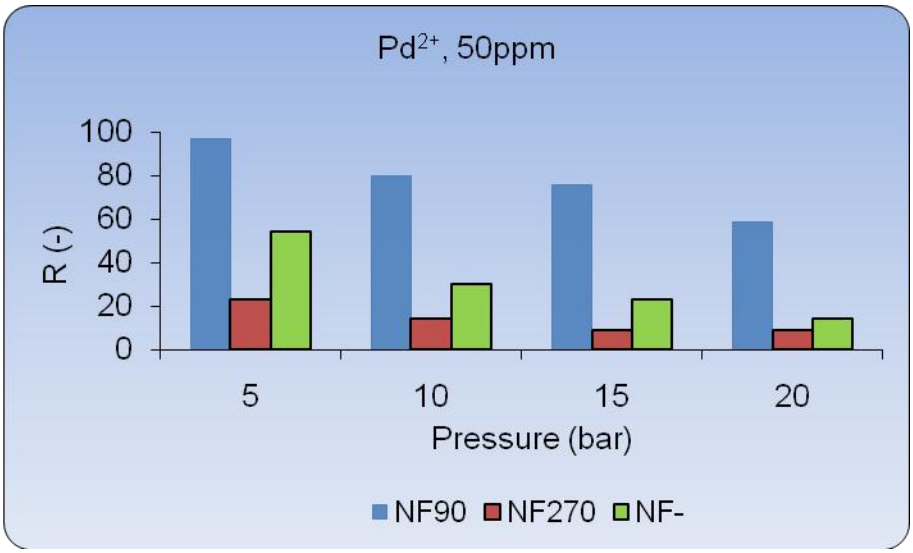

Figure 4.24 Plot vs rejection of $PdCl_2$ on NF membranes at 50 ppm.

At 50 ppm, a similar decreasing rejection trend of Pd^{2+} ion was also observed on NF90 membrane (Figure 4.24). Rejection of 96%, 80% and 79% were achieved at 5, 10 and 15 bar respectively. While at 20 bar a low rejection of 60% was observed. In the case of NF-, rejection of 58% and 39% were achieved at 5 and 10 bar respectively. As the pressure was increased from 15 to 20 bar, the rejection decreased further to about 20%. It appears that at 50 ppm, Pd^{2+} ion was highly rejected than at 20 ppm. This indicates that an electrostatic interaction of Pd^{2+} ion and the membrane surface at 50 ppm, seemed to be stronger than at 20 ppm. In the case of NF270, low rejection was obtained compared to NF-. Rejection of 20% at 5 bar was observed while at 10, 15 and 20 bar, rejections of less than 15% were achieved. The low rejections achieved by NF270 were also due to large pore size. The rejection observed after sequence was that NF90 > NF- > NF270 for Pd^{2+} ion.

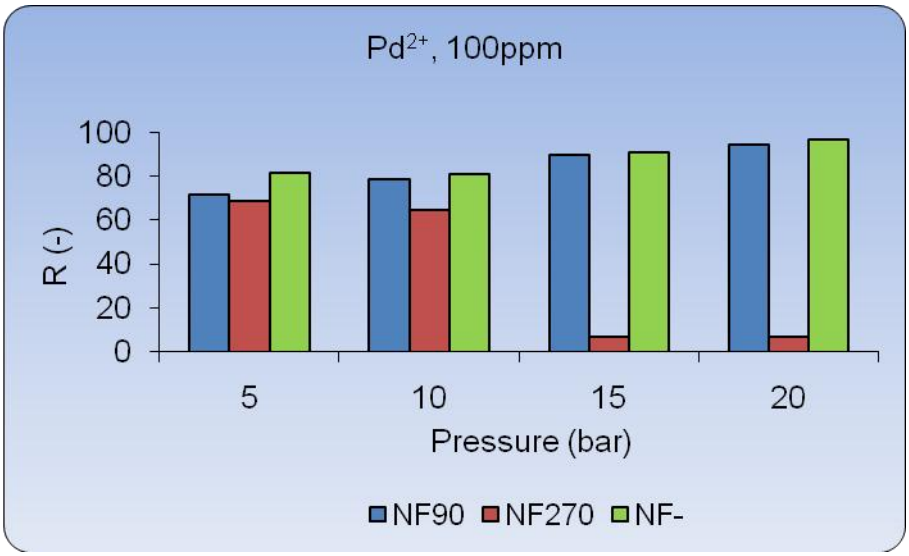

Figure 4.25 Plot of rejection vs pressure of $PdCl_2$ on NF membranes at 100 ppm.

At 100 ppm (Figure 4.25), an increasing rejection trend at varying pressure on NF90 and NF- was observed, unlike at 20 and 50 ppm. Rejection of 76% and 80% at 5 bar and 10 bar respectively, were achieved on NF90. While at 15 and 20 bar, the rejection increased from 82% to 95%. In the case of NF-, the rejection increased from ≈ 81% at 5 bar to ≈ 83% at 10 bar, respectively. Rejection of 90% and 93% were observed at 15 and 20 bar, respectively. It can be assumed that, an increase in rejection behaviour of these two membranes (NF90 and NF-) for Pd^{2+} ion was independent of the pressure applied.

Murphy and Chaudhai [8] reported similar results using Ni^{2+} ion and confirmed that an increase in rejection, was because the ion transportation due to convection becomes significant compared to diffusion. As for NF270, rejection of 72% and 70% were achieved at 5 and 10 bar. Interestingly, rejection decreased by about 65% at 15 and 20 bar. This low rejection performance on NF270 at 15 and 20 bar, was due to membrane's large pore sizes as it has been mentioned before. Therefore, this implies that some of Pd^{2+} and Cl^- ion went through the membrane.

4.10.2 Single salt rejection: *Pd^{4+}as $(NH_4)_2PdCl_6$*

The effect of rejection capacity for Pd^{4+} ion was compared to Pd^{2+} ion on NF membranes in order to investigate the influence of charge density. Figure 4.26 illustrate the rejection performances of Pd^{4+} ion on all membranes.

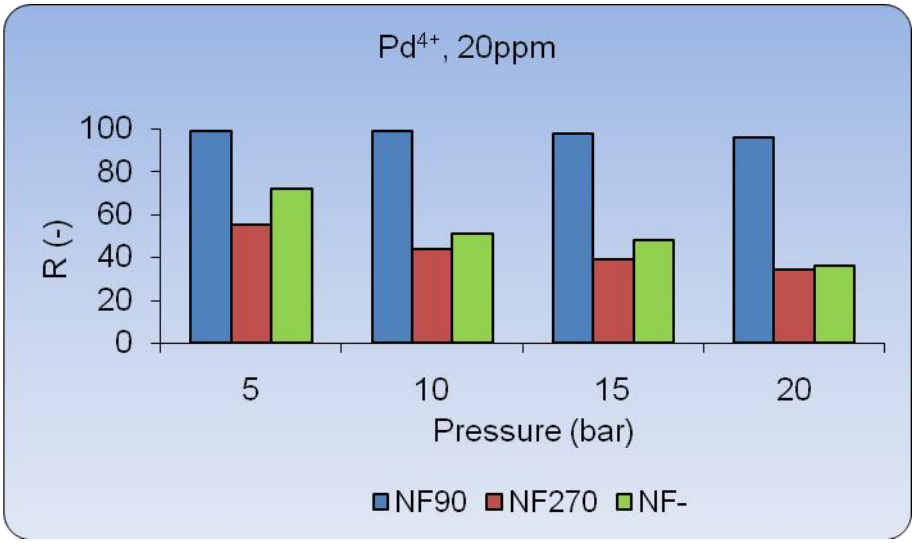

Figure 4.26 Plot of rejection vs pressure of $PdCl_6$ on NF membranes at 20 ppm.

In Figure 4.26, Pd^{4+} ion tends to have a constant rejection of ≈ 99,99%, from 5 to 20 bar on NF90. While NF- showed a slight decrease in rejection from 74% at 5 bar to 49% at 10 bar. Rejection decreased to ≈ 40% when the pressure was increased to 15 and 20 bar. In the case of NF270, a decrease in rejection of 52% and 40% at 5 and 20 bar respectively was achieved. Once again, NF90 proved to be the best performing membrane with high rejection of Pd^{4+} ion. Therefore, the high rejection of Pd^{4+} ion compared to Pd^{2+} ion was due to high ionic charge and solute size of the ions. Similar rejection sequence of Pd^{4+} ion, was found that NF90>NF->NF270 as with that for Pd^{2+} ion.

At 50 ppm (Figure 4.27), the constant rejection trend of 81% was observed from 5 to 20 bar on NF90. This suggests that NF90 is independent of pressure. However, NF- achieved rejection of 60% and 40% at 5 and 10 bar respectively. While at 15 and 20 bar (28% and 23%) were observed. While in the case of NF270, the membrane had a constant rejection of 25% from 10 to 20 bar. The rejection results for NF90 clearly show that, it is the best performing NF membranes amongst the three, due to its small pore size.

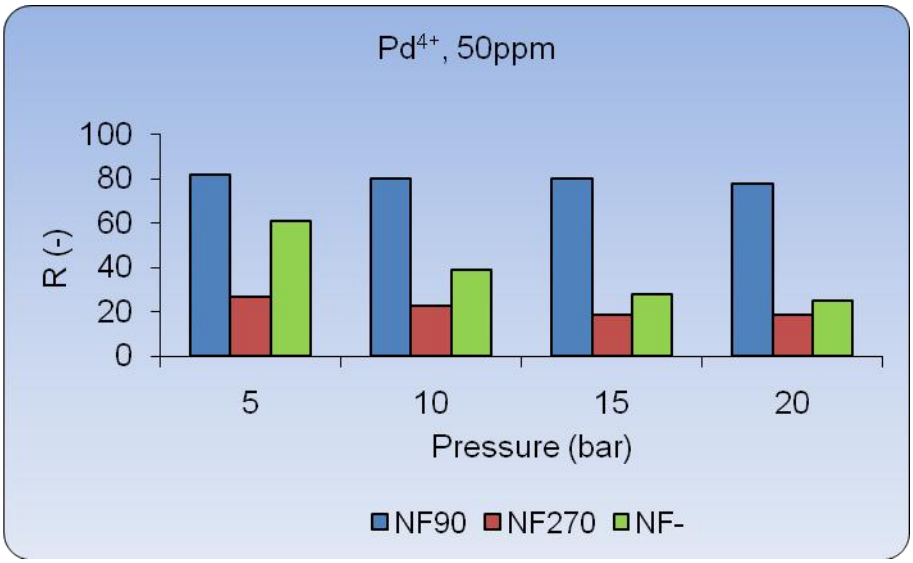

Figure 4.27 Plot of rejection vs pressure of $PdCl_6$ on NF membranes at 50 ppm.

At 100 ppm (Figure 4.28), rejection of ≈ 63% was observed at 5 and 10 bar on NF90. But the rejection of Pd^{4+} increased when the pressure was increased from 15 to 20 bar (80% and 93%) was observed. As for NF-, a slight decrease in rejection was observed when pressure was increased. The rejection of 40% and 35% at 5 and 10 bar were achieved respectively. However, at 5 and 20 bar, constant rejection of ≈ 35%, was achieved on this membrane.

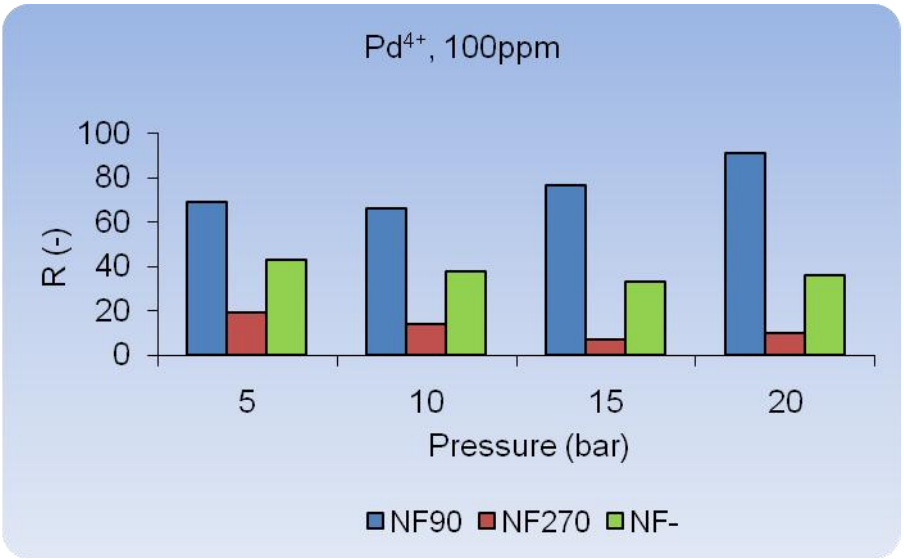

Figure 4.28 Plot of rejection vs pressure of $PdCl_6$ on NF membranes at 100 ppm.

Under the current conditions, this shows that these two NF membranes are concentration and pressure dependent. On the other hand NF270 showed rejections of 19% and 15% (5 and 10 bar), while 10% and 12% (15 and 20 bar) were observed. This decrease in rejection could also be associated with the possibility of concentration polarization accumulation, since high concentration leads to flux decline and low rejection performance of NF membranes [4, 9].

4.10.3 Single salt rejection: *Cu^+ as CuCl*

The monovalent ion (Na^+) tends to have a low rejection compared to multivalent ion (Mg^{2+}) due to their unequal ionic charge and solute size [10, 11]. Figure 4.29 shows the rejection ability of NF membranes for the monovalent (Cu^+) ion at 20 ppm.

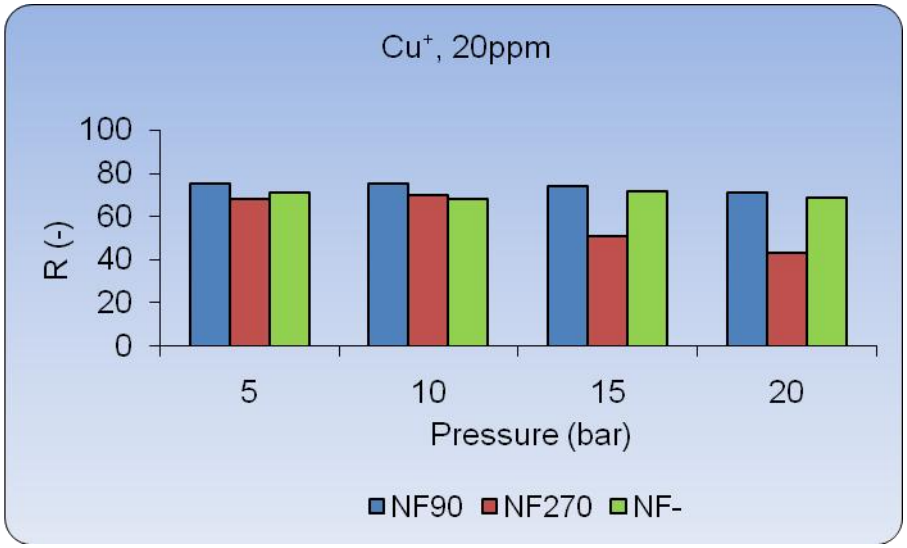

Figure 4.29 Plot of rejection vs pressure of CuCl on NF membranes at 20 ppm.

A constant rejection of ≈ 75% from 5 to 20 bar for Cu^+ ion, was achieved on NF90 (Figure 4.29). In the case of NF-, a constant rejection of ≈ 68% was achieved from 5 to 20 bar. However, NF270 had a slight lower rejection amongst the other two membranes, with about 68% (highest) and 43% (lowest) at 5 and 20 bar respectively. The rejection performances of the membrane on the monovalent ion (Cu^+), showed a low performance at 20 ppm. This was due to the fact that some Cu^+ ions went through the membrane as a result of small solute size and charge of the ion. This indicates that the pressure applied had little influence on the rejection of the monovalent ion.

At 50 ppm (Figure 4.30), an increasing rejection was observed as the pressure is increased. Rejection of 59% and 80% at (5 and 10 bar), was achieved, with constant rejection of 96% at 15 and 20 bar. In the case of NF- high rejection capacity of 96% and 95% was observed at 5 and 10 bar respectively. But a huge decrease in rejection performance of NF from 15 bar (R ≈ 15%) to 20 bar (R ≈ 40%) was observed. This huge decrease in rejection at (15 to 20 bar) could imply that, the membrane was adsorbing some of the Cu^+ and Cl^- ions, even though some went through membrane layers as permeate.

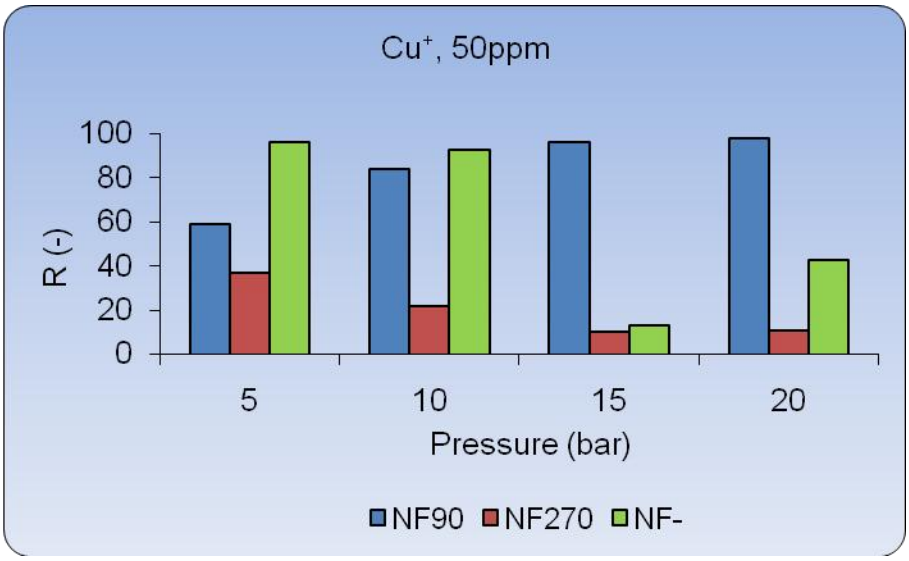

Figure 4.30 Plot of rejection vs pressure of CuCl on NF membranes at 50 ppm.

NF270 had a poor rejection performance of 37% and 11% at 5 bar and 20 bar respectively. At higher concentration (50 ppm) the rejection was high as compared to 20 ppm. This could be due to the fact that, the membrane had an easy passage for Cu^{+} ion to pass through polymeric membrane layers at 20 ppm, as compared to 50 ppm. In essence, the membrane (NF90 and NF-) pore sizes were occupied by ions as the concentration increases from 20 to 50 ppm which leads to high rejection measurements.

At 100 ppm (Figure 4.31), a very low rejection of Cu^{+} ion was achieved on NF90 and NF- membranes compared to 20 and 50 ppm. Rejection of 63% and 20% on NF90 were observed at 5 and 10 bar, respectively. But the rejection performance of the membrane decreased from 15% (15 bar) to 10% (20 bar). On other hand, NF- had a better rejection compared to NF90 achieving 77% and 70% at 5 and 10 bar respectively. While from 15 to 20 bar, a constant rejection of ≈ 43%, was achieved.

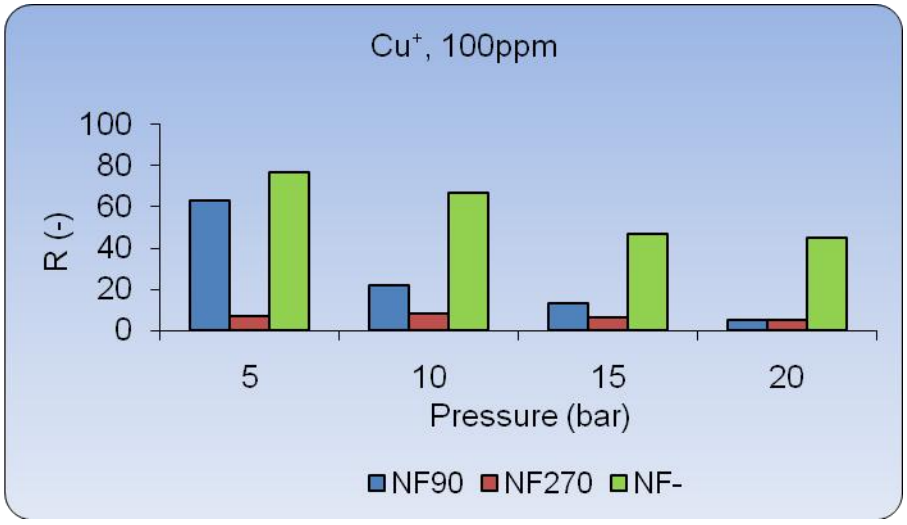

Figure 4.31 Plot of rejection vs pressure of CuCl on NF membranes at 100 ppm.

NF270 had a very low rejection of 7% at 5 bar, while it maintained a constant rejection of 5% from 10 to 20 bar. This could be related to the bigger pore size as seen with high flux measurement in Figure 4.5 in Section A (Chapter 4). Therefore, it can be reported that, high concentration solutions tend to lead to low rejection measurements on NF membranes as the pressure is increased. The lowest rejection of Cu^{+} ion at high concentration (100 ppm) level, could lead to concentration polarization or fouling accumulation as reported by Ahmad and Ooi [4].

4.10.4 Single salt rejection: *Cu^{2+} as $CuCl_2{\cdot}2H_2O$*

Rejection of Cu^{2+} ion as $CuSO_4$ has been previously reported using NF90-2540 nanofiltration membrane in an acidic medium [12, 13]. The response was satisfactory with the rejection of 98% achieved. In this study, the rejection of Cu^{2+} ion as $CuCl_2{\cdot}2H_2O$ is evaluated using NF90, NF270 and NF- membranes at pH 2.0 while varying concentrations and pressure. Figure 4.32 illustrates the rejection of Cu^{2+} ion on NF membranes at 20 ppm.

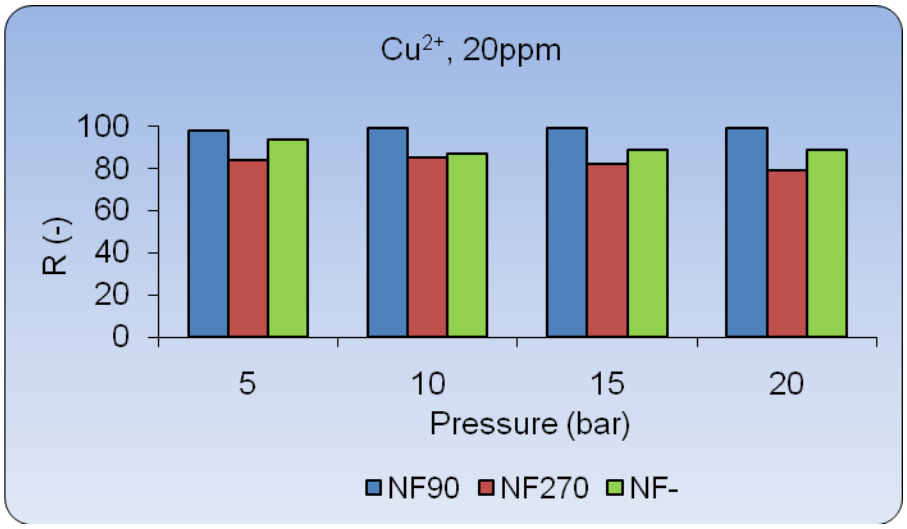

Figure 4.32 Plot of rejection vs of $CuCl_2$ on NF membranes at 20 ppm.

In Figure 4.32, a very high rejection on NF90 was achieved as the pressure was increased. Constant rejections of (98%) at pressure (5-20 bar), were achieved for Cu^{2+} on NF90. This implies that, the 2+ oxidation state of copper metal is not influenced by pressure as with Cu^{+} ion at 20 ppm. The high rejection of Cu^{2+} ion against Cu^{+} ion, is due to the fact that ionic charge and molecular weight of Cu^{2+} ion, is larger than that of Cu^{+} ion. However, NF270 and NF- achieved constant rejection trend of ≈90% from 5 to 20 bar. This high increase in rejection for Cu^{2+} ion was due to membrane surface layer charge density (positive at low pH) which could repel positive ion. This rejection was also influenced by the smallest pore size of the membrane. Similar results were obtained as reported by Karakulski *et al*. [12], and Ahmad *et al* [13].

Figure 4.33 indicates that at 50 ppm, rejection of 80% and 77% at (5 and 10 bar) for Cu^{2+} ion on NF90 were achieved. The rejection slightly decreased to 74% at 15 bar and 64% at 20 bar. The data shown in Figure 4.33, indicates that the rejection of the membrane is pressure and concentrations dependent. In the case of NF-, rejection of about 95% was achieved at 10 bar, while at 5 bar it was 85%, and at 20 bar (75%) was achieved.

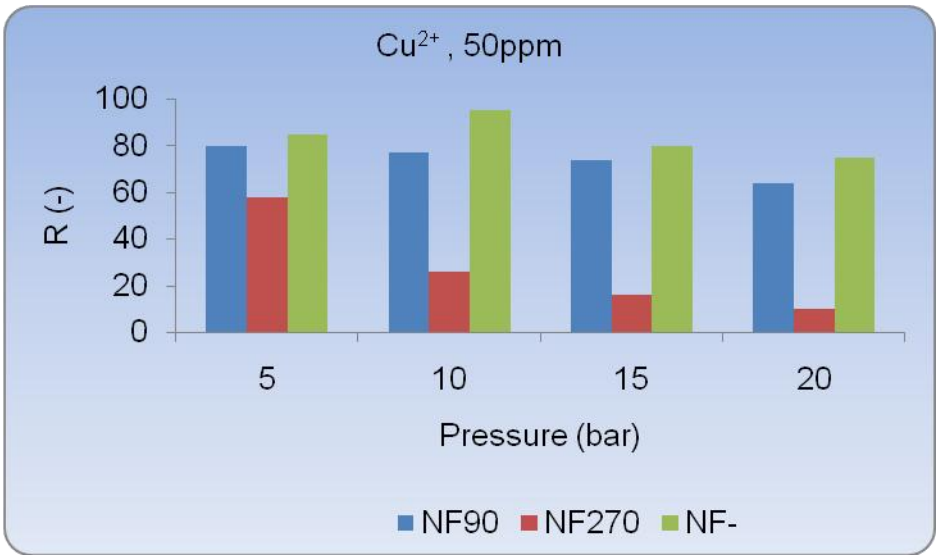

Figure 4.33 Plot of rejection vs pressure of $CuCl_2$ on NF membranes at 50 ppm.

If two rejection trends on 20 ppm and 50 ppm can be compared, it will indicate that at 20 ppm, there is high rejection as compared to 50 ppm. This means that, the passage of the solvent was favoured as compared to that of the solute, which remains quasi-constant [14]. The rejection on NF270 was 58% and 26% at 5 and 10 bar respectively, while 16% and 10% were achieved at 15 and 20 bar, respectively. Again, NF270 performed poorly compared to other NF membranes due to its large pore sizes.

At 100 ppm (Figure 4.34), rejection of 80% (5 bar) and 77% (10 bar) for Cu^{2+} ion, was observed on NF90. While 15 bar and 20 bar, a constant rejection of 70% was achieved. It is clear that, the decrease in rejection trend at 100 ppm, was not much as compared to Cu^{+}, Pd^{2+} and Pd^{4+} ions on NF90. In the case of NF-, constant rejection of (85%) for Cu^{2+} ion was observed from 5 bar to 20 bar.

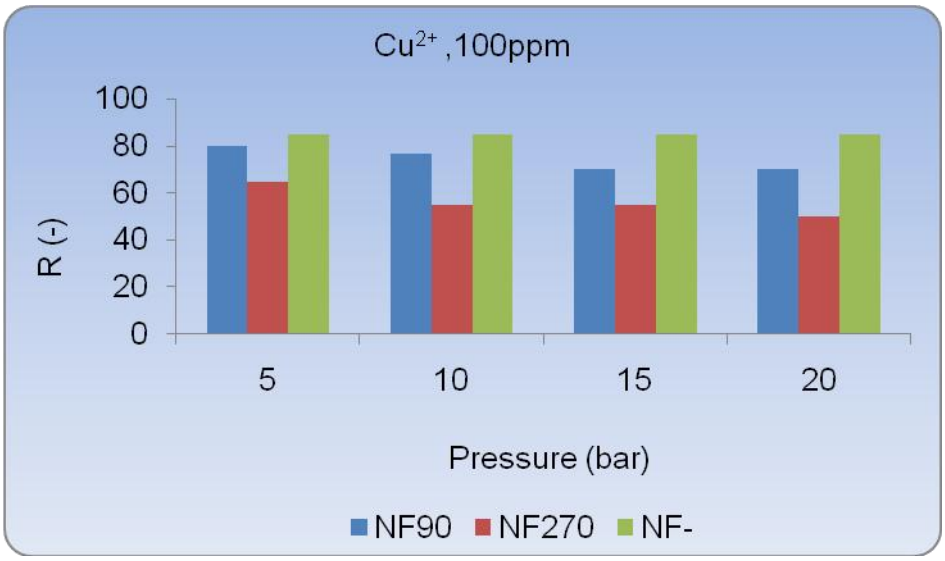

Figure 4.34 Plot of rejection vs pressure of $CuCl_2$ on NF membranes at 100 ppm.

The performance of NF- shows that, pressure did not have any major influence during rejection behaviour of the membrane. In the case of NF270, the rejection was also low with about 65% (5 bar) and 55% (10 and 15 bar), and at 20 bar (50%). Therefore, it can also be mentioned that, high concentration exposed on NF membranes can lead to possibility of fouling the membrane. This can also lead to flux decline and low rejection percentage. In general, rejection of Cu^{+} against Cu^{2+} ion is lower with regard to the solute size.

4.10.5 Single salt rejection: *Ni^{2+} as $NiCl_2{\cdot}6H_2O$*

The rejection of Ni^{2+} ion as $NiCl_2{\cdot}6H_2O$ is evaluated using NF90, NF270 and NF- membranes at pH 2.0 while varying concentrations and pressure. Figure 4.35, illustrate the rejection behaviour of the membranes at 20 ppm.

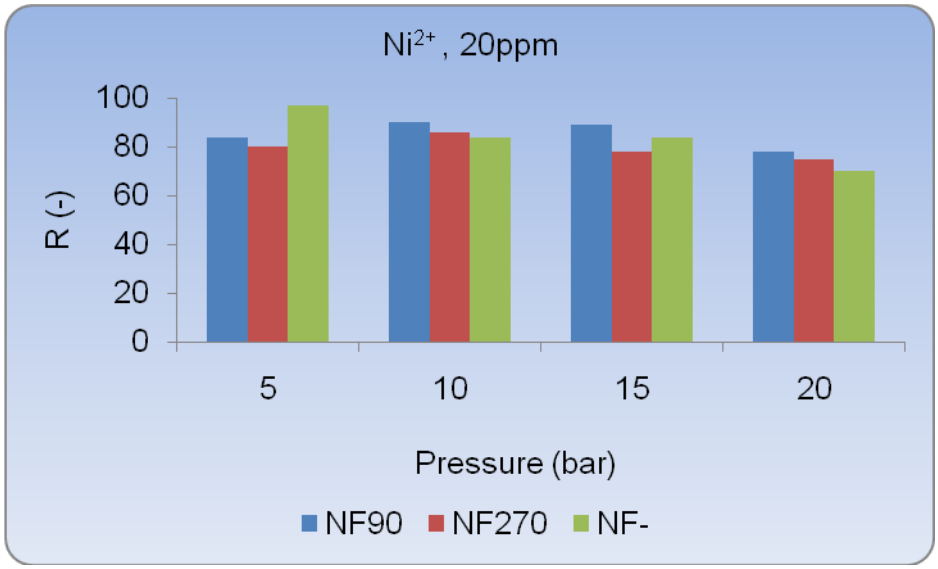

Figure 4.35 Plot of rejection vs pressure of $NiCl_2$ on NF membranes at 20 ppm.

At 20 ppm (Figure 4.35), R=84% and R=90% at 5 and 10 bar respectively, were obtained on NF90. At 10 and 15 bar, the rejection value shows a constant rejection, but decrease at 20 bar. This could be interpreted that due to the strong interaction between membrane material (surface layer) and the solute, has tendency to increase the rejection capacity of the membrane. On the other hand, NF- rejection of 97% (highest) at 5 bar and adopted a constant rejection trend of 84% at 10 and 15 bar respectively, but the rejection decreased to 70% at 20 bar. As for NF270, the membrane proved to have a better rejection performance in the range of 80% and 75% at 5 and 20 bar. The high charge density of the membrane (NF270), resulted in an increase in rejection ability.

In Figure 4.36, a constant rejection of 98% was achieved on both NF90 and NF- membranes from 5 to 20 bar at 50 ppm. In essence, both membranes were not influenced by concentration, and their predicted pore sizes are close as seen during water flux measurement in Figure 4.2 Section A (Chapter 4). But in the case of NF270, slight decrease in rejection from 61% (5 bar) to 56% at (10 bar), were obtained. The large pore size of NF270, lead to a low rejection performance of the membrane.

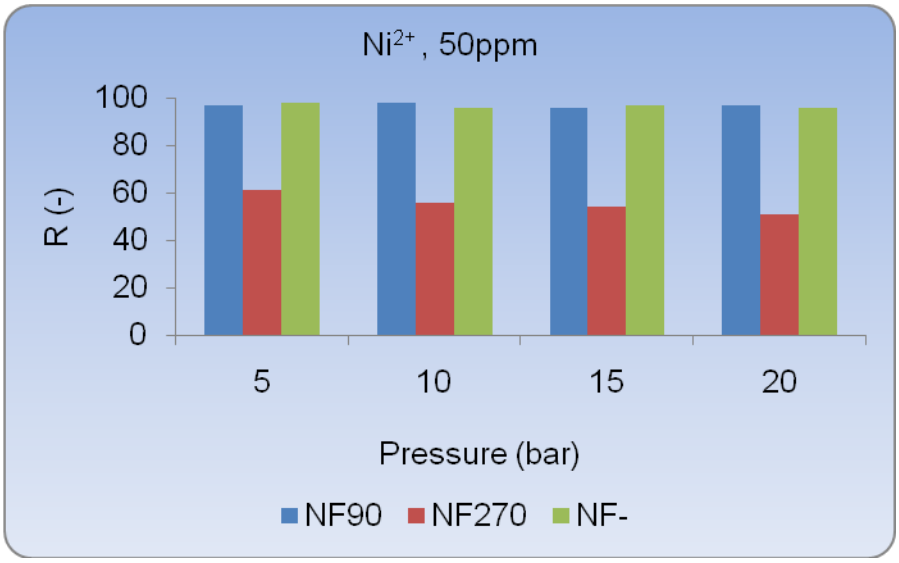

Figure 4.36 Plot of rejection vs pressure of $NiCl_2$ on NF membranes at 50 ppm.

At 100 ppm (Figure 4.37), NF90 had high rejection of Ni^{2+} ion compared to Cu^{2+} and Pd^{2+}. A constant rejection of ≈ 98% from 5 to 15 bar was achieved. While at 20 bar, 85% in rejection was observed. On the other hand, NF- had 92% and 78% at 5 and 10 bar respectively. But at 15 bar, the rejection increased slightly to ≈ 96%, while at 20 bar it decreased to 80%. This shows that, the rejection in this membrane is dependent on pressure. But in the case of NF270, rejection of 85% (highest) at 5 bar and 50% (lowest) at 20 bar, were achieved.

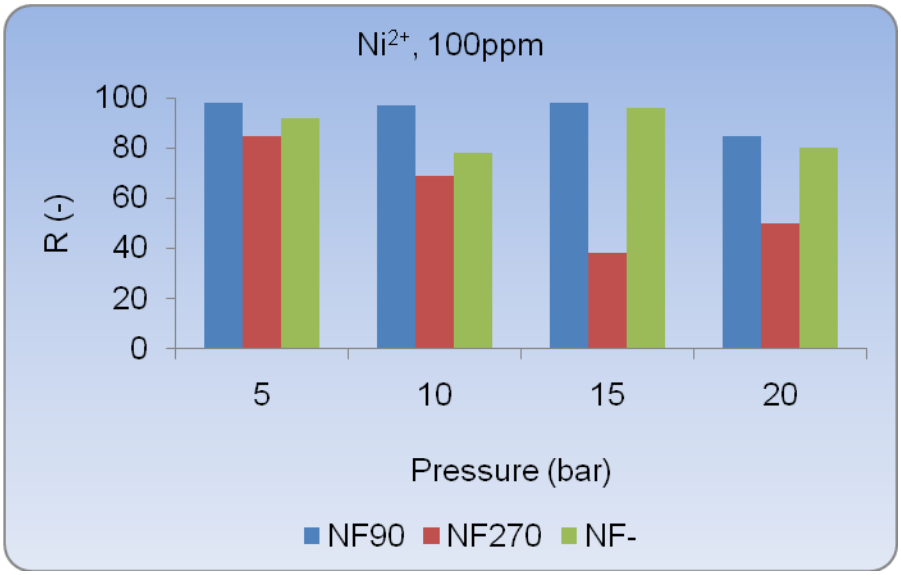

Figure 4.37 Plot of rejection vs pressure of $NiCl_2$ on NF membranes at 100 ppm.

The high concentration tends to lead to low rejection, especially in the case of NF270. In essence, this situation can cause fouling depending on the nature and stability of the ion when increasing an applied pressure. In another study [15] it was also observed that NF90 rejected Ni^{2+} ion higher than NF- at pH 2.4 than at pH 3.2. This was due an increase in protonation of H^+ in a solution mixture at pH 2.4. Murphy and Chaudhari [8] observed similar rejection trend and reported that, the rejection of Ni^{2+} ion decreases when the concentration of the feed solution increases.

4.10.6 Single salt rejection: *Ag^+ as AgCl*

The effect of single salt (AgCl) on NF membranes was investigated with the view of monitoring the movement of Ag^+ ion in the membrane. The rejection of Ag^+ ion, were done at varying pressure and concentration as illustrated in Figure 4.38.

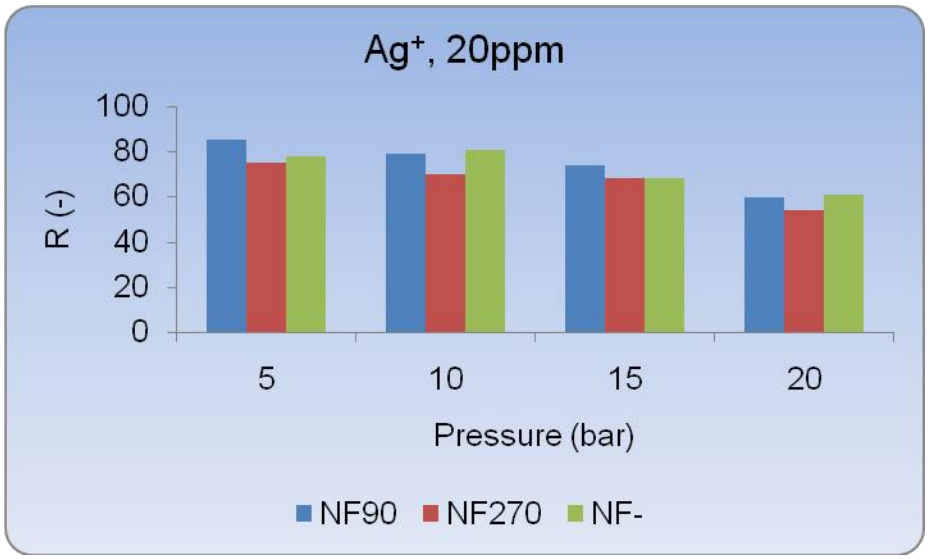

Figure 4.38 Plot of rejection vs pressure of AgCl on NF membranes at 20 ppm.

In Figure 4.38 (20 ppm), NF90 had the rejection of 85% and 79% at 5 bar and 10 bar respectively, 76% and 60% were achieved at 15 and 20 bar respectively for Ag^+ ion. While for NF-, rejection of 78%, 80% and 70% were observed at 5, 10 and 15 bar, respectively. In this case, the rejection was not huge. But at 20 bar, 60% was achieved as the lowest rejection. However, in the case of NF270 the rejection was 76% at 5 bar and 59% at 20 bar. Again NF270 performed poorly as compared to the other two NF membranes, due to its large pore sizes. Therefore, amongst all membrane tested in the study, NF270 is not the suitable membrane for the filtration of metal ions.

At 50 ppm (Figure 4.39), NF90 had a constant rejection of ≈ 90% from 5 bar to 20 bar. The high rejection observed is due to high molecular weight of the ion as compare to Cu^+ ion. While in the case of NF-, rejection of 90% and 87% at 5 and 10 bar respectively, were observed. As the pressure increases from 15 bar to 20 bar, the rejection decreased drastically to 20%.

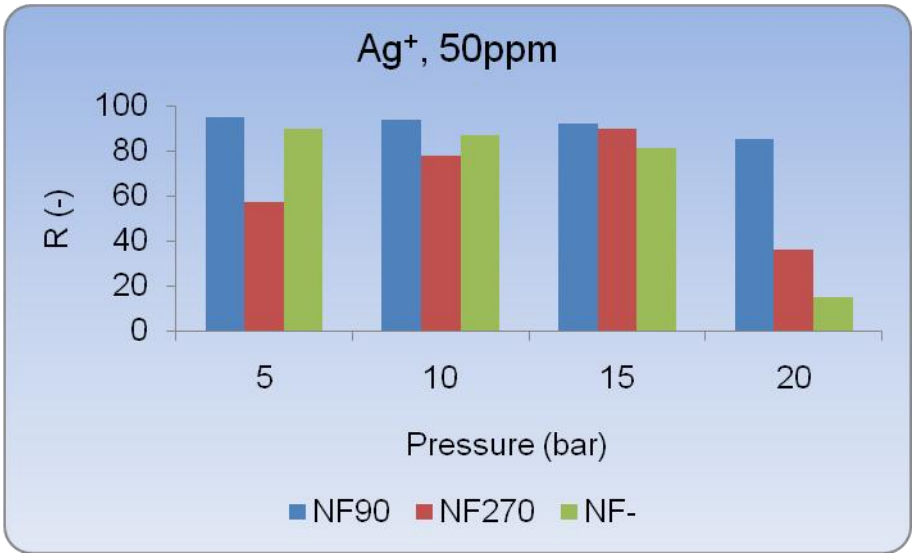

Figure 4.39 Plot of rejection vs pressure of AgCl on NF membranes at 50 ppm.

NF270 also performed poorly amongst the three membranes due to its large pore sizes. This membrane achieved 58% and 77% at 5 bar and 10 bar respectively, with 90% (highest) at 15 bar and 38% (lowest) at 20 bar. NF90 and NF- seems to be the best membranes for metal ions rejection compared to NF270 during membranes processes. This is because the pore sizes for NF270 are large enough to allow some of the metal ions to pass through as permeate [5].

Figure 4.40 illustrates that at 100 ppm, NF90 showed a decreasing trend in rejection of Ag^+ ion from 5 to 20 bar. Constant rejection of 79% at 5 and 10 bar was observed. While a decrease in rejection from 43% at 5 bar to 17% at 20 bar, were achieved. While NF-, rejected 85% at 5 bar and 76% at 15 bar respectively. This rejection behaviour was influenced by concentration as the pressure increases. Both NF90 and NF-, has shown a dependency of pressure.

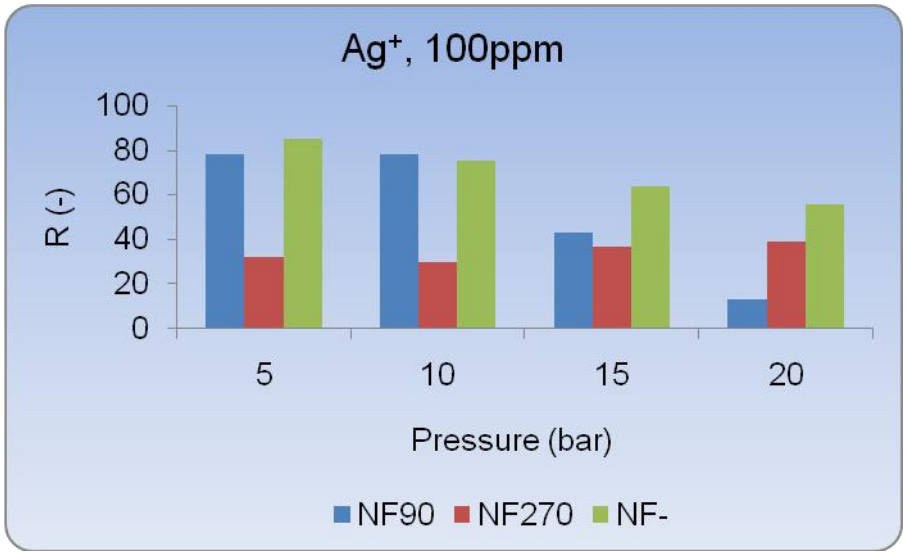

Figure 4.40 Plot of rejection vs pressure of AgCl on NF membranes at 100 ppm.

In the case of NF270, less than 40% of Ag^+ ion was rejected, while Cl^- ion was transported through the membrane as permeate due to counter ion with the membrane surface layer and small ionic charge. As a result, monovalent ions are rejected lower than divalent and multivalent ions [16].

4.11 Effects of pH on NF90 rejection

The polymeric membrane (NF90) has generally proven to be the best performing membrane compared to NF- and NF270. This has to do with the small pore sizes and membrane's surface charge density layer. This membrane (NF90), has a positive charge at low pH. Negative charge tendencies are also gained at high pH [17]. This is due to the charge of the amide group on the membrane surface. According to water permeability study on NF membrane in Section A (Chapter 4), NF90 has larger pore size density compared to NF-. Figure 4.41, illustrate pH influence on the rejection of metal ions (Pd^{2+}, Cu^{2+} and Ni^{2+}) performed at 5 bar.

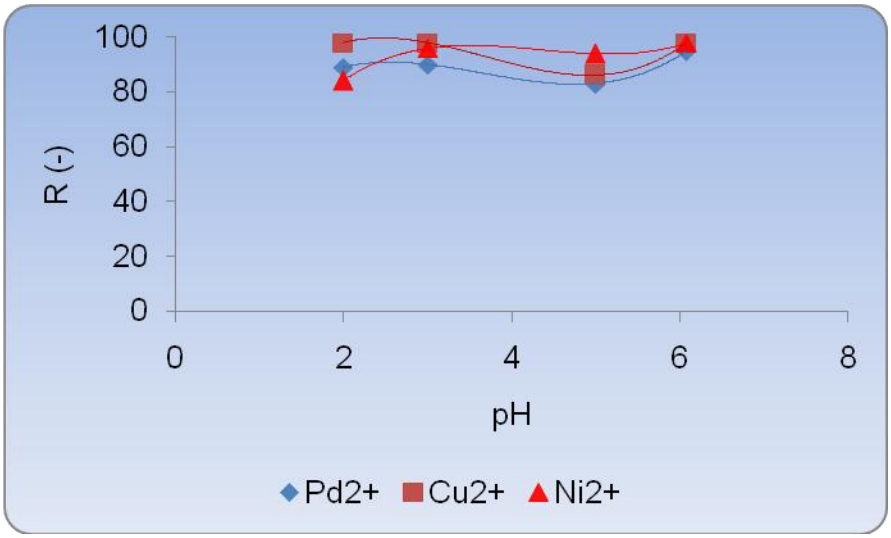

Figure 4.41 Plot of rejection vs pH of ionic metals at varying pH on NF90 at 5 bar.

In Figure 4.41, Cu^{2+} ion shows an almost S-shaped like from pH 2.0 to 6.1. Rejection of 98% was achieved between pH 2.0 and 3.0. A lower pH and hence higher H^{+} concentration will cause an electric double layer of positive charges on the membrane surface [18]. But a slight decrease in rejection between pH 3.0 and 5.0 was observed with an increase at pH 6.1. A slight decrease in rejection at pH 3.0 indicates an isoelectric point (IOP), which is a net or zero charge of the membrane. This IOP was also observed during rejection of charged solutes (NaCl and $MgCl_2$) in Section A (Chapter 4). At pH 6.1, the solution of metal ions precipitated. This was caused by an increase in Cl^{-}content with increasing pH level, which resulted in fouling the membrane pores. It could also be caused by tendency of metal ions to undergo reduction/oxidation into other states. Similar S-shaped trend like was found for Pd^{2+} and Cu^{2+} ions. Pd^{2+} ion had rejection of about 89%, and was less compared to Cu^{2+} ion which had a rejection of about 98% at pH 2.0. Though Pd^{2+} has high molecular weight compared to Cu^{2+} ion, the membrane charge density could also be responsible for Pd^{2+} ion during membrane separation process.

As for Ni^{2+} ion, an opposite rejection trend was observed to that of Pd^{2+} and Cu^{2+} ion. Even though it has been mentioned that at pH 6.1, precipitate is formed in a solution

during rejection experiments, it was observed that Ni^{2+} ion resulted in high rejection on the membrane (NF90). Precipitation formation or fouling on the membrane surface reduces the membrane's life-time, while causing slow movement of ion to pass through the membrane. Therefore, rejection of these metal ions on the NF90 membrane shows a dependence on pH. Generally, pH has an influence in separation and rejection membrane processes.

4.12 Binary mixtures

4.12.1 Salt rejection: Rejection of $PdCl_2/CuCl_2$ (Pd^{2+}/Cu^{2+})

The binary salt ($PdCl_2/CuCl_2$) mixtures of 20 ppm each were exposed and filtered on NF90 and NF- membranes at pH 2.0. The results are shown in Figure 4.42 and Figure 4.43. NF90 and NF- membranes gave satisfactory rejection. This was generally proven for metal ions rejection from Figure 4.24 to Figure 4.34. It is clear NF270 membrane is not good for rejecting metal ions. An example of NF270 membrane's poor performance was shown in Figure 4.27 (Section 4.10.2) for CuCl rejection at 100 ppm. The rejection for CuCl as Cu^{+} ion on NF270 was the poorest amongst all metal ions rejection. Therefore, NF270 will be excluded during binary and trinary solution mixture experiments.

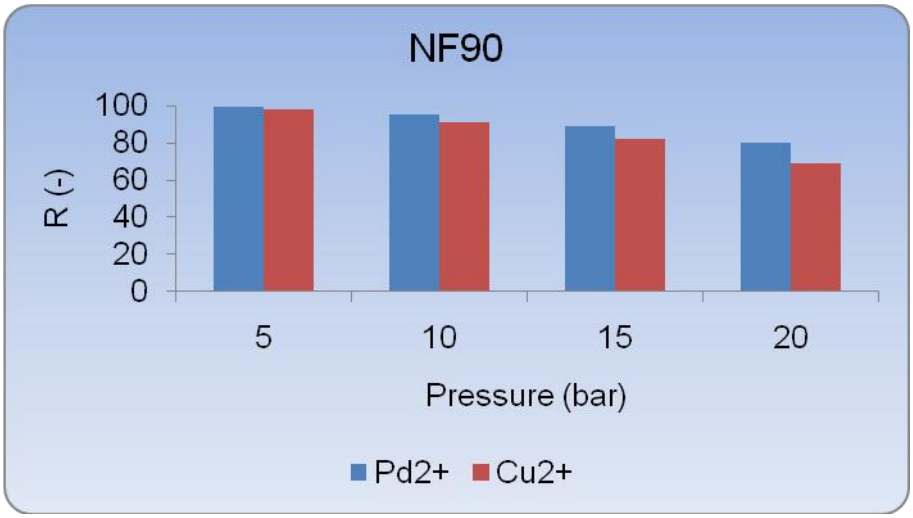

Figure 4.42 Plot of rejection vs pressure of $PdCl_2/CuCl_2$ on NF90 at 20 ppm.

At 20 ppm (Figure 4.42), Pd^{2+} ion had high rejection of 98% and 95% on NF90, at 5 and 10 bar respectively. The rejection slightly decreases at 15 bar (92%) and 20 bar (90%). The same rejection trend was observed for Cu^{2+} ion with, rejection of 96% (5 bar) and 94% (10 bar), respectively. These results indicate that, Pd^{2+} ion is lower as compared to Cu^{2+} ion, which lead to an increase in rejection of Pd^{2+} ion than that of Cu^{2+} ion.

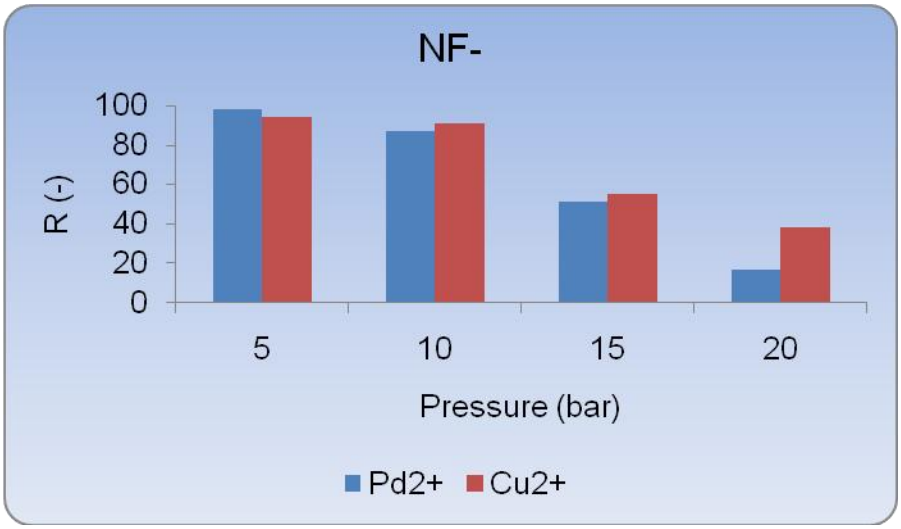

Figure 4.43 Plot of rejection vs pressure of $PdCl_2/CuCl_2$ on NF- at 20 ppm.

In the case of NF- (Figure 4.43), Cu^{2+} ion seems to be permeating more as compared to Pd^{2+} ion. As a result, an increase in pressure leads to a decrease in rejection of the Cu^{2+} ion. Rejection on NF- of between 95% and 97% at (5 -10 bar), were achieved while 45% and 38% were observed at 15 bar and 20 bar respectively. On the other hand, rejection of Pd^{2+} ion on NF- was 99.1% at 5 bar and 93% at 10 bar respectively. While from 10 bar to 20 bar, the membrane's performance for Pd^{2+} ion decreased to about 51% (15 bar) and 19% (20 bar).

In general, distribution movement of Cu^{2+} ion seems to be lower than that of Pd^{2+} ion, which resulted in higher Cu^{2+} ion rejection than Pd^{2+} ion. This had to do with the metal ions molecular weight.

4.12.2 Rejection of $PdCl_2/NiCl_2$ (Pd^{2+}/Ni^{2+})

The difference in rejection of the two ions (Pd^{2+} and Ni^{2+}) in a binary mixture was evaluated on two NF membranes. Figure 4.44 and Figure 4.45 illustrates the rejection of these ions as binary mixture at 20 ppm.

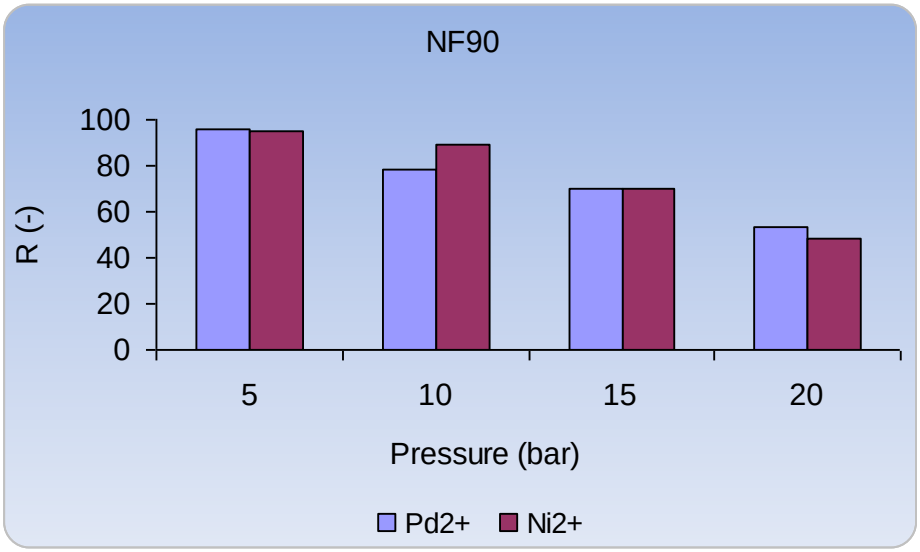

Figure 4.44 Plot of rejection vs pressure of $PdCl_2/NiCl_2$ on NF90 at 20 ppm.

In Figure 4.44, highest Pd^{2+} ion rejection of 98% and 80% at 5 and 10 bar were observed on NF90. While at 15 and 20 bar, 72% and 45%, were achieved respectively. In the case of Ni^{2+} ion, 96% and 90% at (5 and 10 bar) were observed, while for 15 and 20 bar, 70% and 56% was obtained. However, distribution movement of Pd^{2+} ion was low compared to Ni^{2+} ion. This had to do with the charge and molecular weight of Pd^{2+} ion which resulted in high rejection than Ni^{2+} ion.

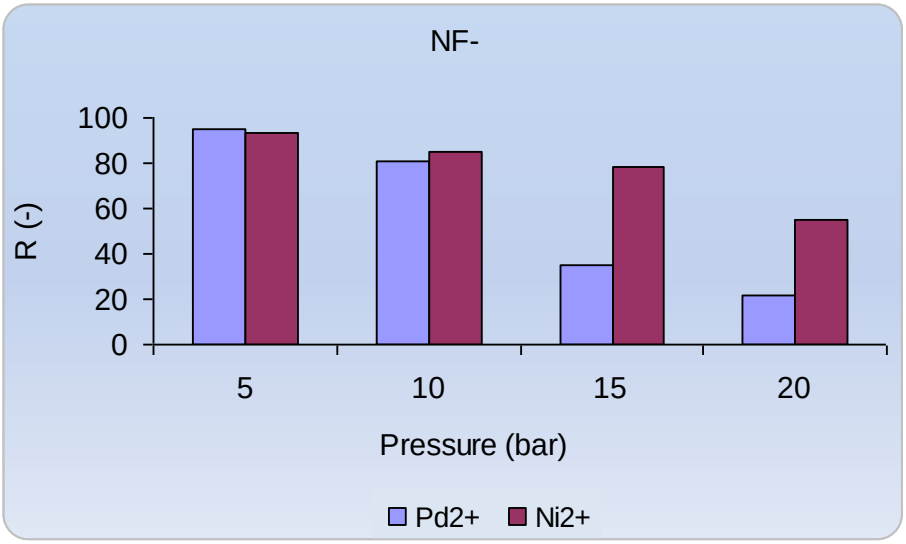

Figure 4.45 Plot of rejection vs pressure of $PdCl_2/NiCl_2$ on NF- at 20 ppm.

In the case of NF- (Figure 4.45), Ni^{2+} ion mostly dominated in rejection as compared to Pd^{2+} ion. Rejections of 96% at 5 bar and 60% at 20 bar, were achieved respectively. As for Pd^{2+} ion, 98% was rejected at 5 bar and 23% at 20 bar. In this case, Ni^{2+} ion was favoured by NF-. Therefore, high rejection on NF membranes is not only based on molecular weight but also the charge of the ion [19].

4.12.3 Rejection of $CuCl_2/NiCl_2$ (Cu^{2+}/Ni^{2+})

Mohsen-Nia *et al.* [20] employed reverse osmosis (RO) membrane for removing Cu^{2+} and Ni^{2+} as binary mixtures and reported that, 98% of metal ions were recovered at low pressure. Figure 4.46 and Figure 4.47, indicate the rejection capability of NF90 and NF- on binary solution mixtures of Cu^{2+} and Ni^{2+} ions for varying pressure (5, 10, 15 and 20 bar) and 20 ppm.

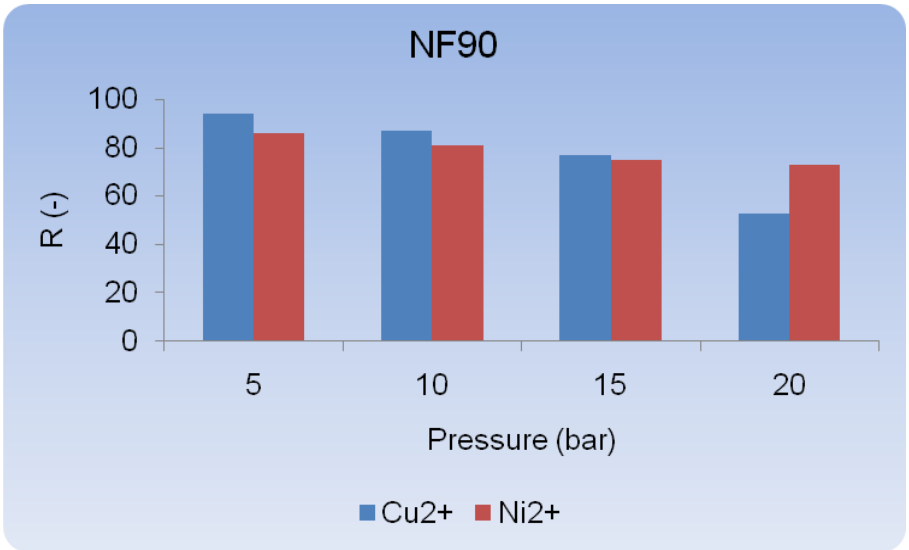

Figure 4.46 Plot of rejection vs pressure $CuCl_2/NiCl_2$ on NF90 at 20 ppm.

In Figure 4.46, rejection of both metal ions seems to have similar decreasing trend with increasing pressure on NF90. Rejection of 97% and 87% at 5 and 10 bar respectively, were observed for Cu^{2+} ion. As the pressure was increasing at (15-20 bar), 88% and 50% rejections were achieved. On the other hand, rejection of Ni^{2+} ion was 86% (5 bar) and 81% (10 bar), while at 15 bar (78%) and 20 bar (75%) were achieved. As a result, Cu^{2+} ion was rejected the most throughout the entire applied pressure, except at 20 bar.

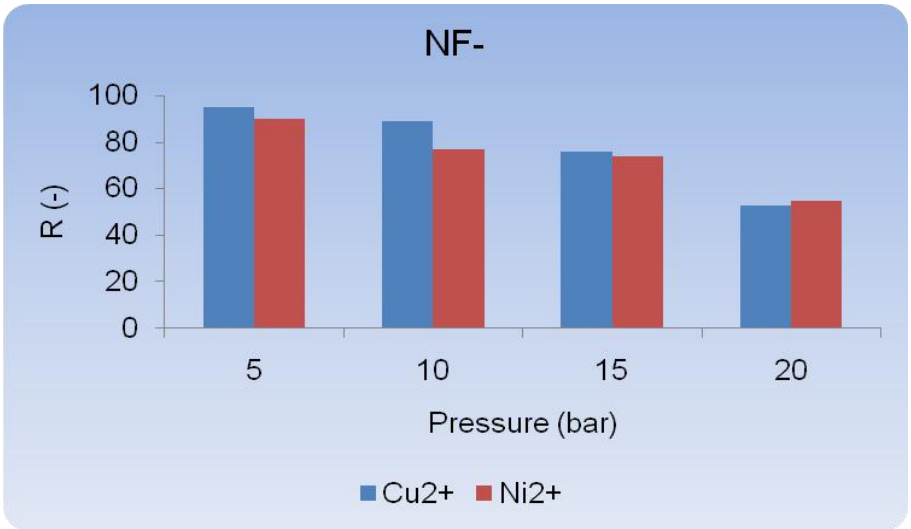

Figure 4.47 Plot of rejection vs pressure ($CuCl_2$/$NiCl_2$) on NF- at 20 ppm.

As for NF- (Figure 4.47), rejection of Cu^{2+} ion was also high with rejection of 95% and 88% at 5 bar and 10 bar, respectively. But Ni^{2+} ion, was lessly rejected with <95% and <40% also at 5 bar and 20 bar. This implies that, an ion with a high molecular weight (Cu^{2+}) was highly rejected as compared to (Ni^{2+}). These results correspond with the one reported by Mohsen-Nia *et al.* [20]. Under acidic condition, the membranes are able to perform best at low pressure and concentration levels. However, the charge density of the polymeric membrane also determines the rejection capacity of the ions.

4.13 Trinary salt mixture:

4.13.1 Salt rejection: $PdCl_2$/$NiCl_2$/$CuCl_2$ (Pd^{2+}/Ni^{2+}/Cu^{2+})

Investigations of rejection of “trinary” salt mixture using NF membrane have not been considered much. The competition amongst metal ions in the same solution is monitored, using ion distribution mechanism (Donnan exclusion) during co-ions analysis. The concentrations of the solution considered were 20 ppm and 100 ppm at

pH 2.0. However, the solution at pH 5.0 was ignored, since it lead to precipitation on the membrane top layer due to an increase in chloride (Cl^-) content and subsequent fouling.

Figure 4.48, indicates the rejection of three metal ions (Cu^{2+}, Ni^{2+} and Pd^{2+}) on NF membranes. All ions had the rejection of ≈ 97% on 20 ppm at low applied pressure of 5 bar. But the rejection decreased as the pressure was increased. This showed that, at lower pressure the membrane performs best during rejection. In the case of Pd^{2+} ion, the rejection was constant with ≈ 96% from 5 bar to 15 bar, and ended with 65% rejection at higher pressures. Ni^{2+} and Cu^{2+} ion shared the same deceasing rejection trend from 5 bar to 20 bar with increasing pressure. This implies that, NF membranes are able to reject metals better at low concentration solution and at low pressures.

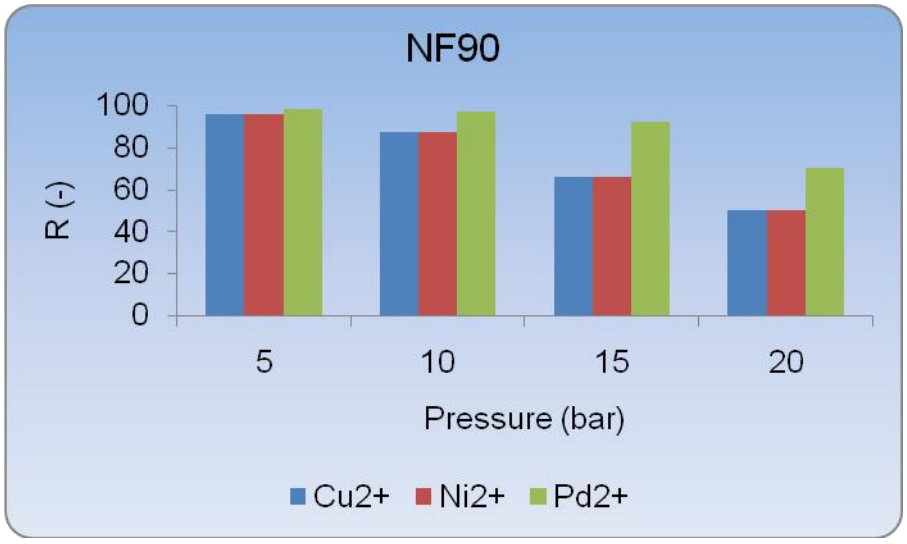

Figure 4.48 Plot of rejection vs pressure of $PdCl_2$/$NiCl_2$/$CuCl_2$ on NF90, 20 ppm.

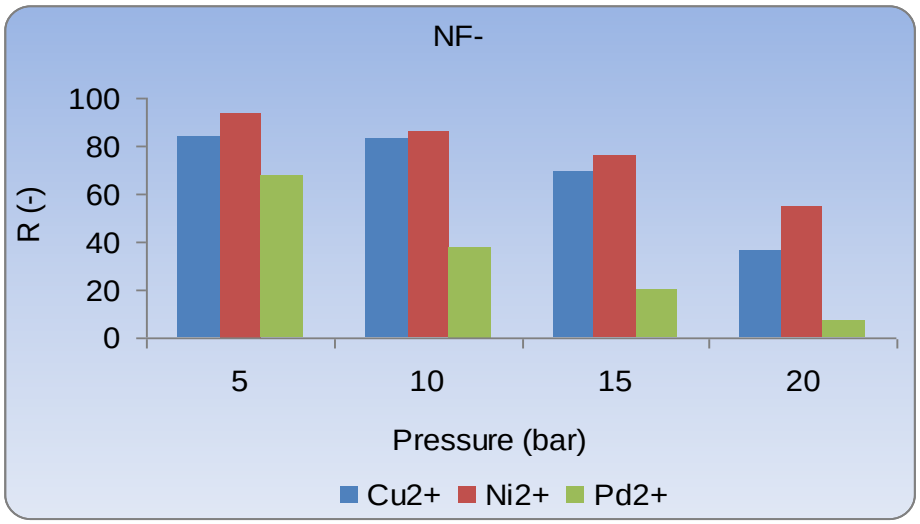

Figure 4.49 Plot of rejection vs pressure $PdCl_2/NiCl_2/CuCl_2$ on NF-, 20 ppm.

NF- shows a decrease in rejection of all ions as shown in Figure 4.49. Ni^{2+} ion remained highly rejected from low to high pressure applied. But Pd^{2+} ion which was expected to be highly rejected due to its high molecular weight exhibited low rejection. As for Cu^{2+} ion, the rejection was 90% at 5 bar but decreased to 58% at 20 bar. It can be explained that, the charge density of Ni^{2+} ion is less strong than that of Pd^{2+} and Cu^{2+} ions when they are all in a solution mixture and at these conditions. This could also be because, an electrostatic interaction between the membrane and the solute, was reduced by the functional group (NH^-) that make up the surface charge.

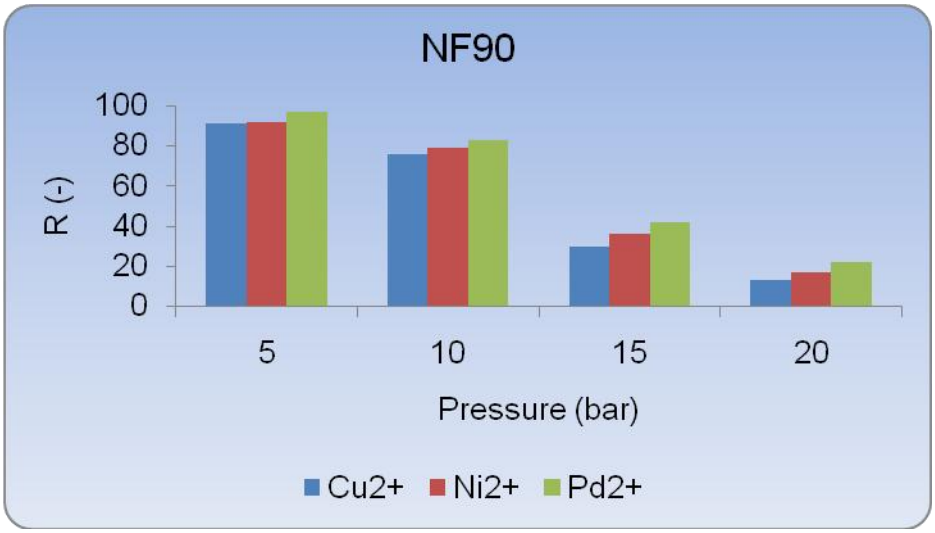

Figure 4.50 Plot of rejection vs pressure of $PdCl_2/NiCl_2/CuCl_2$ on NF90, 100 ppm.

In Figure 4.50, NF90 had highest rejection of about 100% for Pd^{2+} ion at 5 bar when the pressure was increased at 100 ppm. But a low rejection was observed at high pressures. Ni^{2+} and Cu^{2+} were rejected with about < 95% as compared to Pd^{2+} ion at low pressures (5 bar). These results are comparable to NF- membrane at 100 ppm. This indicates that their rejection of metal ions on these NF membranes, are independent of concentration but dependent on the pressure applied at this conditions.

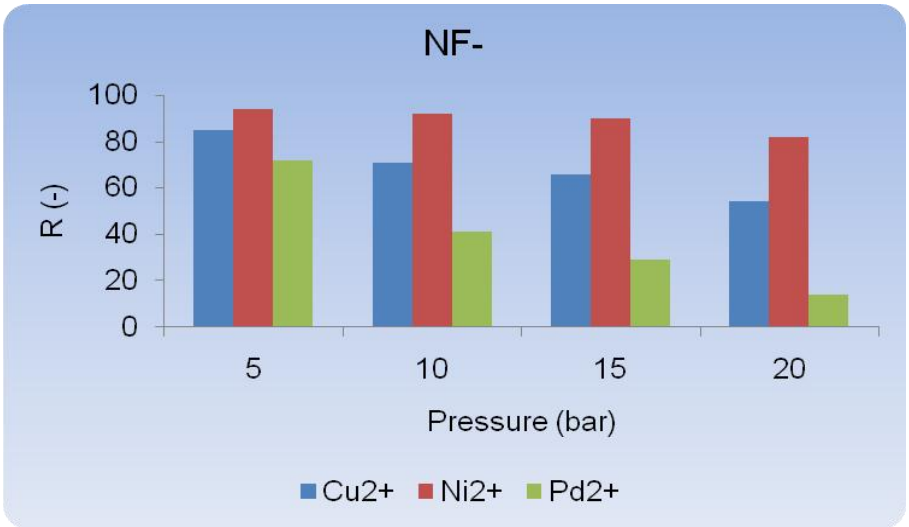

Figure 4.51 Plot of rejection vs pressure for $PdCl_2/NiCl_2/CuCl_2$ on NF-, 100 ppm.

In the case of NF- (Figure 4.51), the highest rejections are associated with low concentration solution mixtures and varying pressure applications. Ni^{2+} ion rejection was < 95%, while that of Cu^{2+} ion was < 90% followed by Pd^{2+} ion with < 80%. Therefore, the sequence of the rejection trend follows that $Ni^{2+} > Cu^{2+} > Pd^{2+}$ ion at 100 ppm. The permeation of ions on the membrane is dependent of molecular weight of the solute or salt solution.

In general, high concentration solution exposure to the membrane, can lead to either higher or lower rejection capacity. This also depends on the charge density on the membrane surface material. Therefore, lower concentration solution and applied pressure conditions during membrane separation processes; result in high rejection performances of NF membranes.

It can be summarised that, the metal ion oxidation states influence the membrane capacity during rejection, and thus depends on the chemical stability of the metal ion. Hence, it was proved that higher the valence electron of the metal ion e.g. Pd^{4+} and Pd^{2+}, Cu^{2+} and Cu^{+} ions, the higher the rejection on NF membranes. Therefore, NF membranes can be operated at an acidic medium to reject metals even better. This was proven in this study, during rejection measurements of the ions.

4.14 Fouling

4.14.1 SEM images of used membranes

Fouling or concentration polarization, leads to flux decline during membrane processes [21, 22]. This is due to deposition of materials which will lead to build-up on the membrane surface during permeation [9]. Scanning electron microscopy was employed to capture images of fouled and cake layer formation on NF- membrane surface layer. Figure 4.52 indicate crystallization of foulants (Ag^+ and Cl^-) and other materials at 20 ppm. While Figure 4.53, is an image of definite cake-layer formation at 100 ppm. Particles magnification at 900 X shows the scattered foulants after forming crystallization at pH 3.0. As mentioned in Figure 4.1, in Section A, the membrane (NF-) is characterised as having low flux measurement with a smooth surface layer. This was because the deposition of foulants easily clogs the membrane as they have small pore sizes.

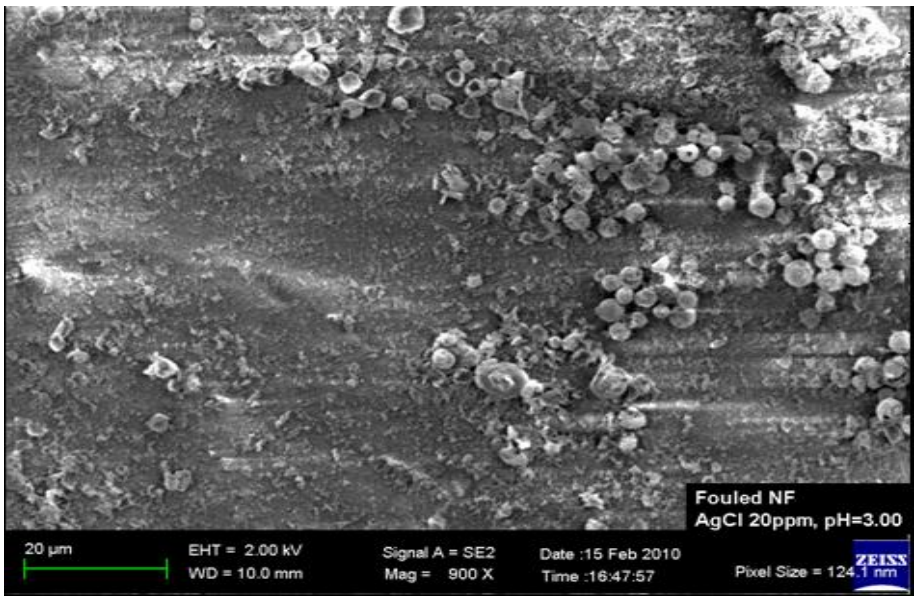

Figure 4.52 SEM image of fouled NF-membrane by AgCl at pH 3.0, 20 ppm.

AgCl, due to its lowest solubility in water and other chemicals or solvents, has a tendency of being reduced from Ag^{+} to Ag^{0}. Therefore, the concentration polarization (fouling) which was caused by Ag^{+} and Cl^{-} ions, were adsorbed on the membrane surface layer. These lead to a cake layer formation on the membrane as shown on Figure 4.53. This situation can lead to flux decline and reduce the membrane lifetime operation. The composition of AgCl and other elements found on the membrane surface as foulants are listed in Table 4.3 as elemental composition by weight percentages.

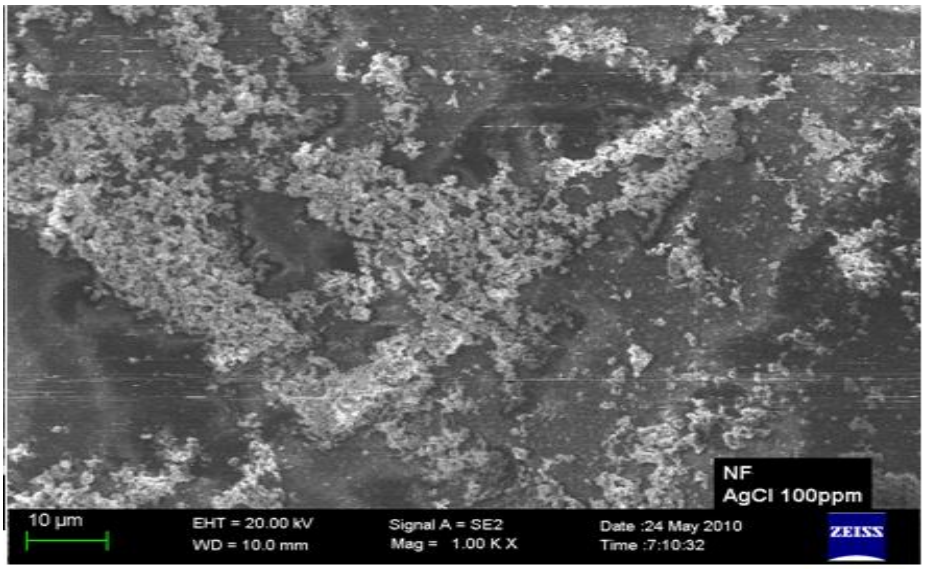

Figure 4.53 SEM image of fouled NF- membrane by AgCl at pH 3.0, 100 ppm.

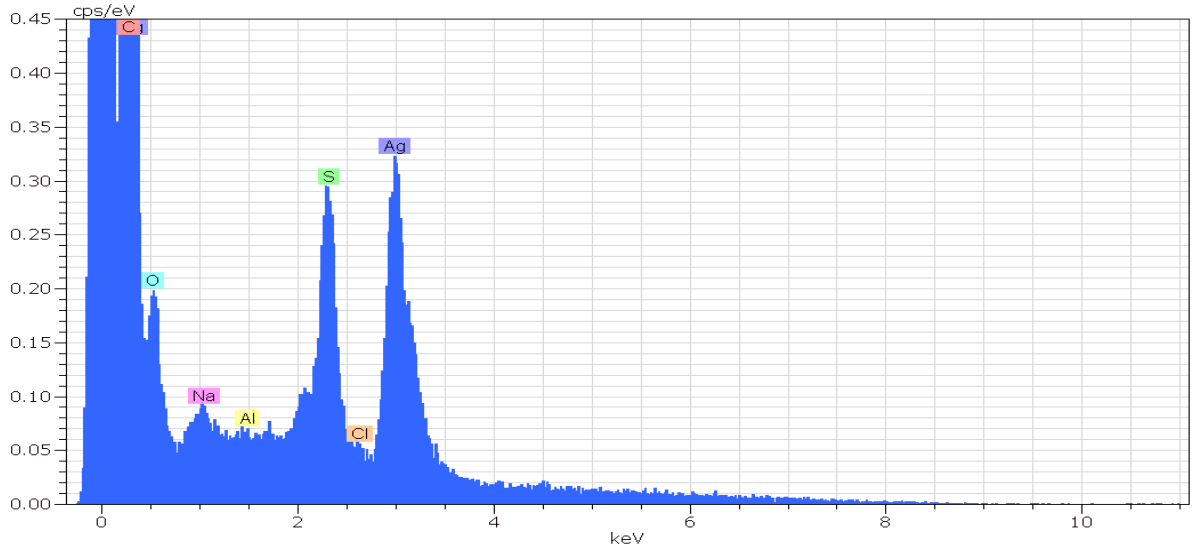

Figure 4.54 EDX elemental composition specta

The amounts of elemental composition by weight percentage present on the membrane surface layer and pores are listed on Table 4.3. Silver (Ag^{+}) is one with the highest content of 38.45%, followed by Na^{+} ion with about 16.45% and so forth. Oxygen (O_2^{2-}) was the lowest with an indication that, most of it went through the membrane since it is a counter ion as the membrane surface layer.

Table 4.3 SEM/EDX elemental composition by weight.

Element	S	Ag	Na	Al	Cl^{-}	C	O
Composition %	15.93	38.45	16.45	13.91	2.12	13.19	-10.78

References

1. A. N. Zhu, F. Long, X. L. Wang, W. P. Zhu, J. D. Ma. The negative rejection of H^+ in NF of carbonate solutions and its influences on membrane performance, *Chemosphere* **67** (2007) p1558-1565.

2. M. Mänttäri, T. Pekuri, M. Nyström. NF270, a new membrane having promising characteristics and being suitable for treatment of dilute effluents from the paper industry, *Journal of Membrane Science* **242** (2004) p107-116.

3. A. Simon, l. Duc Nghiem, P. Le-Clech, S. J. Khan, J. E. Drewes. Effects of membrane degradation on the removal of pharmaceutically active compounds (PhACs) by NF/RO filtration processes, *Journal of Membrane Science* **340** (2009) p16-25.

4. A. L. Ahmad, B. S. Ooi. A study on acid reclamation and copper recovery using low pressure nanofiltration membrane, *Chemical Engineering Journal* **156** (2010) p257-263.

5. A. Simon, L. D. Nghiem, P. Le-Clech, S. J. Khan, J. E. Drewes. Effects of membrane degradation on the removal of pharmaucitically active compounds (PhACs) by NF/RO filtration processes, *Journal of Membrane Science* **340** (2009) p16-25.

6. N. Hilal, H. Al-Zoubi, N. A. Darwish, A. W. Mohammad, Nanofiltration of magnesium chloride, sodium chloride, and calcium sulphate in salts solutions, *Separation Science and Technology* **40** (2005) p3299-3321.

7. T. Y. Chayang, Y-N. Kwon, O. J. Leckie. Effects of membrane chemistry and coating layer on physiochemical properties on thin film composite polyamide RO and NF membranes. I. FTIR and XPS characterization of polyamide and coating layer chemistry, *Desalination* **242** (2009) p149-167.

8. Z. V. P. Murphy, L. B. Chaudhari. Application of nanofiltration for the rejection of nickel ions from aqueous solutions and estimation of membrane transport parameters, *Journal of Hazardous Materials* **160** (2008) p70 -77.

9. L. J. Moitsheki. Nanofiltration: Fouling and chemical cleaning. Msc thesis, Potchefstroom University, South Africa (2003).

10. A. L. Ahmad, B. S. Ooi, A. W. Mohammad, J. P. Choudhury. Composite Nanofiltration Polyamide Membrane: A study on the diamine ratio and its performance evaluation, *Industrial Engineering Chemicals* **43** (2004) p8074-8082.

11. L. Ouyang, R. Malaisamy, M. L. Bruening. Multilayer polyelectrolyte films as nanofiltration membranes for separating monovalent and divalent cations, *Journal of Membrane Science* **310** (2008) p76-84.

12. K. Karakulski, M. Gryta, A. W. Morawski. Membrane processes used for separation of effluents from wire productions, *Chemical Papers* **63** (2009) p205-211.

13. A. L. Ahmad, B. S. Ooi. A study on acid reclamation and copper recovery using low pressure nanofiltration membrane, *Chemical Engineering Journal* **156** (2010) p257-263.

14. N-E. Belkhouche, M. A. Didi, S. Taha, N. B. Farés. Zinc rejection from leachate solutions of industrial solid waste-effects of pressure and concentration on nanofiltration membrane performances, *Desalination* **239** (2009) p58-65.

15. E. Chilyumova, J. Thöming. Nanofiltration of bivalent cations-model parameter determination and process simulation, *Desalination* **224** (2008) p12-17.

16. E. Cséfalvay, V. Pauer, P. Mizsey. Recovery of Copper from process waters by nanofiltration and reverse osmosis, *Desalination* **240** (2009) p132-142.

17. K. Boussu, Y. Zhang, J. Cocquyt, P. Van der Meeren, A. Volodin, C. Van Haesendonck, J. A. Martens, B. Van der Bruggen. Characterization of polymeric nanofiltration membranes for systematic analysis of membrane performance, *Journal of Membrane Science* **278** (2006) p418-427.

18. C. Niewersch, K. Meier, T. Wingtgens, T. Melin. Selectivity of polyamide nanofiltration membranes for cations and phosphoric acid, *Desalination* **250** (2010) p1021-1024.

19. M. R. Teixeira, M. J. Rosa, M. Nyström. The role of membrane charge on nanofiltration performance, *Journal of Membrane Science* **265** (2005) p160-166.

20. M. Mohsen-Nia, P. Montazeri, H. Moderress. Removal of Cu^{2+} and Ni^{2+} from wastewater with a chelating agent and reverse osmosis processes, *Desalination* **217** (2007) p276-281.

21. M. Nyström, L. Kaipia, S. Lugue. Fouling and retention of nanofiltration membranes, *Journal of Membrane Science* **98** (1995) p249-262.

22. A. I. Schäfer, A. G, Fane, T. D. Waite. Fouling effects on rejection in the membrane filtration of natural waters, *Desalination* **131** (2000) p215-224.

CHAPTER 5

CONCLUSIONS AND RECOMMENDATIONS

5.1 Conclusion

Rejection measurements study of both charged solute and metal ions as might occur in mining wastewater, were successfully evaluated on NF membranes. This was done through varying their oxidation states at varying concentrations, pressure and pH levels. Therefore, the hypothesis was proven and the objectives were achieved with regard to the rejection performances of the NF membranes for the platinum group metals. The performance of the NF90 and NF- gave satisfactory and convincing rejection values of > 90% compared to NF270. This was even so when operated at low pressure and concentration in acidic (pH 2.0) medium and at concentrations as low as between 20 ppm and 50 ppm. Since pH influence the separation and rejection process, pH 2.0 on average, gave a high rejection trend as compared to pH 3.0 and pH 5.0. This was due to an increase in protonate (H^+) on the positively surface layer material. But at pH 7.0, the rejection of both metals and charged solutes, tends to increase in rejection as pressure applied increase.

During membrane characterization, flux measurements using pure water in Section A (Chapter 4), revealed the characteristics of the membranes before a sample could be exposed to it. An increasing trend in flux measurements at an increasing pressure, was in accordance with the membrane permeability performance sequence of NF270 > NF90 > NF-, at all concentrations of 20 ppm, 50 ppm and 100 ppm. As for rejection study of the charged solutes, divalent (Mg^{2+}) ion gave a highest rejection than monovalent (Na^+) ion. Amongst membranes employed, NF90 gave a high rejection levels. The counter ion (Cl^-), which seemed to permeate through the membranes, did so due to the opposite charged (counter ion) with the membrane surface charge density.

NF90, which is also regarded as loose reverse osmosis type, proved to be excellent in rejecting single salts and inorganic metals as divalent (Cu^{2+} and Ni^{2+}) ion and multivalent (Pd^{4+}) ion with > 95% and ≈ 99,91% at low pressures and concentrations. But Pd^{2+} seemed to be favoured on NF90 than NF-, with rejection > 90%. Even though during membrane characterization, NF90 was found to have slightly higher flux measurements as compared to NF-, but had high rejection ability than NF-. Its charged

surface layer made of polyamide, contributed during an electrostatic interaction with the solute thus leading to high rejections. In the case of monovalent (Ag^{+} and Cu^{+}) ions, although most would permeate through the membrane, a fair rejection of > 85% was achieved at low concentration and in acidic medium.

As for binary and trinary solution mixture, the competition amongst the ions was high, due to their molecular weight. Ni^{2+} and Pd^{2+} ions were rejected on a varying trend on both NF90 and NF-, but NF- favoured Ni^{2+} while NF90 did so for Pd^{2+}, at both 20 and 100 ppm solution mixtures.

NF270 membrane was eliminated during metals rejection of binary and trinary inorganic metal solution mixtures, due to its low performance on average of < 80%. This membrane performed well, however during charged solute rejection studies. This could be linked to the fact that, the varying oxidation state and metal ionic charge had an influence on the performance of this membrane.

In general, NF- had almost similar rejection trends as with NF90 on all experiments carried during the studies. The characteristics which are closer to NF90 during flux measurements on the membranes were also observed. Therefore, the two membranes recommended for rejection of metals at acidic mediums. It can be reported that, the more solution is concentrated, the lower the flux and rejection which will lead to concentration polarization or fouling on NF membranes. This was justified by SEM/EDX spectra analysis during elemental compositions of the foulants in Figure 4.26 and Figure 4.27 (Chapter 4 under Section A). It can be further emphasized that, the performance of NF- membranes are dependent on pH, concentration and pressure.

5.2 Recommendations

NF membranes have abilities to remove or reject metal ions depending on the surface charge density of the membrane. Therefore, the following points can be outlined for further improvement on membrane rejection performance:

- An acidic medium should be considered for NF membranes applications during wastewater treatment, since they have capability to remove metals at both high and low concentration levels.
- Low pressure operation should be utilized for high cations or metals rejection, in order to minimize the energy consumption during membrane processes.
- Coating or impregnation of NF membranes with a chelating agent e.g. EDTA to increase surface layer to obtain > 95% of the metals ions.
- The process for NF membrane process should be viable and easy to operate at high pilot plant scale as experienced on dead end module.